STUDIES ON SEMICONDUCTIVITY IN Transition Metal Compounds

MAY 1966

Mrs. P. P. JOGALEKAR
M. Sc.

STUDIES ON SEMICONDUCTIVITY IN TRANSITION METAL COMPOUNDS

A THESIS
SUBMITTED TO
THE UNIVERSITY OF POONA
FOR
THE DEGREE OF DOCTOR OF PHILOSOPHY
(IN CHEMISTRY)

by
Mrs. PRADNYA PRABHAKAR JOGALEKAR, M.Sc.,
National Chemical Laboratory,
Poona-8. (INDIA).

MAY - 1965

ACKNOWLEDGEMENTS

I am deeply indebted to Dr.A.P.B.Sinha for his keen interest, valuable guidance and encouragement during the pursuit of this work.

I am grateful to Dr.A.B.Biswas for his help and valuable suggestions during the course of this work. I am also grateful to Mr. M.M.S.Murthy for going through the various drafts of this thesis and making valuable suggestions for its improvement.

I take this opportunity to express my sincere thanks to the Director, National Chemical Laboratory, Poona-8, for allowing me to submit the research work carried out at N.C.L. in the form of a thesis.

Finally, thanks are due to the Council of Scientific & Industrial Research, New Delhi, for the award of Junior Research Fellowship during 1961-1965 which made this study possible.

CONTENTS

		Pages
INTRODUCTION		
0.1.	General Introduction.	1
0.2.	General Proporties of Manganites.	3
PART I.	ELECTICAL PROPERTIES OF ZINC-LITHIUM MAGANITES AND ZINC-COPPER MARGANITES.	
1.1.	Introduction.	11
1.2.	Hoppint machanism of electrical conductivity in transition metal oxides.	15
1.3.	Experimental Techniques.	19
1.4.	Experimental Results.	31
	(A) Zinc-lithium manganites.	31
	(B) Zinc-copper manganites.	59
1.5.	Discussion.	76
	(A) Zinc-lithium mananites.	76
	(B) Zinc-copper manganites.	92
PART II.	MAGNSTIC PROPERTIES OF ZINC-LITHIUM MAGNANITES AND ZINC-COPPER MANGANITES.	
2.1.	Introduction.	96
2.2.	Experimental Techniques.	105
2.3.	Experimental Results.	109
2.4.	Discussion.	
	(A) Zinc-lithium manganites.	114
	(B) Zinc-copper manganites.	122
PART III	JAHN-TEILER DISTORTION IN MIXED MANGANITES.	
3.1.	Introduction.	127
3.2.	Results and discussion.	134
SUMMARY		148
REFERENCES.		150

◆ ◆ ◆ ◆

INTRODUCTION

0.1. General Introduction

3d transition metal oxides exhibit many interesting electrical properties. As these solids have incompletely filled 3d bands, they would be expected to be conductors, but a number of them are known to be either insulators or semiconductors[1,2]. It is generally believed that in such compounds the charge carriers are localised and the electrical conduction takes place through occasional hops of these carriers from one site to another[3,4].

Oxidic semiconductors containing both Mn^{3+} and Mn^{4+} ions would be expected to have an additional interesting feature. At octahedral sites the Mn^{3+} ions produce a strong Jahn-Teller distortion and such distortion is expected to be localised around Mn^{3+} ions only. The electron transport in these compounds which would take place by exchange of electrons between neighbouring Mn^{3+} and Mn^{4+} ions will lead to an unstable configuration as the new Mn^{4+} (at the old site of Mn^{3+}) would be surrounded by a distorted octahedral arrangement of oxygen ions, and the new Mn^{3+} ion by a cubic octahedron of O^{2-} ions. So each electron exchange will have to be associated with a rearrangement of surrounding oxygen ions which would require an additional activation energy. With a view to investigate this behaviour some manganites (AMn_2O_4) containing both Mn^{3+} and Mn^{4+} ions were synthesized and their electrical properties were studied.

The magnetic properties of such compounds are also known to be very interesting. Lanthanum strontium manganites and a few other similar compounds have been prepared which contain both Mn^{3+} and Mn^{4+} at the octahedral sites of the perovskite structure and they are found to be ferromagnetic[5]. This behaviour has been explained by Zener[6] (1951) on the basis of double exchange. Double exchange is also known to occur in $Li_xMn_{1-x}Se$[7] and all these compounds exhibit metallic type conductivity. Some spinel type compounds containing Mn^{3+} and Mn^{4+} ions were therefore investigated for the possible existence of double exchange and its correlation with the electrical properties of these substances.

In the present studies, a controlled formation of Mn^{3+} and Mn^{4+} ions was achieved by incorporating Li ions in the homogeneous solid phase of zinc manganite ($ZnMn_2O_4$). ZnO, Mn_2O_3 and Li_2O were reacted in the appropriate proportion at elevated temperatures in air. The presence of Li ions created a controlled amount of Mn^{4+} in the zinc manganite structure. The other method where one prepares a non-stoichiometric compound with a small proportion of the transition metal ions in a different state of ionisation could not be used because of the experimental difficulties in controlling the extent of non-stoichiometry.

Another series of compounds was formed by the so-called 'dilution method', where one prepares a solid solution of two or more compounds of widely different

conductivities. Copper manganite is known to have a high p-type conductivity ($\rho_{R.T.} \sim 30$ ohm x cm)[8]. This is understood to arise because of a large concentration of Mn^{4+} ions at the octahedral sites. By forming suitable solid solutions with $ZnMn_2O_4$ which contains only Mn^{3+} ions at octahedral sites, compounds having a predetermined ratio of Mn^{3+} to Mn^{4+} at octahedral sites were obtained. The present work describes the results of two series of compounds, $Zn[MnLi]_2O_4$ and $(ZnCu)[Mn]_2O_4$. In addition, new spinels of formulae $(Ni^{2+}Mn^{3+}Cr^{3+})O_4$, $(Cu^{2+}Fe^{3+}Mn^{3+})O_4$ and $(Cu^{2+}Cr^{3+}Mn^{3+})O_4$ have also been synthesized as they were expected to exhibit Jahn-Teller distortion, and their structural and electrical properties have been investigated.

0.2. General properties of manganites

Before going into the experimental results and their discussion it would be useful to discuss some general structure of the manganites as known from the earlier studies. The manganites chosen for this study have the general formula Me_3O_4 where Me stands for a mixture of ions such as Mn^{3+}, Mn^{4+}, Li^{1+} and several others. The metal ions are present in such a ratio that the total charge over three Me's is 8+. These manganites belong to the well-known family of compounds called 'spinels'. They crystallise in either the cubic spinel structure or the tetragonal hausmannite structure. Some general features of these structures are given below.

0.2.1. Cubic spinel structure

The unit cell edge of the cubic spinels varies from substance to substance, but is usually of the order of 8.3 Å. The space group is $Fd3m$, (O_h^7) and there are 8 molecules of Me_3O_4 per unit cell. The positions of the ions in the unit cell are given as :

8 metal ions at : 8(a) positions

$0,0,0;\ \frac{1}{4},\frac{1}{4},\frac{1}{4}$ (+ f.c.c.)

16 metal ions at : 16(d) positions

$\frac{5}{8},\frac{5}{8},\frac{5}{8};\ \frac{5}{8},\frac{7}{8},\frac{7}{8};\ \frac{7}{8},\frac{5}{8},\frac{7}{8};\ \frac{7}{8},\frac{7}{8},\frac{5}{8}$ (+ f.c.c.)

32 oxygen ions at : 32(e) positions

$u,u,u;\ u,\bar{u},u;\ \bar{u},u,\bar{u};\ \bar{u},\bar{u},u;$

$\frac{1}{4}-u,\ \frac{1}{4}-u,\ \frac{1}{4}-u;\ \frac{1}{4}-u,\ \frac{1}{4}+u,\ \frac{1}{4}+u;$

$\frac{1}{4}+u,\ \frac{1}{4}-u,\ \frac{1}{4}+u;\ \frac{1}{4}+u,\ \frac{1}{4}+u,\ \frac{1}{4}-u$ (+f.c.c.)

f.c.c. translations are $0,0,0;0,\frac{1}{2},\frac{1}{2}$; $\frac{1}{2},0,\frac{1}{2}$; $\frac{1}{2},\frac{1}{2},0$.

These oxygen ions form an almost perfect cubic close packing and the metal ions are distributed over the octahedral and tetrahedral interstices. In a unit cell there are 32 octahedral and 64 tetrahedral holes, but only 16 of the former (16d) and 8 of the latter (8a) are occupied by the metal ions.

0.2.2. Tetragonal spinel structure

Manganites such as Mn_3O_4 and $ZnMn_2O_4$ do not exhibit

the usual cubic symmetry. The unit cell is tetragonal and contains 4 molecules of the formula unit. The space group assigned to such spinels is $I4_1/amd - D_{4h}^{19}$ and the coordinates for the various ions are :

metal ions at 4(a) position : $0,0,0$; $0,\frac{1}{2},\frac{1}{4}$;

and 8(d) position : $0,\frac{1}{4},\frac{5}{8}$; $0,\frac{3}{4},\frac{5}{8}$;

$\frac{1}{4},0,\frac{3}{8}$; $\frac{3}{4},0,\frac{3}{8}$; and

oxygen ions at 16(f) positions : $0,0,0$

$0,\bar{x},z$; $0,x,z$; and

$0,\frac{1}{2}+x,\frac{1}{4}-z$; $\frac{1}{2},\frac{1}{2},\frac{1}{2}$

$0,\frac{1}{2}-x,\frac{1}{4}-z$;

$\bar{x},0,\bar{z}$; $x,0,\bar{z}$;

$x,\frac{1}{2},\frac{1}{4}+z$; and

$\bar{x},\frac{1}{2},\frac{1}{4}+z$

The body centred tetragonal spinel can be compared with face centred cubic spinel by converting it into a larger face-centred tetragonal spinel on its 'c' face diagonals. Thus, the lattice parameters for the new cell are $a' = a\sqrt{2} \simeq 8\text{Å}$ and $c' = c \simeq 9\text{Å}$ with its volume twice that of the original cell. This tetragonally distorted spinel containing 8 molecules of Me_3O_4 has the atomic positions similar to those in a cubic spinel. The metal ions, in this structure also,

are distributed over the various interstitial positions. The interstitial positions corresponding to the octahedral sites of the ideal cubic spinel, have six oxygen neighbours, four of which are situated in the plane defined by the axes a and b and the other two along the normal to this plane. The first four are closer to the central metal ion than the other two approximately by a factor of a'/c'. The tetrahedral site has four equidistant oxygen neighbours. However, the angular distribution does not correspond to the ideal cubic arrangement in so far as the Me-O-Me angles have two values.

In spinels where there are only two metal ions e.g. AB_2O_4, a systematic classification for the distribution of 8A and 16B cations, in both cubic and tetragonal spinels, over the octahedral and tetrahedral sites, has been proposed by Barth and Posnjak[9] (1932). When all the 8A ions occupy the tetrahedral sites and all the 16B ions occupy the octahedral sites, the structure is said to be 'normal'. When 8B ions occupy tetrahedral sites and the remaining 8B ions along with 8A ions occupy octahedral sites in a completely random arrangement, the structure is referred to as 'inverse'. If 8A and 16B ions are distributed randomly among the 8 tetrahedral and 16 octahedral sites the structure is referred to as 'random'.

The formula of a spinel is conveniently written by putting the metal ions located at the tetrahedral site first, and then the metal ion located at the octahedral site in a

square bracket followed by the oxygen ions. Thus, $Cd[Mn_2]O_4$, $Zn[Mn_2]O_4$ are normal spinels; $Mn[MnMi]O_4$ is an inverse spinel, and $Fe_{1/3}Mn_{2/3}[Mn_{4/3}Fe_{2/3}]O_4$ is a random spinel.

However, it is now known that these are three special cases only; in general, the cations can be distributed in any proportions between the two sites. The most general formula for cation distribution is then,

$$(A_mB_{1-m})_{tet.}[A_{1-m}B_{1+m}]_{oct.}O_4$$

where m can have any value between 0 and 1. The normal, inverse and random models are obtained with the values of m = 1, 0, 1/3 respectively.

The structure of a number of manganites has been determined by various investigators. Some of the results have been summarised in Table 1. It can be seen from the table 1 that a number of manganites crystallise in the tetragonal spinel structure (Hausmannite structure). The tetragonal distortion of spinels has been discussed in detail in a later chapter.

Table - 1

The structure of various manganites

No.	Compound	Structure	c (A^0)	a (A^0)	c/a	Probable cation distribution	Ref.
1.	$CuMn_2O_4$	Cubic		8.33 8.30 8.28		$Cu[Mn]_2O_4$	10,12 14 19
2.	$NiMn_2O_4$	Cubic		8.37 8.38 8.39		$Mn[NiMn]O_4$	10 14 18
3.	$MnMn_2O_4$ or Mn_3O_4	Tetragonal	9.44 9.45 9.454	8.15 8.151 8.157	1.16 1.159 1.159	$Mn^{2+}[Mn_2^{3+}]O_4$	10 14 15,16
4.	$CdMn_2O_4$	Tetragonal	9.87	8.22	1.20	$Cd^{2+}[Mn_2^{3+}]O_4$	10,11
5.	$ZnMn_2O_4$	Tetragonal	9.24 9.228 9.224 9.254	8.10 8.087 8.092 8.087	1.14 1.141 1.142 1.144	$Zn^{2+}[Mn_2^{3+}]O_4$	10 14 15,16 17
6.	$MgMn_2O_4$	Tetragonal	9.28 9.31	8.07 8.07	1.15 1.15	$Mg^{2+}[Mn_2^{3+}]O_4$	10,13 14
7.	$CoMn_2O_4$	Tetragonal	9.31	8.10	1.15	$Co^{2+}[Mn_2^{3+}]O_4$	14

0.2.3. Effect of temperature on the structure of distorted manganites

Distorted manganites when heated to elevated temperatures transform from the tetragonal to the cubic spinel structure. McMurdie and Golovato[20] (1948) during their investigation on the oxides of manganese by the high temperature x-ray diffraction and the differential thermal analysis,

observed a transformation of Mn_3O_4 from the tetragonal to the cubic symmetry at 1170°C. Romeijn[21] (1953) supported the same by his observation of a discontinuity in the resistivity of $ZnMn_2O_4$ at 1025°C and forecast that $ZnMn_2O_4$ would transform from tetragonal to cubic spinel structure at this temperature. Irani, Sinha and Biswas[22] (1962) determined the structure of many tetragonal manganites as a function of temperature and found a transformation to cubic phase in all cases. Finch, Sinha and Sinha[23] (1957) have treated the problem theoretically on the basis of an order-disorder process. This model has been investigated in detail by Wojtowicz[24] (1959). Kanamori[25] (1961) on the other hand treats the cubic phase as arising due to resonance between the various possible distorted structures.

0.2.4. <u>Effect of removal of Mn^{3+} ions from octahedral sites</u>.

The effect of removal of the Mn^{3+} ions on crystal distortion was first studied by Finch, Sinha and Sinha[23]. They replaced the Mn^{3+} ions by non-distorting cations through the formation of solid solution of tetragonal (Mn_3O_4) and cubic (AFe_2O_4) spinels. They analysed the results on the assumption that the Mn^{3+} ions occupied the octahedral sites in the solid solutions as they did in the parent Mn_3O_4. Wickham and Croft[26] (1958) made a similar assumption in their studies on the systems $Zn_xGe_{1-x}Mn_2O_4$, $Zn_xGe_{1-x}Co_{2-2x}Mn_{2x}O_4$ and $Zn_xLi_{1-x}Mn_2O_4$.

Irani, Sinha and Biswas[27] (1960), who studied the system Mn_3O_4-$MgAl_2O_4$ and $MgMn_2O_4$-$MgAl_2O_4$, determined the cation distribution from an analysis of the x-ray diffraction intensities and plotted the unit cell dimensions as a function of the number of Mn^{3+} ions at the octahedral sites. They observed that c' and a' do not change linearly with composition but remain more or less constant and then show an abrupt change at a critical composition beyond which c' = a' and the systems take up cubic spinel structure. This critical composition is one where 9.3 ± 0.2 sites out of the 16 octahedral sites are occupied by Mn^{3+} ions. Finch, Sinha and Sinha[23] (1957), Sojtowicz[24] (1959) and Kammeri[25] (1961) have treated this transformation theoretically.

+ + + +

PART I

ELECTRICAL PROPERTIES

OF

ZINC LITHIUM MANGANITES

AND

ZINC COPPER MANGANITES

1.1. Introduction.

Although the electrical conductivity of a number of oxides has been investigated, only a very limited study has been made on the manganites. This is due to the fact that most of the manganites have been synthesized and their interesting structural properties brought to light only very recently. The earlier conductivity work was usually on mixed substances and not on single phase compounds. Also no attempt was made to identify the phases present.

The electrical conductivity of sintered samples of mixed oxides of cobalt and manganese, was measured by Ikuo Aoki[28] (1952). He obtained the specific resistance R and the temperature coefficient $\frac{dR}{dT}$. The specific resistance was minimum when the mole ratio of Co:Mn was 2:1 (I). This sample had a spinel structure which would be designated as (I) $(Mn,Co)[CoMn]_2O_4$. It had a comparatively high $\frac{dR}{dT}$. In the case of specimens consisting only of Co_3O_4 and CoO, a larger R and a smaller $\frac{dR}{dT}$ was observed than for a mixture of Co and Mn oxides.

Masahide Kamiyama and Ziro Nara[29] (1952) prepared some samples by sintering the mixtures of MnO_2 and NiO in various ratios at 1300°C for 3 hours and annealing at 500°C for 24 hours. On sintering, MnO_2 changed to Mn_3O_4. They measured the electrical resistance R of these samples at various temperatures. The compositions (MnO_2 : NiO ratio in weight) of the compounds studied and the corresponding activation energies are given below :

(I) 1:0 pure Mn_3O_4, 0.48 eV; (II) 4:1, 0.31 eV; (III) 3:2, 0.33 eV; (IV) 2:3, 0.36 eV; (V) 1:4, 0.46 eV; (VI) 0:1 pure NiO, 0.61 eV and for (VII) 7:3, the minimum for E corresponding to a minimum of R has been observed. On measuring the thermoelectric power, they found that samples (I), (II) and (VI) were p-type while (III, (IV), (V) were n-type. The 7:3 sample was n-type below 200°C and p-type above that temperature. Using x-ray diffraction techniques they found that (VII) consisted of (II) and (III).

Suchet[30] (1955) found from his studies on the variation of electrical resistivity with temperature in the systems consisting of the oxides of manganese and nickel that the behaviour was best represented by the equation :

$$\rho = AT^b \exp.\left(\frac{B}{T}\right)$$

where ρ = resistivity, b, A and B = constants and T = absolute temperature. A third corrective constant b has been introduced. This equation fits with the experimental observation over a wider temperature range.

Heikes and Johnston[31] (1957) have studied the effect of Li substitution on the electrical properties of MnO, CoO, NiO and CuO. The addition of Li ions changes some divalent metal ions to 3+ ionisation state according to the following equation :

$$(1-x)MnO + \frac{x}{2} Li_2O + \frac{x}{4} O_2 = Mn^{2+}_{1-2x} Li^{1+}_{x} Mn^{3+}_{x} O$$

With increasing concentration of Li^{1+} the activation energy and resistivity initially decrease rapidly and then level off. They have treated the conduction process as a thermally activated diffusion of positive holes i.e. Me^{3+}. The activation energy is a consequence of the self-trapping of the moving hole by its own polarisation field. In general, the activation energy is built up of two parts (i) loosening energy and (ii) a transport term. The former depends upon the distance between the transport level and the acceptor levels. The latter is determined by the self-trapping. The activation energy for conduction increases abruptly near the antiferromagnetic Curie point.

Sabane[8] (1960) has studied the variation of electrical conductivity as a function of temperature for the manganites of copper, nickel, manganese, cobalt, magnesium, zinc and cadmium. He has observed that Wilson's law is obeyed for all these manganites only in the higher temperature range. He has also studied the electrical conductivity in the solid solutions : $NiMn_2O_4$-$CuMn_2O_4$; $NiMn_2O_4$-Mn_3O_4; $NiMn_2O_4$-$CoMn_2O_4$; $NiMn_2O_4$-$MgMn_2O_4$; Mn_3O_4- $CoMn_2O_4$; Mn_3O_4-$CuMn_2O_4$; $CoMn_2O_4$-$CuMn_2O_4$; and $CuMn_2O_4$-$MgMn_2O_4$. The thermoelectric coefficient measurements carried out by him indicate that all the manganites studied showed p-type conduction. He has also discussed the mechanism of electrical conductivity on the basis of the electron hopping process.

Larson, E.G., Arnott, R.J. and Wickham, D.G.[32] (1962) have prepared a series of compounds with the general formula

$Ni_{1-x}Mn_{2+x}O_4$. They have studied the semiconduction and low temperature magnetization of this system. The compounds with the values of x less than 0.42 crystallize with cubic symmetry and others with the values of x greater than 0.42 exhibit tetragonal symmetry. From the results of Seebeck coefficient measurements they observed that n-type conduction occurs in cases of compounds with $x < 0.46$ and p-type conduction occurs when $x > 0.46$. A sharp change in the low temperature magnetization takes place as the value of x is increased from 0.36 to 0.42. According to them, if the formula of the above systems is written as :

$$(1-\beta)Mn_x^{2+}Mn_{1-x}^{3+}[Ni_{1-x}^{2+}Mn_{1+x}^{3+}]O_4 + \beta\, Mn^{2+}[Ni_{1-x}^{2+}Mn_{2x}^{3+}Mn_{1-x}^{4+}]O_4 ,$$

the electrical conductivity results from the transfer of electrons from B site Mn^{3+} ions to the neighbouring B site Mn^{4+} ions. The possible contribution to the conductivity from A site ions is neglected because the distance between them is too great to allow a comparable transfer of charge by a hopping mechanism according to which an electron jumps directly from one cation to a neighbouring cation.

Recently, M.Rosenberg, P.Nicolou, R.Manaida and P.Pausasau[33] (1963) have prepared $Cu_xMn_{3-x}O_4 (o \leqslant x \leqslant 0.2)$, $Zn_{1+x}Mn_{2-x}O_4 (o \leqslant x \leqslant 0.2)$, $Mg_xMn_{3-x}O_4$ $(o \leqslant x \leqslant 1)$ and $Zn_xMn_{3-x}O_4$ $(o \leqslant x \leqslant 1)$ by co-precipitation methods and studied their electrical conductivity. From the studies of the

crystal symmetry as a function of composition and of electrical conductivity as a function of composition and temperature, they have concluded that the electrical conductivity involves the hopping mechanism of electrons between Mn^{3+} and Mn^{4+} ions at octahedral sites.

1.2. Hopping-Mechanism of electrical conductivity in transition metal oxides.

De Boer and Verwey[3] (1937) were the first to attempt to explain the electron transport in the oxide semiconductors. They pointed out that the collective electron treatment of Bloch[34,35] (1928, 1930) and Wilson[36] (1931), although very successful in explaining the electrical behaviour of metals, is not a correct approximation for the oxide semiconductors. Later Mott[4] (1949) has also shown that the band picture of solids does not satisfactorily explain the electron transport in oxide semiconductors such as NiO. The Heitler-London approximation based on localised atomic wave functions should be used here.

Morin[37] (1951) made a systematic investigation of the conduction mechanism in oxides whose cations have a partially filled d level. The electrical conductivity, Hall effect and Seebeck effect were measured on two sets of polycrystalline samples of α-Fe_2O_3 and α-Fe_2O_3 containing from 0.05 to 1.0 atomic percent titanium (n-type impurity).

In one set, the sample was containing 0.6% excess of iron (n-type impurity), while the second set had 0.6 atomic percent deficiency of iron (p-type impurity). It was observed that the conductivity of pure α-Fe_2O_3 was independent of the amount of stoichiometric deviation. He used the Seebeck data to study the temperature variation of the Fermi-Level. The temperature variation of the carrier concentration was determined from Fermi levels, and mobility from the carrier concentration and conductivity. The results on the carrier concentration indicated that each added titanium ion was donating approximately one electron for the conduction process. From the further extensive investigation of conductivity, Seebeck effect and optical transmission of α-Fe_2O_3 and NiO, Morin analysed the results using two alternative models : (i) involving conduction in d levels of the metal ions; and (ii) involving conduction in the sp band of the oxygen ions. The observed low mobility was explained by means of the first model. A large variation of the mobility with the impurity concentration and temperature was observed in both α-Fe_2O_3 and NiO, and was associated with an activation energy of 0.1 eV. Morin has suggested that this energy could be accounted for in two different ways : (i) energy required to transfer a charge carrier from one Fe ion to another or (ii) energy related to the anti-ferromagnetic exchange energy kTc.

Yamashita and Kurosawa[38,39,40] (1958, 1960, 1961) have discussed the problem of conduction in semiconductors

with incomplete d shells. They have proposed the Heitler-London approach to explain the conduction in such compounds and have assumed that the wave function of the electron is localised closely around an ion. However, the localised state is a stationary state only in the first approximation. The electron jumps from an ion to its nearest neighbour ions with a certain probability due to the perturbing influence of the neighbouring ions. Considering the conservation of energy, this transition of the electron must be accompanied by emission and absorption of many phonons. This therefore becomes a thermally activated process and the mobility is associated with an activation energy term.

It has been concluded by Yamashita that when mobility is much larger than 1 cm^2/sec.x volt, the usual Bloch theory could be used, while the H-L approach might be good when the mobility is much smaller than 1 cm^2/V x sec. If the mobility is smaller, activation energy becomes larger. Also, if the density of donors is low, the main part of the activation energy comes from the work required to separate an electron from the vicinity of the donor to a distant point in the lattice.

Holstein[41] (1959) has treated this problem for a simplified one dimensional lattice composed of hydrogen like molecules. He has found that if the lattice spacing is large the localised states have a lower energy. He has also calculated the matrix element for transition of the hole between the nearest neighbour orbits.

Dogonadze and Chizmadzhev[42] (1962) have also studied, theoretically the problem of electronic conduction in polar crystals where the mobility of charge carriers is very low.

Recently, Sinha and Sinha[43] (1963) have studied the electronic conduction in some polar semiconductors where the carriers are assumed to be localised. The electron lattice coupling is separated into two parts, one dependent and the other independent of the coordinates of the excess charge carriers. The independent part gives rise to lattice polarisation, while the dependent part, treated as the perturbation, superposes some excited orbital states on the ground orbital state of the carrier located at the metal ion. The static potential of the other ions, treated as the perturbation, causes transition of the carrier from one site to another. This formulation automatically takes into account the role of the intermediate excited states in the hopping process. They have found that, under favourable conditions, these intermediate states furnish an easier path for conduction. In the higher temperature region the dependence of carrier mobility on temperature is nearly exponential. This behaviour is in agreement with the experimental observations of some transition metal compounds.

In what follows we present the results of our investigations on the electrical properties of zinc lithium manganites and copper zinc manganites.

1.3. Experimental technique.

In this section we deal with the experimental techniques employed for the preparation of samples and for the measurements of their electrical and structural properties.

1.3.1. Preparation of compounds.

A series of compounds of the general formula $Zn(Li_{2x}Mn_{2-2x})O_4$, where x had the values as 0.05, 0.10, 0.15, 0.20, 0.25, 0.30 was prepared by a high temperature reaction between ZnO, Mn_2O_3 and Li_2CO_3. All the three components were spectroscopically pure. The sesquioxide of manganese was obtained by a prolonged heating of a sample of specpure Mn_3O_4, in a platinum crucible, at 850°C. Li_2CO_3 decomposes to Li_2O at the reaction temperature i.e. 850°C. The mixtures of ZnO, Li_2CO_3 and Mn_2O_3, taken in appropriate proportions, were thoroughly mixed under alcohol, in an agate mortar with pestle till they appeared homogeneous. The reaction was carried out for several hours in an electric furnace where the temperature could be controlled to $\pm$ 5°C. In some cases, regrinding and prolonged heating was required for the completion of the reaction. The completion of the reaction was checked by taking x-ray diffraction patterns. The heating was continued till no diffraction lines due to the unreacted free oxide appeared. The x-ray diffraction powder patterns were obtained by means of 14 cm. Debye-Scherrer camera and Mo-K_α ($\lambda = 0.709$ Å) radiation filtered through a zirconium foil.

Finally, the compounds were quenched from 850°C to room temperature. The details of the heat treatment are given in Table 2.

Table - 2

Heat treatment given to the compounds of the series $ZnLi_{2x}Mn_{2-2x}O_4$.

Composition	Heat treatment
$ZnLi_{.1}Mn_{1.9}O_4$	850°C / 96 hours
$ZnLi_{.2}Mn_{1.8}O_4$	850°C / 96 hours
$ZnLi_{.3}Mn_{1.7}O_4$	850°C / 100 hours
$ZnLi_{.4}Mn_{1.6}O_4$	850°C / 100 hours
$ZnLi_{.5}Mn_{1.5}O_4$	850°C / 120 hours
$ZnLi_{.6}Mn_{1.4}O_4$	850°C / 136 hours

The other series of compounds with the general formula $Zn_yCu_{1-y}Mn_2O_4$ was prepared by the solid state reaction between ZnO, CuO and Mn_2O_3 taken in appropriate ratios. The oxides used here were specpure materials. Different values given to y were 0.05, 0.10, 0.15, 0.20, 0.25 and 0.50. These thoroughly mixed oxides were fired in the furnace at 950°C.

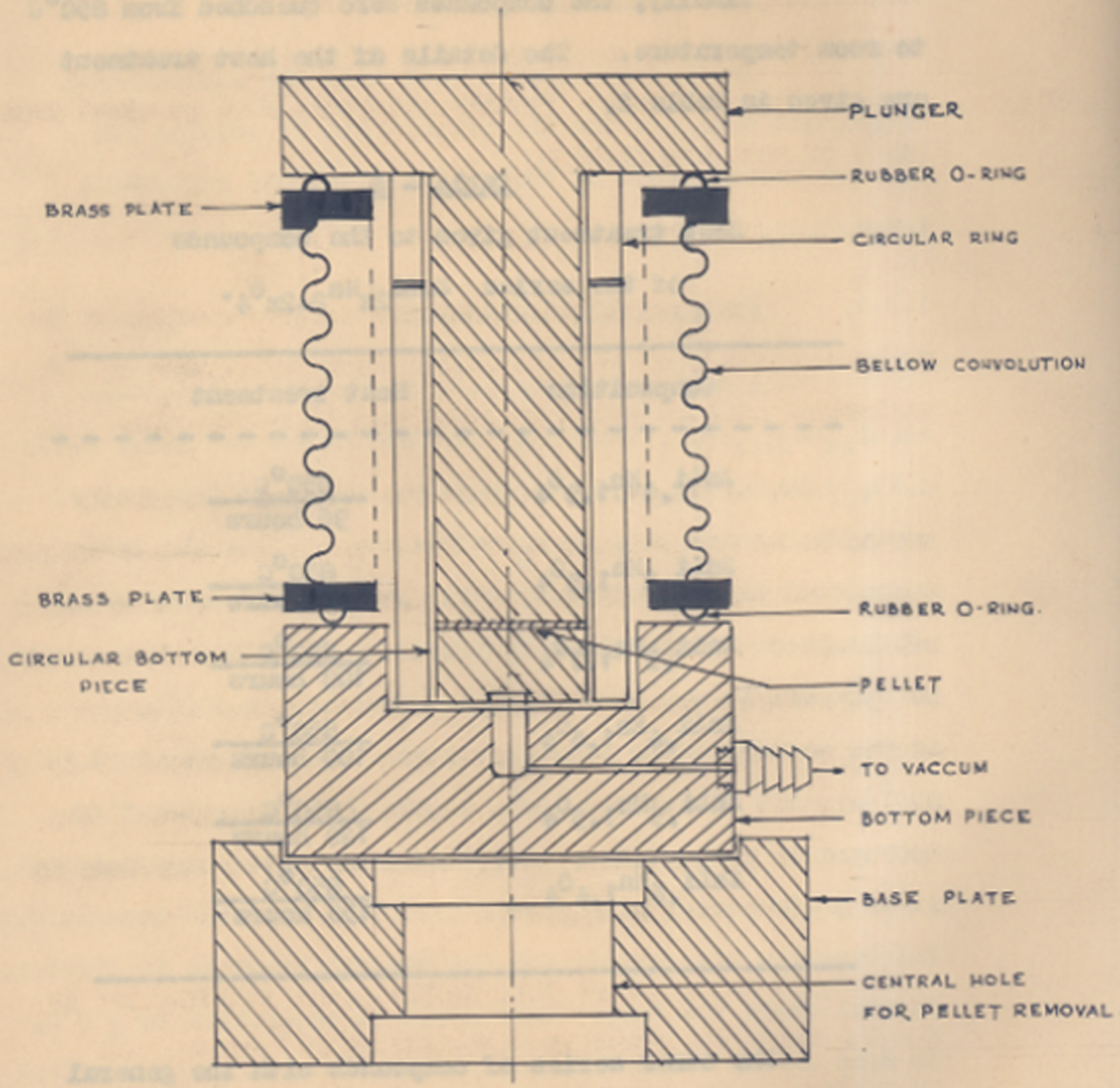

A DIE FOR PRESSING THE PELLET.

FIG-1

The heating was continued till the reaction was complete. This was checked by means of x-ray diffraction patterns, as described earlier. Finally compounds were quenched from 950°C to room temperature.

1.3.2. Preparation of Pellets.

The general procedure for the preparation of the pellets consists of the standard ceramic techniques of powdering, mixing, grinding, moulding, sintering etc.

The compounds of both the systems were finely ground in an automatic grinder for 8 hours and passed through a standard 325 ASTM sieve. The particle size thus obtained was smaller than 44 microns. About 1 cc of 3% solution of the polyvinyl acetate in acetone was then added to about 1 gm. of the powder. The binder used here has been found to be the most convenient for the systems under consideration. The moulding of the compounds along with the binder was done in a die as shown in the Fig. 1.

A pressure of 5000-10,000 p.s.i. was applied to the die and while pressing, a vacuum of 10^{-2} mm Hg. was maintained. The operation was performed on a Carver laboratory press fitted with a calibrated pressure guage.

The pellets were normally of a diameter of 2 cms and the thickness varied from 0.15 to 0.2 cm. The pellets thus obtained were slowly heated in air at 300°C for about

half an hour, when the binder was burnt completely. The temperature of the furnace was then increased gradually to the sintering temperature i.e. 850°C. For the compounds from the first system, x-ray diffraction patterns were obtained after heating at 850°C, 950°C, 1050°C and 1150°C. It was found that the compounds decomposed at 950°C. Wickham and Croft had also made similar observation in case of $Li^{1+}_{1-x}Zn^{2+}_{x}Mn^{3+}_{1+x}Mn^{4+}_{1-x}O_4$. They found that these compounds decompose above 900°C. Hence, the pellets were sintered at 850°C for several hours. Finally, they were quenched to room temperature in air when sintered, crackfree circular pellets were obtained. A careful grinding was carried out to obtain pellets with rectangular cross-section and parallel faces.

1.3.3. Measurement of the electrical conductivity.

The electrical conductivity was studied as a function of temperature. A suitable furnace was constructed for these measurements.

A cavity, where the junction of the thermocouple could conveniently rest, was made on the surface of the opaque silica tube, the diameter of which was 2". One of the junctions of the calibrated chromel-alumel thermocouple was placed in this cavity. An insulating mica sheet was wrapped on this cavity. A standard resistor Kanthal (A_1) wire was wound over this wrapped mica sheet. The whole assembly was

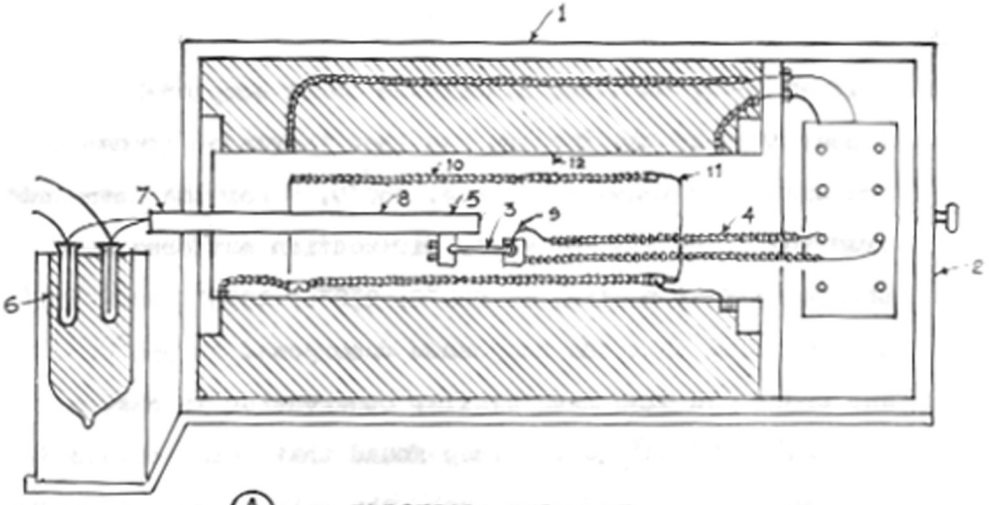

(A) ELECTRIC FURNACE

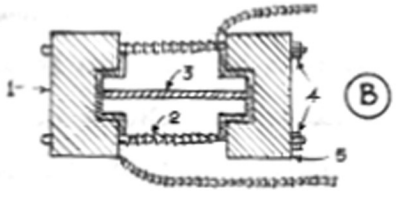

(B)

SAMPLE HOLDER ASSEMBLY

(A)

1 - FURNACE BOX
2 - FURNACE DOORS
3 - SAMPLE HOLDER ASSEMBLY
4 - PLATINUM WIRE LEADS
5 - Pt/Pt-Rh THERMOCOUPLE MESURING JUNCTION
6 - Pt/Pt-Rh THERMOCOUPLE REFERENCE JUNCTION.
7 - CERAMIC THERMOCOUPLE SHEATH.
8 - SILICA " "
9 - PELLET.
10 - REGISTOR WIRE WINDING.
11 - INNER SILICA TUBE.
12 - OUTER " "

(B)

1 - PLATINUM FOIL
2 - CERAMIC INSULATING BEADS
3 - PELLET
4 - NUT BOLT ASSEMBLY FOR PRESSURE CO
5 CERAMIC BASE.

FIG - 2

fixed up in a box made up of asbestos cement sheets. The thermocouple introduced here was connected to a small automatic controller (Hartmann and Braun, chopper bar type) which was in series with the variac (8 amps. 220-270 volts) in a primary of a 5 KVA power transformer 220/110-55 V. The variac, along with the controller was used to control the heating of the furnace. The furnace was thermally well-insulated by suitable lagging. Suitable arrangements were done to take out the electrical leads from the furnace to the conductivity bridge. From one end of the furnace, another calibrated chromel-alumel thermocouple covered with a protective silica sheath was introduced in such a way that the measuring junction of the thermocouple was at the centre of the furnace, while the pellet in the sample holder assembly was introduced from the other end of the furnace as shown in Fig. 2. The temperature was fairly uniform at the centre of the furnace where the sample holder assembly was placed.

A 'PYE' type portable potentiometer was used to measure the thermocouple e.m.f. The potential of 10 μV to 17V could be read with this potentiometer. Accuracy in this measurement was ± 0.1%.

A thin layer of platinum paste (supplied by Johnson Mathey and Co. No.758) was coated on the two end faces of each pellet. An electrically conducting, chemically inert coating was thus formed.

FIG. 2 : Jone's Conductivity Bridge.

The pellet having electrically conducting faces was then pressed in a ceramic sample-holder as shown in Fig. 2. The ceramic sample-holder consisted of a pair of ceramic clits with an adjustable nut-bolt assembly. The platinum foil electrical assembly was set in between. 2 mm diameter platinum wires, insulated with porcelain beads, served as leads. The assembly was found to withstand temperatures upto 750°C indefinitely, and for short periods upto 1000°C.

Resistances of the order of 10^{-3} to 10^{8} ohms (D.C. or A.C. at frequencies 500-2000 cycles/sec) were measured with a Leeds and Northrup precision Jone's conductivity bridge. (Fig. 3). The A.C. or D.C. measurements in the range of 10^{-3} to 60,000 could be directly measured on the bridge. The higher resistances i.e. resistances of the order of 6×10^{4} to 1×10^{8} ohms were measured by shunting a standard resistance of 30,000 ohms from the bridge circuit across the unknown one. However, the accuracy of the bridge drops down for these higher order resistances. Generally, A.C. measurements at a frequency of 500 cycles/sec. were done.

The conductivity has been measured at various temperatures from room temperature upto 300°C. The temperature of the furnace was gradually increased by varying the voltage supply through the variac. At each setting of the variac the temperature was allowed to reach a steady value. The resistance of the pellet was measured at that temperature. A set of different values of resistances at different temperatures was thus obtained.

If Wilson's law is obeyed, the conductivity of these specimens should be given by a simple relation

$$\sigma = \sigma_0 \exp\left(-\frac{\Delta E}{KT}\right)$$

or $$\rho = \rho_0 \exp\left(+\frac{\Delta E}{KT}\right)$$

$$\log \rho = \log \rho_0 + \frac{\Delta E}{KT}$$

where σ = specific conductivity;

ρ = specific resistivity;

ΔE = the thermal activation energy;

K = Boltzmann's constant;

T = Absolute temperature in ^{o}K.

Graphs of $\log_{10}\rho$ as a function of $\frac{1}{T}$ were therefore plotted in all cases. The slope of the graph $\log_{10}\rho$ vs. $\frac{1}{T}$ was specified in electron volts (eV). Further, the plots of the activation energy vs. the composition and the $\log_{10}\rho$ at 28°C vs. the composition were also obtained.

1.3.4. <u>X-ray examination</u>.

The x-ray powder diffraction technique was employed to check the completion of the reaction and to determine the crystal structure of the compounds formed. The samples were filled in thin glass capillaries and Debye-Scherrer patterns were taken on a Philips x-ray machine using Mo-K_α radiation ($\lambda = 0.709$ Å) filtered through a zirconium foil, in a 14 cm camera. The d values were obtained from the

powder diffraction data in the usual way and the lattice parameters were calculated from the observed 'd' values. The cubic and tetragonal patterns were indexed with the help of the standard charts. The cation distribution was determined by visually estimating the intensities of different diffraction lines and comparing them with those calculated for different cation distribution. The details of these calculations are given later.

1.3.5. Chemical analysis.

The compounds of the system $Zn[LiMn]_2O_4$ were analysed for the amount of Li^{1+} and Mn^{4+} ions. A flame photometric method was used for the quantitative estimation of lithium. A Lange flame photometer model 6 operating on petrol gas, and air at a pressure of 0.6 atmosphere was employed. A calibration curve for lithium concentration in p.p.m. was obtained by means of standard solutions of Li_2CO_3 containing 100, 80, 60, 40, 20 and 10 mgs of Li/litre. The compounds under investigation were taken in such a way that the approximate concentration of lithium in solution was in the range of 2 to 20 p.p.m. of lithium ion. A weighed amount of compound was leached with water. The residue was filtered out. The filtrate was boiled to concentrate and tested for the presence of the Li by the flame photometer. The filtrate did not give any indication of the presence of lithium. This clearly showed that all the lithium had entered the spinel structure and no free lithium salt was

present. The residue was very carefully dissolved in hydrochloric acid. A known volume of the solution was prepared. The amount of lithium in mg/L was then determined for the compounds under investigation by making use of the calibration curve.

The amount of Mn^{4+} ions formed due to the presence of Li^{1+} ions was determined by reduction with oxalic acid.

A known excess of standard oxalic acid, in the presence of H_2SO_4 was added to a weighed amount of the compound. Mn^{3+} and Mn^{4+} ions present in the solid were reduced to Mn^{2+} by the oxalic acid. The unreacted oxalic acid was then back-titrated with standard $KMnO_4$ solution.

In the compound $ZnLi_{2x}Mn_{2-2x}O_y$, let 'a' be the number of Mn^{4+} ions. The oxygen absorbed from the atmosphere during the formation of the compound would be equal to a/2 and the molecular formula for the compound becomes :

$$Zn[Li_{2x}Mn^{3+}_{(2-2x-a)}\ Mn^{4+}_{a}]\ O_{(4-2x+a/2)}$$

Here, Mn^{3+} ion is capable of taking up 1 electron to become stable divalent manganese, while Mn^{4+} is capable of taking up two electrons to become divalent. Hence, one gram mole of the above compound will react with $[2-2x-a]+2a = 2-2x+a$ gm. equivalents of oxalic acid. Knowing the amount of oxalic acid reacted, the value of 'a' could easily be determined as the value of x was already known for the different compounds.

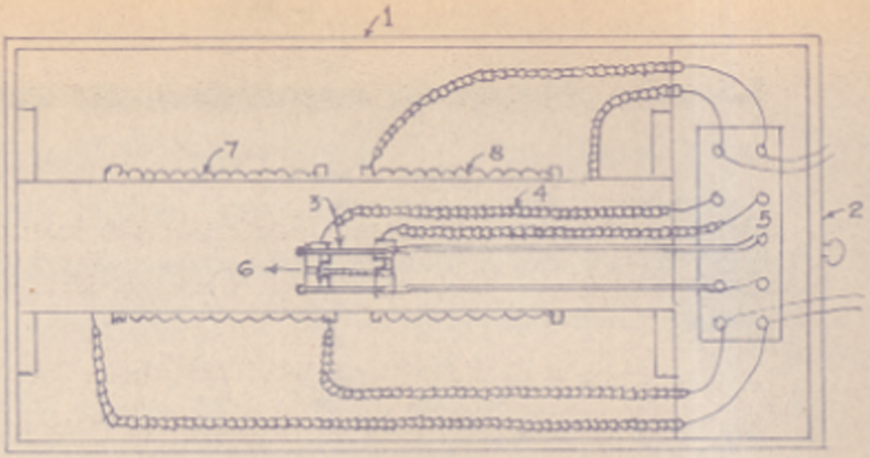

FIG. 4

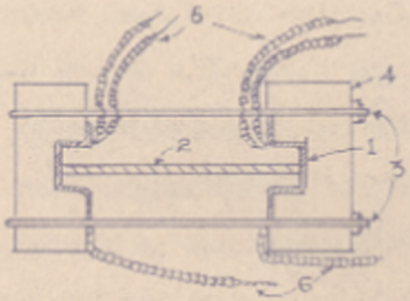

FIG. 4 A

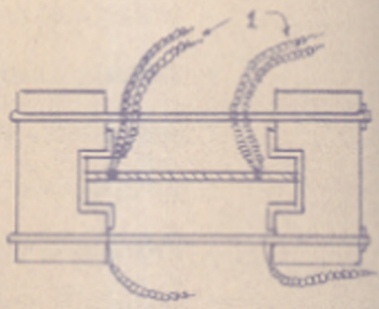

FIG. 4 B

FIG. 4

1 FURNACE BOX

2 FURNACE DOORS

3 SAMPLE HOLDER ASSEMBLY

4 PLATINUM WIRE LEADS

5 TWO CHROMEL-ALUMEL-THERMOCOUPLES.

6 PELLET

7 FURNACE WINDINGS

8 — do —

FIG. 4 A.

1 PLATINUM FOIL

2 PELLET

3 NUTBOLT ASSEMBLY FOR PRESS CONTACT.

4 CERAMIC BASE

5 THERMO COUPLES SOLDERED TO PLATINUM FOILS.

6 PLATINUM WIRE LEADS.

FIG. 4 B.

1 THERMOCOUPLES INSERT IN THE HOLES DRILLED THE PELLET.

FIG. 4 FURNACES AND THE SAMPLE HOLDER ASSEMBLY FOR THE THERMOELECTRIC COEFICIENT MEASUREMENT.

1.3.6. Thermoelectric coefficient measurements.

It is known that a potential difference arises when the two ends of a semiconductor are held at different temperatures. This e.m.f. is known as thermoelectric e.m.f.

An apparatus of the following description was designed and constructed to measure the thermo e.m.f. of our samples at various temperatures. Two electric furnaces of the type shown in Fig. 4 were made by winding standard resistor Kanthal (A_1) wire over a 2" diameter opaque silica tube. Both furnaces were wound on the same silica tube and a gap of $\frac{1}{4}$" was kept between the two. The silica tube was placed in a box made up of asbestos cement sheets. The furnace was thermally insulated by packing the box with magnesia asbestos powder. One end of the silica tube was closed and the sample holder assembly was introduced from the other end. The heating of the furnace was controlled by introducing a variac (rated for 8 amps, 220-270 volts). Stabilised voltage supply was fed to the variac through A.C. voltage stabiliser with input 180-250 V, output 230 V, stability ± 1%, 500 watt.

The temperature profile in the furnace was determined and it was observed that the temperature was remaining fairly uniform (± 0.5°C) in the gap of $\frac{1}{4}$" between the two furnaces (Fig. 4). By adjusting the voltage supply it was possible to obtain a temperature difference of

20-50°C between the two ends of the sample placed in the gap.

A sample holder assembly similar to that used for conductivity measurements was also constructed. Silver foils were employed for electrical contacts. The silver wires (2 mm diameter) were fused to the silver foils. These wires were electrically insulated with porcelain beads and were brought out of the furnace for T. e.m.f. measurements.

Temperature measurements were done by two different arrangements. Two small holes, just sufficient to insert thermocouple wires of 28 guage, were drilled near the two ends of the sample as shown in figure 4B. Two calibrated chromel-alumel thermocouples of 28 guage were, then inserted in the holes. These were taken out through the connectors. In the other arrangement, chromel-alumel thermocouples were silver-soldered to the outside ends of the two silver foils as shown in figure 4A. These were then calibrated against a standard thermometer which could read upto 500°C. However, the hole-drilling technique did not work for many of the present samples because they were very soft due to the low sintering temperature used. But in cases such as $CuMn_2O_4$ where both methods worked, the therme e.m.f. got by these two methods always gave practically identical results.

The pellet was pressed in the ceramic sample holder as shown in Fig. 4B. A potentiometer, which read upto 10 microvolts was used to measure thermocouple e.m.f. as well as

thermoelectric e.m.f. The average temperature of the same sample was obtained by taking the mean of the temperatures at the two ends.

The thermoelectric coefficient has been measured at various temperatures ranging from 150°C to 400°C. As the resistivity of the samples of the first system, is of the order of 10^6 ohms, the e.m.f. at lower temperatures could not be measured with the instrument used. Also, the temperature difference was kept at 40-45°C in order to minimise the error in e.m.f. measurement.

+ + + +

1.4. Results.

(A) Zinc-lithium manganites.

Compounds having the general formula $ZnLi_{2x}Mn_{2-2x}O_4$ with x = 0.05, 0.10, 0.15, 0.20, 0.25 and 0.30 were prepared from specpure oxides by the method described earlier.

1.4.1. (i) Chemical composition.

The compounds were analysed for the amount of lithium actually incorporated in the homogeneous phase by the flame photometric method discussed earlier. The results of the analysis are given in Table 3.

Table - 3

Li ion concentrations in zinc-lithium manganites

Compound x	expected Li/gm.mole	observed Li/gm.mole	Probable composition
0.05	.10	.10	$ZnLi_{0.1}Mn_{1.9}O_4$
0.1	.20	.19	$ZnLi_{0.2}Mn_{1.8}O_4$
0.15	.30	.29	$ZnLi_{0.3}Mn_{1.7}O_4$
0.2	.40	.38	$ZnLi_{0.4}Mn_{1.6}O_4$
0.25	.50	.49	$ZnLi_{0.5}Mn_{1.5}O_4$
0.3	.60	.58	$ZnLi_{0.6}Mn_{1.4}O_4$

It can be seen from the above table that nearly the entire

amount of lithium that was initially taken has been incorporated in the zinc lithium manganite. As the difference between the expected value and the observed value is of the order of the experimental errors involved in our measurements, we have rounded the figures and put the probable composition in the last column of Table 3. The amount of Mn^{4+} ions formed was determined by the volumetric method given in the last chapter. The chemical formulae thus determined for the various compounds are given in Table 4.

Table - 4

Chemical formulae for $ZnLi_{2x}Mn_{2-2x}O_4$

Composition	Formula
x = 0.05	$ZnLi_{.1}Mn^{3+}_{1.7}Mn^{4+}_{.2}O_4$
x = 0.10	$ZnLi_{.2}Mn^{3+}_{1.4}Mn^{4+}_{.4}O_4$
x = 0.15	$ZnLi_{.3}Mn^{3+}_{1.1}Mn^{4+}_{.6}O_4$
x = 0.20	$ZnLi_{.4}Mn^{3+}_{.8}Mn^{4+}_{.8}O_4$
x = 0.25	$ZnLi_{.5}Mn^{3+}_{.74}Mn^{4+}_{.76}O_{3.88}$
x = 0.30	$ZnLi_{.6}Mn^{3+}_{.58}Mn^{4+}_{.82}O_{3.81}$

The actual value of the number of oxygen ions, as determined, is within the range $4.00 \pm .02$ for the first four compositions but rounded figures are given because the value $\pm .02$ is within the limits of our experimental error (0.5%).

1.4.2. X-ray Analysis.

As mentioned previously, x-ray diffraction patterns of the compounds under investigation were taken using Mo-K_α radiation on a 14 cm Debye Scherrer camera. From the x-ray diffraction patterns obtained, the 'd' values were computed by the usual method. The unit cell of $ZnLi_{0.6}Mn_{1.4}O_4$, $ZnLi_{0.5}Mn_{1.5}O_4$ and $ZnLi_{0.4}Mn_{1.4}O_4$ was found to be cubic, and hence the cell dimension was easily calculated. In case of $ZnLi_{0.3}Mn_{1.7}O_4$, $ZnLi_{0.2}Mn_{1.8}O_4$ and $ZnLi_{0.1}Mn_{1.9}O_4$, which were found to be tetragonal, the lattice parameters 'c' and 'a' were calculated from the observed 'd' values by the method of successive refinement. First, reflections of the type hko and ool were taken to determine the approximate values of'a' and 'c' respectively. Using these approximate values of 'a' and 'c' refined values of 'a' and 'c' were obtained respectively from the hkl reflections of high h,k and high l. This process of refinement was continued till no further improvement in the calculated values was obtained. From systematic absences of certain reflections it is easy to see that the cubic compounds were isomorphous with the spinels (space group $Fd3m-O_h^7$) and the tetragonal compounds were isomorphous with Mn_3O_4 (space group $I4_1/amd - D_{4h}^{19}$) . The coordinates of the ion-positions were as listed earlier.

For convenience of comparison with true cubic spinel, the tetragonal cells have been converted into bigger

unit cells with $c' = c$ and $a' = a\sqrt{2}$ and the c' and a' parameters have also been given in each table. In tables 5 to 10 the hkl indices, the observed and calculated values of $1/d^2$ and the lattice parameters c, a, c' and a' for all the compounds have been tabulated.

Table - 5

X-ray results for $ZnLi_{.1}Mn_{1.9}O_4$

hkl	obs. intensity	$1/d^2$cal.	$1/d^2$obs.	Lattice parameters
101	-	0.04311	-	$1/c^2 = 0.01191$
112	S	0.11004	0.1105	$1/a^2 = 0.03120$
200	-	0.1248	-	
103	S	0.13839	0.1388	$c = 9.64$ Å
211	VS	0.16791	0.1701	$a = 5.661$ Å
004	-	0.19056	-	$c' = 9.64$ Å
220	M	0.2496	0.2479	$a' = 7.925$ Å
204	-	0.31536	-	$c'/a' = 1.15$
105	W	0.32895	0.3310	
312	VW	0.35964	0.3557	
303	VW	0.38799	0.3855	
321	VW	0.42751	0.4140	
224	M	0.44016	0.4409	
400)		0.49920		
)	M		0.4958	
314)		0.50256		
411	-	0.5423	-	
206	-	0.55356	-	
305	-	0.57855	-	
420	-	0.62400	-	
413		0.63759		

S = Strong; VS = Very strong; M = Medium; W = Weak;
VW = Very weak.

Table - 6

X-ray results for $ZnLi_{.2}Mn_{1.8}O_4$

hkl	obs. intensity	$1/d^2$obs.	$1/d^2$cal.	Lattice parameters
101	-	-	0.04356	c = 9.035 Å
112	S	0.1142	0.11138	a = 5.665 Å
200	-	-	0.1250	$1/c^2$ = 0.01225
103	S	0.1372	0.1414	
211	VS	0.1673	0.1682	$1/a^2$ = 0.03125
004	-	-	0.1960	c' = 9.035 Å
220	M	0.2485	0.24952	a' = 8.007 Å
204	-	-	0.3210	c'/a' = 1.128
105	W	0.3347	0.33744	
312	VW	0.3602	0.3609	
303	VW	0.3864	0.3909	
321	VW	0.4179	0.41772	
224	M	0.4432	0.44552	
400	M	0.5025	0.5000	
314			0.5085	
411	-	-	0.5435	
402	-	-	0.5490	
206	-	-	0.5660	
305	-	-	0.5875	
420	VW	0.6414	0.6256	
413			0.6415	
422	-	-	0.6740	
404	-	-	0.6960	
217	VW	0.7491	0.7535	
316				
008	-	-	0.7839	
431	-	-	0.79475	
501				
424	-	-	0.8210	
415	-	-	0.8375	

Table - 7

X-ray results for $ZnLi_{.5}Mn_{1.7}O_4$

hkl	obs. intensity	$1/d^2$cal.	$1/d^2$obs.	Lattice parameters
101	-	0.4424	-	
112	S	0.11644	0.1151	c = 8.457 Å
200	-	0.12104	-	a = 5.748 Å
103	S	0.15608	0.1580	c'= 8.467 Å
211	VS	0.16528	0.1641	a'= 8.162
004	-	0.22368	-	c'/a' = 1.036
220	M	0.24208	0.2446	
204	W	0.34472	0.3602	
105		0.37936		
312	-		-	
303	-	0.39816	-	
321	W	0.40736	0.4079	
224		0.46571	0.4399	
400	M	0.48416	0.4885	
314		0.52628		
411		0.52840	-	
402	-	0.54008	-	
206	-	0.62444	-	
305	-	0.62184	-	
420	W	0.60520	0.6379	
413		0.64024		

Table - 8

X-ray results for $ZnId_{.4}Mn_{1.6}O_4$

hkl	obs. intensity	$1/d^2$obs.	$1/d^2$cal.	Lattice parameters
111	MW	0·0442	0.04473	
220	MS	0.1164	0.11928	$1/c'^2 = 1/a'^2$
311	S	0.1633	0.16401	$= 0.01491$
400	M	0.2403	0.22856	$c' = a' = 8.19$ Å
331	-	-	0.28629	
422	-	0.3589	0.35784	
511) 333)	S	0.4060	0.4026	
440	S	0·4722	0·4771	
531	-	-	0.5219	
620	-	-	0.5964	
533)	W	0.6397	0.6412	
622)			0.6561	
444	-	-	0.5684	
711) 551)	-	-	0.7605	
642	-	-	0.8351	
731) 553)	W	0.9291	0.8798	
800			0.9545	

Table - 2

X-ray results for $ZnLi_{.5}Mn_{1.5}O_{3.88}$

hkl	obs. intensity	$1/d^2$obs.	$1/d^2$cal.	Lattice parameters
111	VW	0.0444	0.04419	
220	MS	0.1171	0.11784	$1/c'^2 = 1/a'^2$
311	S	0.1633	0.16203	$= 0.01473$
400	M	0.2387	0.23568	
331	-	-	0.2799	$c' = a'$
422	-	0.3557	0.3535	$= 8.242$ Å
511,333	S	0.3963	0.3977	
440	S	0.4664	0.4713	
531	-	-	0.5156	
620	-	-	0.5892	
533	M	0.6291	0.6335	
622			0.6482	
444	-	-	0.7099	
711	-	-	0.7513	
551				
642	-	-	0.8249	
731			0.8692	
553				
	M	0.9289		
800			0.9428	

Table - 10

X-ray results for $ZnLi_{.6}Mn_{1.4}O_{3.81}$

hkl	obs. intensity	$1/d^2$obs.	$1/d^2$cal.	Lattice parameters
111	VW	0.0443	0.04421	
220	MS	0.1143	0.11816	$c' = a' = 8.23$ Å
311	VS	0.1629	0.16247	
400	M	0.2375	0.23632	$1/c'^2 = 1/a'^2$
331	-	-	0.28063	$= 0.01477$
422	MS	0.3573	0.35448	
511,333	S	0.3982	0.39879	
440	S	0.4710	0.47264	
531	-	-	0.5170	
620	-	-	0.59080	
533	M	0.6336	0.6352	
622			0.6486	
444	-	-	0.7089	
711 / 551	-	-	0.7534	
642	-	-	0.8271	
731 / 553	M	0.8628	0.8716	

We now, proceed to determine the distribution of Zn, Li and Mn over tetrahedral and octahedral sites. Since it is difficult to determine the distribution of the three types of ions over the two types of sites from the limited data, we make use of the known sites preference energies. Verwey and Heilmann[44] (1947) have proposed a scheme of cation distribution, which has been further modified by Carter[45] (1954). It can be summarized as follows :

(1) Ions such as Zn^{2+} and Cd^{2+}, Ga^{3+}, Ge^{4+} etc. with filled 3d shells have a tendency to occupy the tetrahedral sites.

(2) The ions Li^{1+}, Mg^{2+}, Al^{3+} and Ti^{4+} which occur in spinels and have a noble gas configuration do not show preference for either coordination.

(3) The ions with half filled 3d shells exhibit spherical symmetry and so they do not possess any individual preference for either of the two positives.

(4) Transition metal ions such as Cr^{3+}, Ni^{2+} or Mn^{4+} with $3d^3$ and $3d^8$ configurations have a marked preference for octahedral positions.

(5) Other transition metals do not have any individual preference.

Recently A.Miller[46] (1959) has extended the calculations of octahedral site preference energy in spinels

to include Madelung, Born's and crystal field terms. He has formulated a set of site preference energies which can be used to predict the ionic distribution of spinels of non-transition as well as transition metal ions.

Table - 11

Octahedral site preference energies for various cations

P - kcal/g. at wt.

Ion	P	Ion	P	Ion	P	Ion	P
Li^{+}	-3.6	Mn^{++}	-14.7	Zn^{++}	-31.6	Cr^{+++}	-16.6
Cu^{+}	-8.6	Fe^{++}	-9.9	Cd^{++}	-29.1	Mn^{+++}	3.1
Ag^{+}	-19.6	Co^{++}	-10.5	Al^{+++}	-2.5	Fe^{+++}	-13.3
Mg^{++}	-5.0	Ni^{++}	9.0	Ti^{+++}	-21.9	Ga^{+++}	-15.4
Ca^{++}	-30.7	Cu^{++}	-0.1	V^{+++}	-11.9	In^{+++}	-40.2

In view of the above results, to start with, we assume that all Mn ions occupy octahedral sites. Both Zn and Li show a preference for tetrahedral sites, however since the total number of these ions is much larger than the available sites, a fraction of them will be forced to occupy the octahedral sites. We, therefore, determine the distribution of these two ions over the octahedral and tetrahedral sites from the x-ray diffraction results.

The distribution can be represented by the formula

$$Zn_{1-\alpha}Li_{\alpha}\,[Li_{2x-\alpha}Mn_{2-2x}Zn_{\alpha}]\,O_4$$

It is now, left to determine the value of α in order to know the cation distribution.

Different values ranging from 0 to 0.1 were given to α . Reflections 220, 400 and 422 were found to be fairly sensitive to the cation distribution. Reflection intensities for these reflections were calculated by using the formula

$$I_{hkl} \propto |F|^2 \times p \times \frac{1 + \cos^2\theta}{\cos\theta \sin^2\theta}$$

where $|F|$ denotes the structure factor, p the multiplicity factor and the remaining part comprises the combined Lorentz and polarisation factors. Corrections for the absorption and thermal vibrations were not applied. The structure factor $|F|$ for each of the reflections was calculated using the ionic scattering power of these different ions ($f_{Zn^{2+}}$, $f_{Mn^{*}}$, $f_{Li^{1+}}$, $f_{O^{2-}}$) at different locations in the lattice. The ionic scattering factor 'f' for the different ions was computed from the values given in the 'International Tables for the determination of crystal structures' Vol.II, 1935.

$f_{Mn^{*}}$ is the weighted average of the scattering powers of Mn^{3+} and Mn^{4+}.

The average scattering powers of ions at tetrahedral site (f_A) and those at octahedral site (f_B) are :

$$f_A = (1-a)\, f_{Zn^{2+}} + a f_{Li^{1+}}$$

$$f_B = \frac{(2x-a) f_{Li^{1+}} + (2-2x) f_{Mn^{3+}} + a f_{Zn^{2+}}}{2}$$

The oxygen parameter was arbitrarily fixed as $u = 0.375$. This was refined later. An arbitrary index of 100 was assigned to the strongest reflection and the reflection intensity values for the others were assigned visually, with reference to the strongest as 100. The ratios of the intensities of reflections I_{220}/I_{422} , I_{422}/I_{400} were obtained. The value of 'a' was then fixed by comparing the calculated ratios of reflection intensities with the observed ones.

Having fixed the value of 'a', we now proceed to determine the value of the oxygen ion parameter 'u'. We see that the reflection most sensitive to changes in 'u' is 111. We calculate the I_{111} as a function of 'u' for the value of 'a' determined earlier. The value of 'u' at which the intensity had the best match was selected. Now, making use of this value of 'u' we redetermine the intensities for 220, 400 and 422 reflections for the different values of 'a', following the above described procedure. This process of repeated refinement was continued till the values of 'u' and 'a' showed no further improvement. The reflection

intensities were then calculated for all the reflections upto 731, 553. This procedure was followed for the three compositions which possess the cubic structure. The calculated and observed intensities are shown in Table 12, 13, 14. It can be seen that the agreement is good.

Table - 12

Observed and calculated reflection intensities for $ZnLi_{.4}Mn_{1.6}O_4$

hkl	$I_{obs.}$	$I_{cal.}$
111	5	2.13
220	45	45.68
311	100	100
222	-	3.8
400	15	14.79
331	-	< 1
422	15	15.12
511,333	40	38.8
440	55	54.19
531	-	< 1
442	-	< 1
620	-	6.36
533	15	16.3
622	-	3.55
444	-	2.01
711,551	-	< 1
642	-	< 1
731,553	10	11.28)
		)
		8.29)

Table - 13

Observed and calculated intensities

for $ZnLi_{.5}Mn_{1.5}O_{3.88}$

hkl	$I_{obs.}$	$I_{cal.}$
111	5	3.76
220	55	55.77
311	100	100
222	-	< 3
400	12	12.68
331	-	< 1
422	15	13.98
511,333	45	44.63
440	50	50.39
531	-	< 1
442	-	< 1
620	-	< 3
533	12	12.74
622	-	4.1
444	-	< 3
711,551	-	< 1
642	-	< 1
731,555	10	6.8 7.9

Table - 14

Observed and calculated intensities

for $ZnLi_{.6}Mn_{1.4}O_{3.81}$

hkl	$I_{obs.}$	$I_{cal.}$
111	5	2.96
220	50	52.04
311	100	100
222	-	1.92
400	15	14.58
331	-	1.836
422	20	17.88
511,333	50	49
440	60	59.46
531	-	<1
442	-	<1
620	-	5
533	12	13.79
622	-	3.8
444	-	1.928
711,551	-	<1
642	-	<1
731,553	12	11
		10

We find that most of the Zn^{2+} ions occupy tetrahedral sites and the Li^{++} ions the octahedral sites. Table 15 gives the cation distribution (last column) together with the crystallographic parameters for the three cubic phases.

Table - 15

Structural data for the cubic zinc-lithium manganites

Comp.	a	u	a	Me-O oct. A^o	Radius of oct. hole	Me-O tet. A^o	Radius of tet. hole	Formula
x=0.3	0.091	0.389	8.23	1.95	0.63	1.99	0.67	$Zn_{.91}Li_{.09}[Li^{1+}_{.51}Mn^{3+}_{.58}Mn^{4+}_{.82}Zn^{2+}_{.09}]O_{3.81}$
x=0.25	0.06	0.392	8.24	1.93	0.61	2.026	0.706	$Zn_{.94}Li_{.06}[Li^{1+}_{.44}Mn^{3+}_{.74}Mn^{4+}_{.76}Zn^{2+}_{.06}]O_{3.88}$
x=0.2	0.075	0.383	8.19	1.985	0.665	1.887	0.56	$Zn_{.925}Li_{.015}[Li^{1+}_{.325}Mn^{3+}_{.8}Mn^{4+}_{.8}Zn^{2+}_{.075}]O_4$

Although the cation distribution in the tetragonal phases has not been determined, it is reasonable to expect that similar distribution is present in these phases also. Moreover, we are primarily interested in the concentration of Mn^{3+} and Mn^{4+} ions at the octahedral sites. As has already been shown it appears almost definite that they are present exclusively at the octahedral sites. Therefore the concentration of Mn^{3+} and Mn^{4+} at the octahedral sites are as presented in Table 16.

Table - 16

The concentration of cations at octahedral sites in $ZnLi_{2x}Mn_{2-2x}O_4$.

x	Mn^{3+}	Mn^{4+}	Other ions (Li^{1+} + Zn^{2+})
.05	1.7	.2	.1
.10	1.4	.4	.2
.15	1.1	.6	.3
.20	.8	.8	.4
.25	.74	.76	.5
.30	.58	.82	.6

This conclusion is also supported by their structures. The manganites have tetragonal structure due to the presence of Mn^{3+} ions at the octahedral sites. The electronic levels of octahedrally coordinated Mn^{3+} split into a lower triplet (t_{2g}) and an upper doublet (e_g).

In weak crystal fields the fourth electron of the Mn^{3+} ion occupies the e_g levels. This configuration is doubly degenerate and is unstable as has been shown by Jahn and Teller. The octahedron around the Mn^{3+} ion therefore distorts to a tetragonal symmetry. If the crystal contains a large number of such distorted octahedra, there is a cooperative interaction and the crystal shows a tetragonal symmetry. However, when the Mn^{3+} ions are replaced by non-disterting cations, the distortion decreases and is absent below a certain critical concentration of Mn^{3+} ions[23,27]. This dependence of distortion on concentration is more or less independent of the nature of the non-distorting ions as has been found for many manganite systems. This known behaviour of manganites can be used to determine, indirectly the number of Mn^{3+} ions at the octahedral sites in the tetragonal systems. This seems to match with what has been given in Table 16.

1.4.3. Electrical conductivity

The compounds under investigation were sintered into pellets by the method described earlier. The apparent densities were calculated from the weight and the dimensions of the pellet and x-ray densities derived from the observed lattice parameters. The ratio $D_{app.}/D_{x\text{-}ray}$ ranges from 0.76-0.80 (see Table 17) indicating the total pore volume to be of the order of 20-25%.

FIG. 5 VARIATION OF SPECIFIC RESISTIVITY AS A FUNCTION OF THE RECIPROCAL OF THE TEMPERATURE FOR THE SYSTEM ZINC LITHIUM MANGANITE

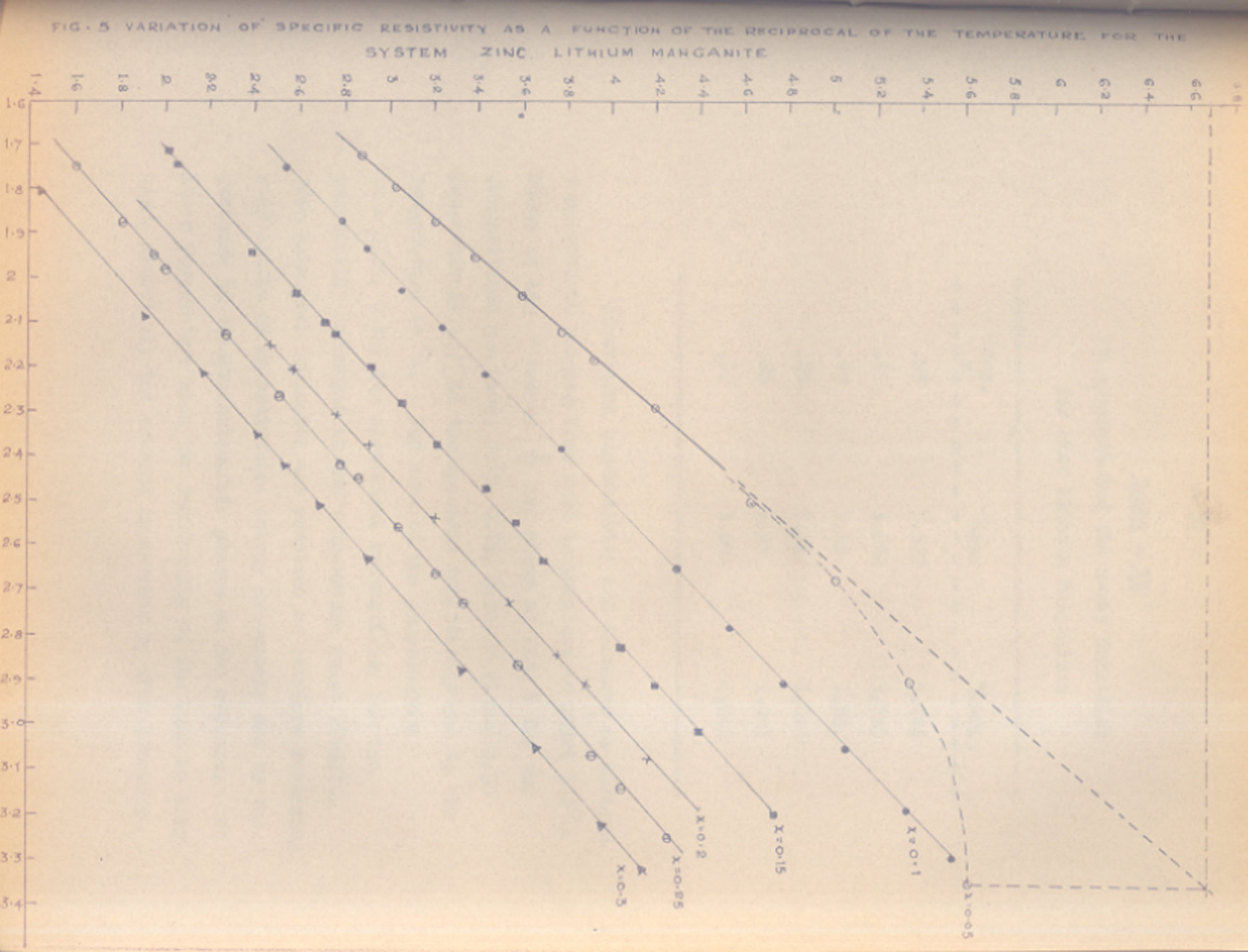

Table - 17

An apparent and the x-ray densities for zinc lithium manganites

Comp. x	$D_{app.}$	D_{x-ray}
.05	3.528	5.144
.10	3.566	5.165
.15	3.66	5.300
.20	3.99	5.320
.25	3.98	5.067
.30	3.89	4.943

Electrical conductivity was measured at various temperatures ranging from room temperature to about 350°C. Plots of log ρ versus $\frac{1}{T}$ are shown in Fig. 5 for the compositions x = 0.05, 0.10, 0.15, 0.20, 0.25 and 0.30 respectively. ρ is the specific resistivity and T, the temperature in °K. For some of the compositions (x = 0.05, 0.10) the electrical conductivity remains practically unchanged in the temperature range 27-50°C. Such behaviour indicates the presence of carriers requiring very little or no activation energy presumably due to the presence of non-stoichiometric phases on the surface. At lower temperature when the resistivity of the bulk is very high, almost all the current is carried by free carriers

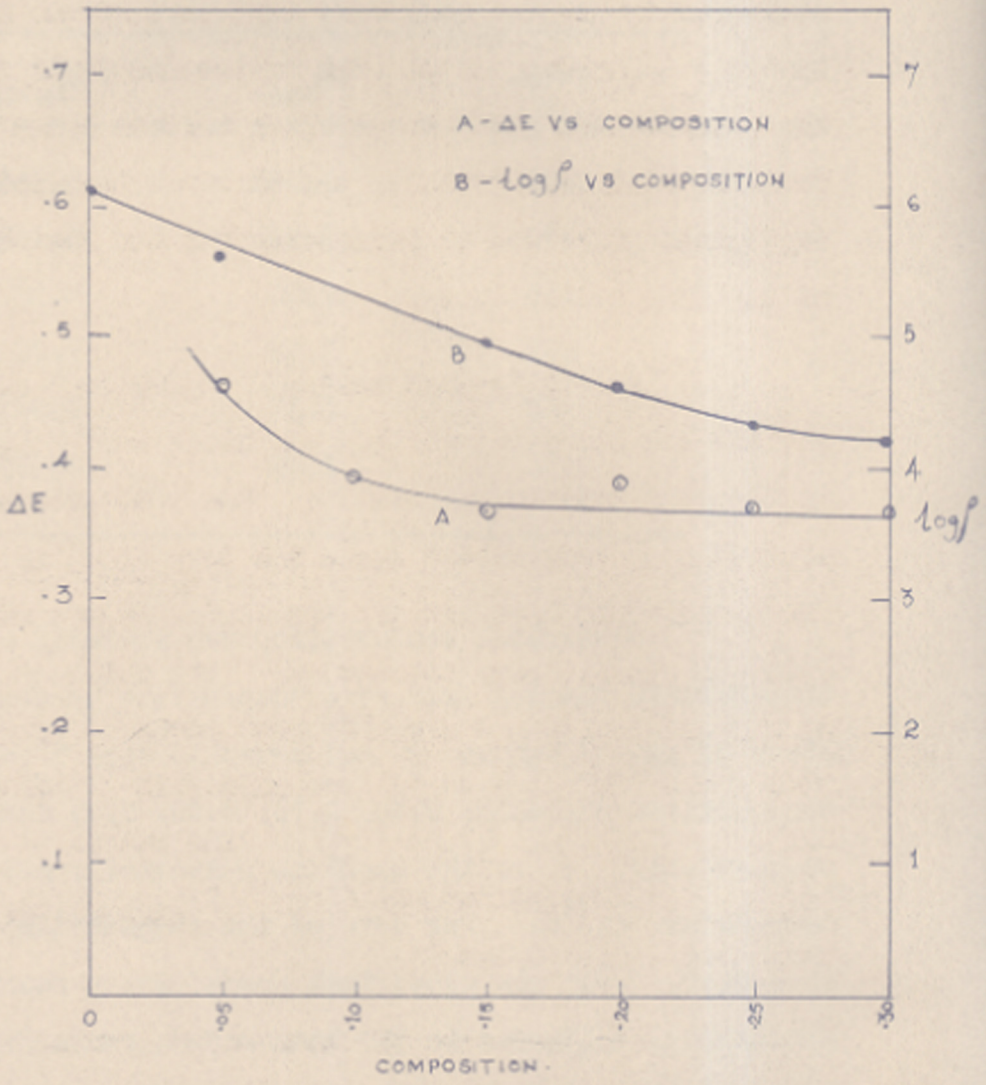

FIG- 6 VARIATION OF ΔE AND LOG ρ AS A FUNCTION OF COMPOSITION.

on the surface. Therefore there is no variation in the conductivity with temperature. At higher temperatures the conductivity of the bulk semiconductor rises. When this conductivity becomes much more than that of the surface, the true behaviour of the bulk semiconductor is noticed. The contribution from the parallel surface conductors being small at high temperatures, the observed temperature dependence would not be different from the true behaviour of the bulk semiconductor.

The activation energy ΔE has been obtained for all the compositions from the slope of the linear plot in the high temperature region. The extrapolation of this plot to room temperature gives the true value of $\log \rho$ which one would have got for the semiconductor if the spurious conductivity was absent. The value of $\log \rho_o$ at $T = \infty$ i.e. $\frac{1}{T} = 0$ has also been obtained by extrapolation. This gives the value of the pre-exponential factor in the Wilson's law $\rho = \rho_o \exp. \frac{\Delta E}{kT}$. The values of ΔE, $\log (\rho_{RT})$ extrapolated and $(\log \rho_o)_{\text{extrapolated}}$ have been tabulated in the table 18.

The variation of these parameters as a function of composition has been plotted in Fig. 6.

Table - 18

Conductivity results for $ZnLi_{2x}Mn_{2-2x}O_4$

Composition x	$\log(\rho_{RT})_{obs.}$	ΔE (eV)	$\log(\rho_{RT})_{ext.}$	$\log(\rho_o)_{ext.}$
0.05	5.6119	0.46	6.710	$\bar{2}.8500$
0.10	5.5254	0.39	5.5254	$\bar{1}.120$
0.15	4.9263	0.365	4.9263	$\bar{2}.820$
0.20	4.5915	0.389	4.5915	$\bar{2}.510$
0.25	4.3060	0.368	4.3060	$\bar{2}.460$
0.3	4.1528	0.364	4.1528	$\bar{2}.180$

1.4.4. Thermoelectric coefficient.

Thermoelectric coefficients were measured at different temperatures in the temperature range 250-400°C. As the specific resistances of the samples are quite high i.e. of the order of 10^5 ohms, e.m.f. imbalance of 1 mv in our circuit would give a current of the order of 10^{-11} amps. The galvanometer was not sensitive enough to detect this small current and hence thermo-e.m.f.s could not be measured. It was possible to get reliable values only at high temperatures when the specific resistivity fell down to a few hundred ohms. The values of thermoelectric coefficients S, and ST are given in Tables 19 to 24 for compositions x = 0.05, 0.10, 0.15, 0.20, 0.25 and 0.30. The positive sign indicates that the cold end

was positive with respect to the hot end and vice-versa for the negative sign. Plots of thermoelectric coefficients and ST for different compositions are shown in figs. 7 to 12.

Table - 19

Thermoelectric coefficients of $ZnLi_{.1}Mn_{1.9}O_4$

(Type of conduction : p-type)

t_1^oC	t_2^oC	T^oK	E e.m.f. in micro-volts	S microvolts /degree	ST volts per degree x temp. ^oK
320	275	570.5	1500	33.3	0.019
330	280	578	1720	34.4	0.01988
344	298	594	1700	37	0.02198
356	302	602	1900	34.6	0.02104
363	314	611.5	1900	38.7	0.02367
376	326	624	1800	36	0.02247
382	326	627	2000	35.7	0.02239
382	335	631.5	1800	38.2	0.02412
388	342	638	1850	40.2	0.02564
402	350	649	2100	40.0	0.02596
446	390	691	2310	41.25	0.0285
454	400	700	2300	42.6	0.0298

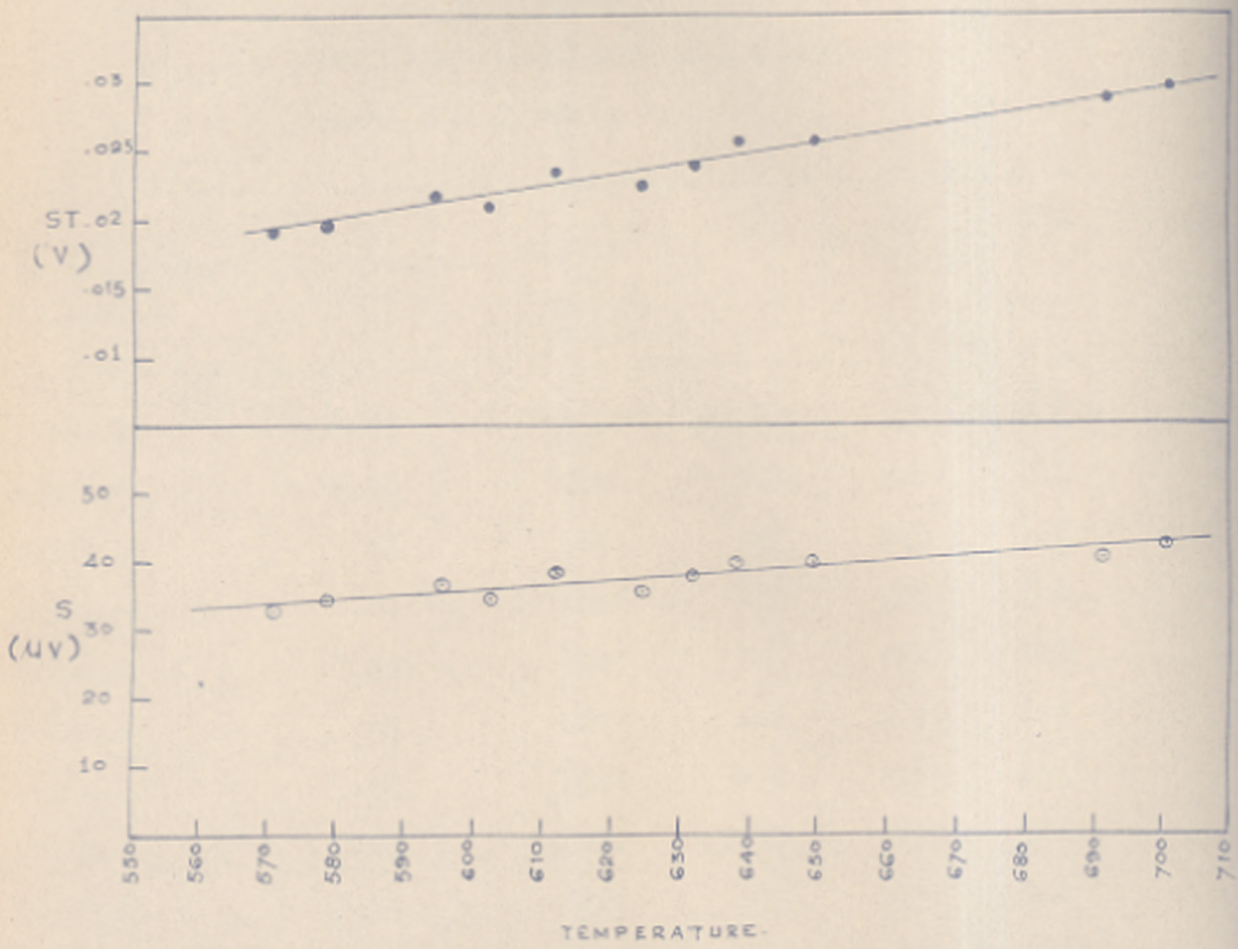

FIG-7 VARIATION OF S AND ST AS A FUNCTION OF TEMPERATURE FOR Zn Li-I $Mn_{1.9}O_4$

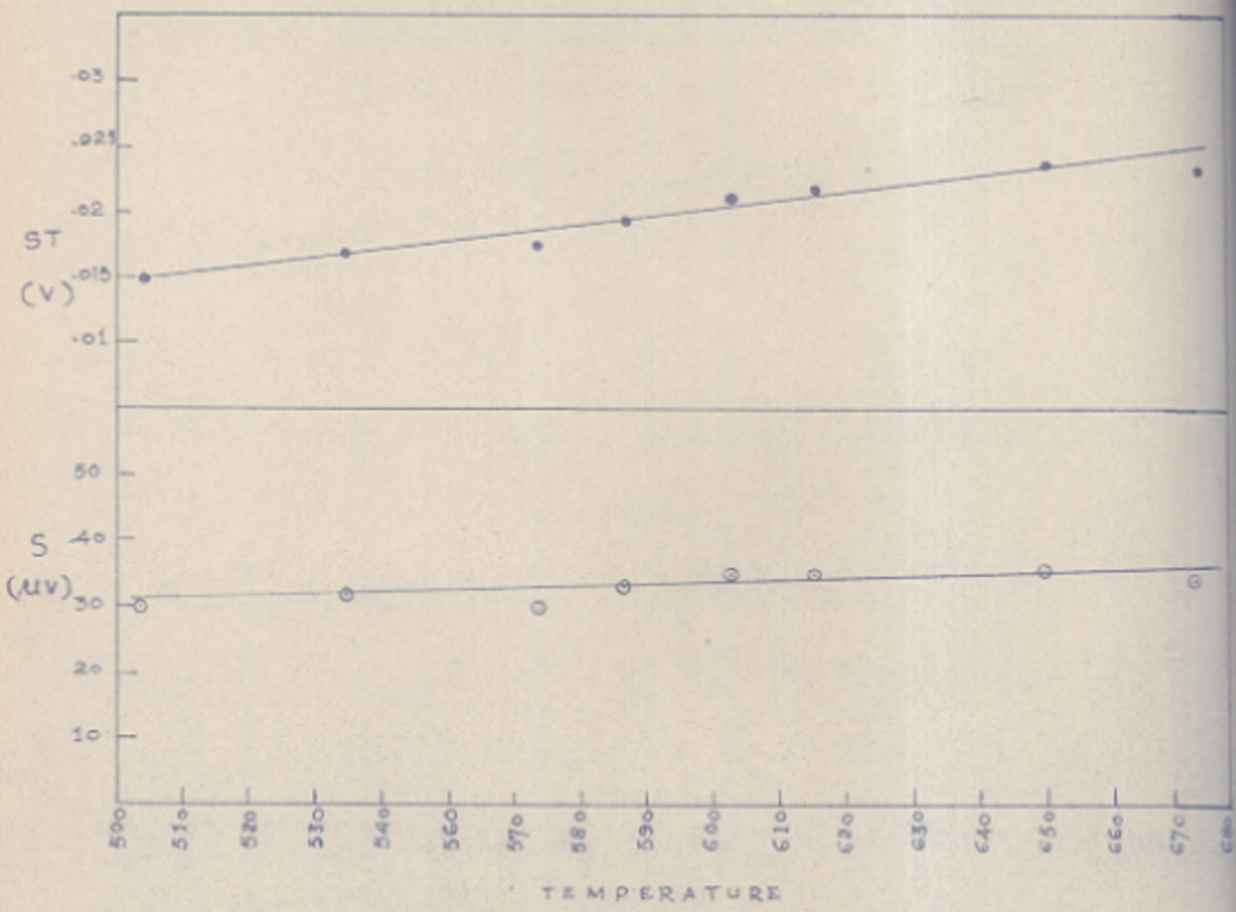

FIG. 8 VARIATION OF S AND ST AS A FUNCTION OF TEMPERATURE FOR $Zn\,Li_{.2}\,Mn_{1.8}O_4$

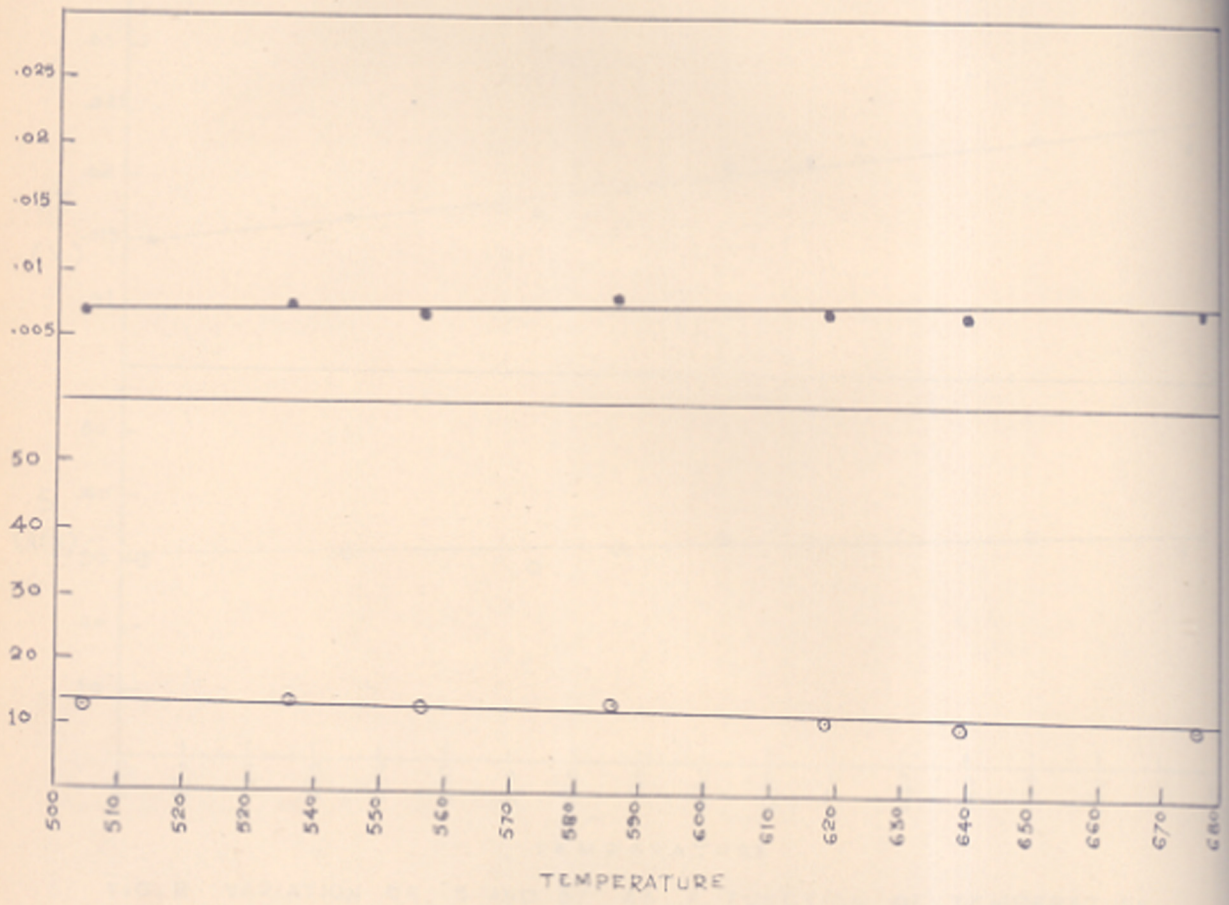

FIG. 9 - VARIATION OF S AND ST AS A FUNCTION OF TEMERATURE FOR $Zn\,Li_{.3}\,Mn_{1.7}O_4$

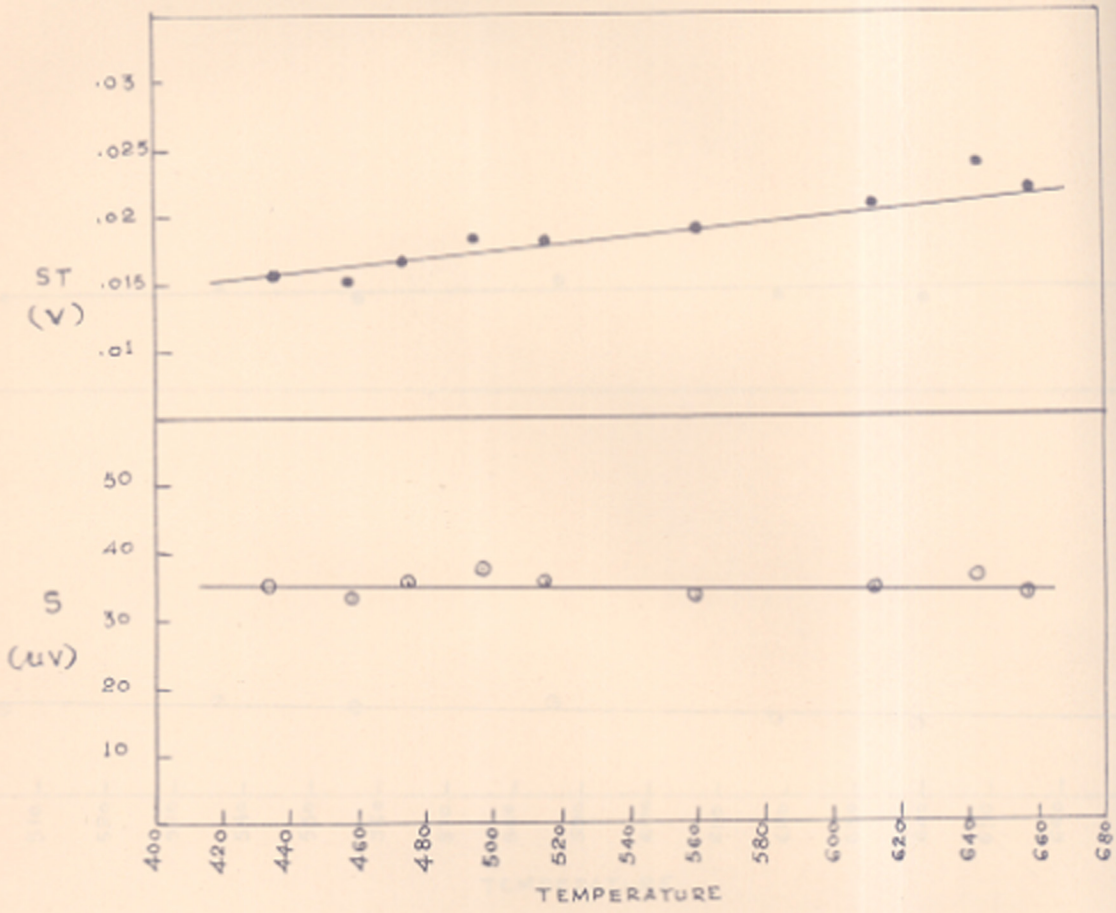

FIG. 10 VARIATION OF S AND ST AS A FUNCTION OF TEMERATURE FOR Zn Li.4 Mn 1.604

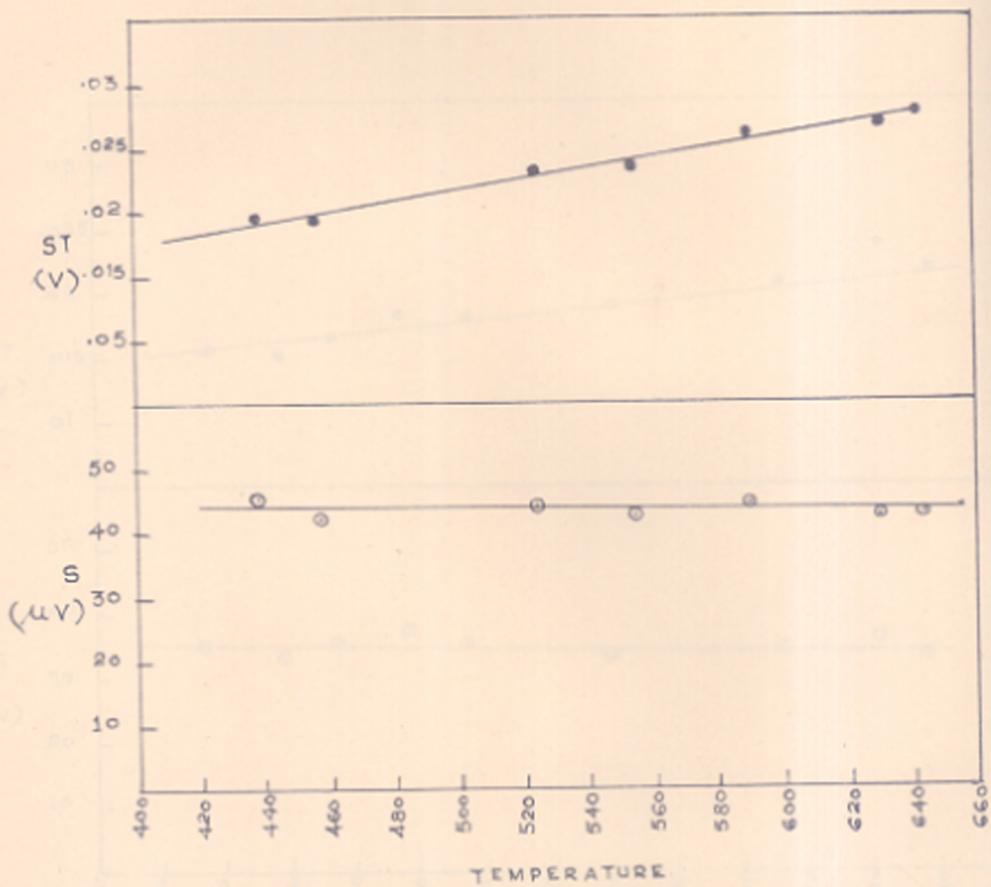

FIG. 11 VARIATION OF S AND ST AS A FUNCTION OF TEMPERATURE FOR Zn Li.5 Mn 1.5 O4.

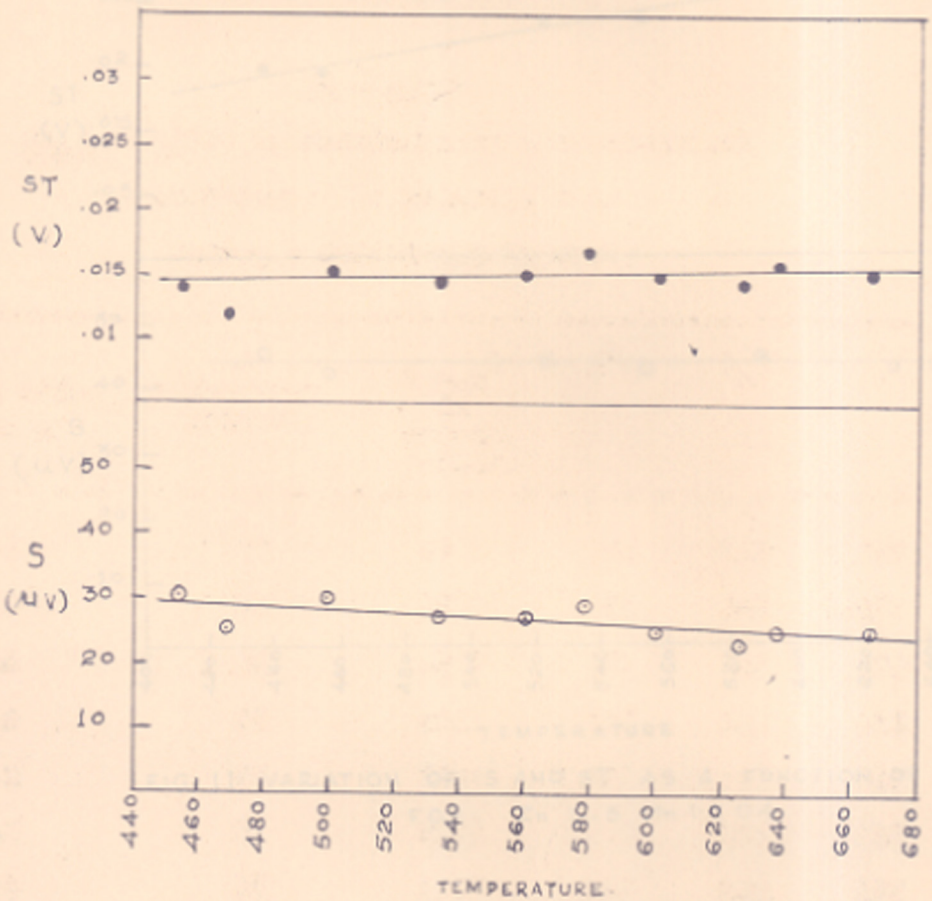

FIG. 12 VARIATION OF S AND ST AS A FUNCTION OF TEMPERATURE FOR $ZnLi_{.6}Mn_{1.4}O_4$

Table - 20

Thermoelectric coefficients of $ZnLi_{.2}Mn_{1.8}O_4$ as a function of temperature.

(Type of conduction : p-type)

t_1^oC	t_2^oC	T^oK	$T_{e.m.f.}$ in micro-volts	S microvolts /degree	ST volts per degree x temp.^oK
250	212	504	1140	30	0.01512
279.5	244	534.7	1135	32	0.01711
320	282	574	1150	30.3	0.01739
334	294	587	1320	33	0.01936
348	311.5	602.7	1280	35	0.02110
360	325	615.5	1225	35	0.02155
392	362	650	1080	36	0.02340
415	387	674	955	34	0.02292

Table - 21

Thermoelectric coefficients of $ZnLi_{.5}Mn_{1.7}O_4$
as a function of temperature
(Type of conduction : n-type)

t_1^oC	t_2^oC	T^oK	$E_{e.m.f.}$ in micro-volts	S microvolts /degree	ST volts per degree x temp.^oK
250	212	504	500	13.4	0.006753
282	244	536	510	13.66	0.007321
303	263	556	520	13.0	0.007228
325	290	585.5	500	14.3	0.008373
368	322	618	560	12.0	0.007416
396	356	639	440	11.0	0.007030
426	381	676.5	525	11.6	0.007847

Table - 22

Thermoelectric coefficients of $ZnNi_{.4}Mn_{1.6}O_4$ as a function of temperature

(Type of conduction : n-type)

t_1^oC	t_2^oC	T^oK	$T_{e.m.f.}$ in micro-volts	S microvolts /degree	ST volts per degree x temp.^oK
177	145	434	1120	35	0.01519
198	170	457	925	33	0.01508
212.2	187.2	472.7	1225	35	0.01654
240	202	494	1400	37	0.01828
267	235	514	1110	35	0.01799
303.5	268	558.7	1170	33	0.01844
355	321	611	1150	34	0.02077
378.4	358	641.2	1095	36	0.02372
402	367	656.5	1150	33	0.02166

Table - 23

Thermoelectric coefficients of $ZnIn_{.5}Mn_{1.5}O_4$
as a function of temperature
(Type of conduction : n-type)

t_1^oC	t_2^oC	T^oK	$\mathcal{E}$ e.m.f. in micro-volts	S microvolts /degree	ST volts per degree x temp.^oK
177.5	148.2	436	1300	44.36	0.01934
199.2	165.8	455.5	1400	41.92	0.01910
268	232.8	523.4	1540	43.75	0.02290
271	248	532.5	1040	45	0.02396
300	260	553	1680	42	0.02322
327.5	304.5	589	1000	43.5	0.02563
368	345	629.5	970	42	0.02643
380	356	641	1020	42.5	0.02725

Table - 24

Thermoelectric coefficients of $ZnLi_{.6}Mn_{1.4}O_4$ as a function of temperature

(Type of conduction : n-type)

$t^{\circ}C_1$	$t^{\circ}C_2$	$T^{\circ}K$	$T_{e.m.f.}$ in micro-volts	S microvolts /degree	ST volts per degree x temp.$^{\circ}K$
190	172	454	540	30	0.014
208	184	469	600	25	0.01172
216	184	473	800	25	0.01182
246	208	500	1150	30	0.015
276	246	534	820	27	0.01442
302	271	559.5	820	27	0.01512
328	284	579	1320	29.3	0.0169
346	310	601	900	25	0.01503
378	328	626	880	23	0.0144
382	346	637	900	25	0.0159
412	375	666.5	920	25	0.01533

1.4.5. (B) Zinc-Copper manganites

In this section we present the results of electrical measurements on zinc copper manganites. Copper manganite ($CuMn_2O_4$) has a normal cubic spinel structure and the copper ions occupy the tetrahedral and the manganese ions the octahedral sites. The high conductivity and low activation energy exhibited by this compound is best explained by assuming that the ionic formula of the compound is $Cu^{1+}[Mn^{3+}\ Mn^{4+}]O_4^{2-}$. It appeared interesting to study the effect of controlled replacement of Mn^{4+} by Mn^{3+} ions on the semiconducting as well as magnetic properties of this compound. In $ZnMn_2O_4$, Zn^{2+} ions prefer tetrahedral sites, and octahedral sites are occupied by Mn^{3+} ions. Hence, an attempt was made to prepare binary solid solutions of $CuMn_2O_4$ and $ZnMn_2O_4$ in the ratio 1-y : y. In other words a system of compounds with the general formula $Cu_{1-y}Zn_yMn_2O_4$ was prepared. The system was prepared by a solid state reaction between specpure ZnO, CuO and Mn_2O_3 taken in appropriate ratios, at high temperatures (900°C) for about 75 hours.

1.4.6. X-ray diffraction results.

X-ray diffraction powder patterns of the system $Cu_{1-y}Zn_yMn_2O_4$ were obtained on a 14 cm Debye Scherrer camera, using Mo-K_α radiations filtered through Zr. Usual methods were employed to get the 'd' values from these patterns.

An attempt was made to index the pattern with log d vs. c/a chart for tetragonal patterns. Although many of the reflections were matching with the reflections for tetragonal unit cell, some reflections could not be indexed. In case of $0.05 \leqslant y = 0.25$, intensities of these reflections were compared with the intensities of reflections from pure $ZnMn_2O_4$ pattern which is isomorphous with hausmannite. It was observed that the intensity of the 112 reflection from the system studied was smaller than that of the 200 reflection, which is not possible for the hausmannite structure. This indicated the presence of some other reflection overlapping with that of 200 of the tetragonal structure. Reflection 220 from the cubic spinel structure has almost the same d value and this experimental result suggest that the cubic phase must also be present. In fact the observed intensities of all reflections could be explained very well if the cubic and tetragonal phases were assumed to be present in a suitable proportion. Reflections which were not overlapping with any cubic reflections were used to calculate the unit cell dimensions of the tetragonal phase. No such distinct reflection was available for the cubic phase. Therefore the overlapping reflections were used to calculate the 'a' value for this phase.

The expected intensity values for different hausmannite, cubic ratios in the mixed phase were calculated by taking the weighted average of the known intensities of

A — HOMOGENEOUS CUBIC PHASE

B — MIXED (CUBIC AND TETRAGONAL) PHASE

C — HOMOGENEOUS TETRAGONAL PHASE

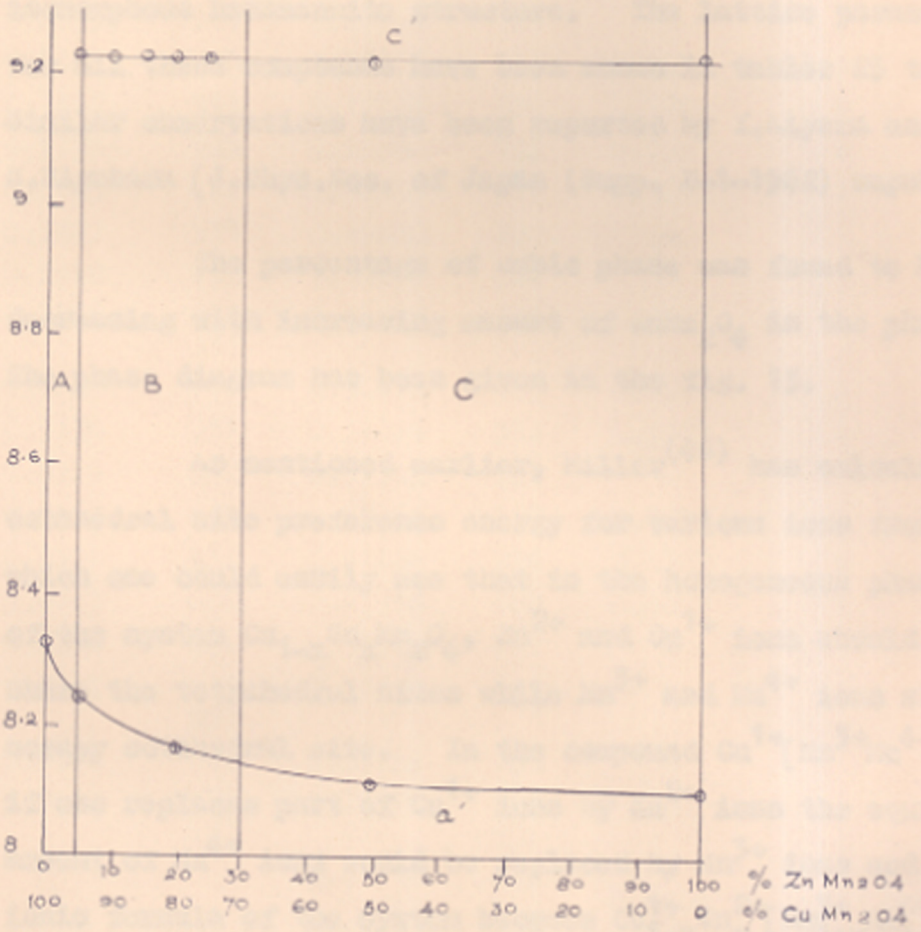

FIG. 13 - PHASE DIAGRAM FOR COPPER - ZINC - MANGANITE

the reflections from pure $ZnMn_2O_4$ (tetragonal) and $CuMn_2O_4$ (Cubic)and were compared with the observed intensities. Thus an approximate ratio of the two phases in the mixed phase was determined. The compounds with $y > 0.25$ were found to be of homogeneous phase and were isomorphous hausmannite structure. The lattice parameters for all these compounds have been shown in tables 25 to 30. Similar observations have been reported by Y.Aiyama and S.Miyahara [J.Phys.Soc. of Japan (Supp. B-1-1962) unpublished].

The percentage of cubic phase was found to be decreasing with increasing amount of $ZnMn_2O_4$ in the phase. The phase diagram has been given in the fig. 13.

As mentioned earlier, Miller[46] has calculated octahedral site preference energy for various ions from which one could easily see that in the homogeneous phase of the system $Cu_{1-y}Zn_yMn_2O_4$, Zn^{2+} and Cu^{1+} ions should share the tetrahedral sites while Mn^{3+} and Mn^{4+} ions should occupy octahedral site. In the compound $Cu^{1+}[Mn^{3+}Mn^{4+}]O_4$ if one replaces part of Cu^{1+} ions by Zn^{2+} ions the equivalent amount of Mn^{4+} ions would be replaced by Mn^{3+} ions and the ionic formula of the system becomes $Cu^{1+}_{1-y}Zn^{2+}_y[Mn^{3+}_{1+y}Mn^{4+}_{1-y}]O_4$. The probable unit cell formulae and the structure have been given in the table 31.

Table - 25

X-ray results for $Zn_{.05}Cu_{.95}Mn_2O_4$

Cubic		Tetragonal		$1/d^2$obs.	$I_{obs.}$	Lattice parameters
$1/d^2$cal.	hkl	$1/d^2$cal.	hkl			
0.04396	111	0.04162	101	-		
0.1172	220	0.10656	112	0.1079	V.W.	
0.1612	311	0.11904	200	.1184	> W	Tetragonal:
0.1759	222	0.1356	103	0.1337	W	c = 9.22 Å
0.2345	400	0.16056	211	0.1612	S	a = 5.796 Å
0.2785	331	0.16608	202	-		c' = 9.22 Å
0.3518	422	0.18816	004	-		a' = 8.231 Å
0.3958	511, 333	0.23888	220	0.2327	W	$\frac{c'}{a'}$ = 1.12
0.4689	440	0.32376	105	0.3210	W	Cubic
0.5130	531	0.34464	312	0.3529	W	a = 8.26 Å
0.5276	442	0.37368	303	-		
0.5862	620	0.39864	321	0.3951	M	
0.6302	533	0.42624	224	0.4303	W	
0.6449	622	0.47616	400	0.4671	M	
0.7034	444	0.51768	411	-		
0.7457	711, 551	0.52320	402	-		
0.8208	642	0.54254	206	-		
0.8648	731, 553	0.56184	305	-		
		0.61176	413			
				0.6325	W	
		0.66432	404			
		0.72110	316			
		0.7528	008			
				0.8635	W	

Table - 26

X-ray results for $Zn_{.1}Cu_{.9}Mn_2O_4$

Cubic		Tetragonal		$1/d^2$obs.	$I_{obs.}$	Lattice parameters
$1/d^2$cal.	hkl	$1/d^2$cal.	hkl			
0.04485	111	0.04234	101	-		
0.1196	220	0.10850	112	0.1092	V.W.	
0.16445	311	0.12175	200	0.1205	W	Tetragonal
0.17940	222	0.13754	103	0.1372	W	
0.23920	400	0.16430	211	0.1660	S	c = 9.166Å
0.2841	331	0.16934	202	-		a = 5.73 Å
0.3586	422	0.19040	004	-		c'= 9.166Å
0.4034	511, 333	0.24350	220	0.2384	W	a'= 8.137Å
						$\frac{c'}{a'}$= 1.127
0.4780	440	0.32790	105	0.3247	W	Cubic
0.5230	531	0.35200	312	0.3590	W	a = 8.176Å
0.5379	442	0.38106	303	-		
0.5977	620	0.40762	321	0.4009	M	
0.6425	533	0.43390	224	0.4365	>W	
0.6575	622	0.48704	400	0.4771	M	
0.7171	444	0.52940	411	-		
0.7621	711	0.53464	402	-		
0.8368	642	0.55016	206	-		
0.8816	731	0.57146	305	-		
		0.62450	413	0.6308	M	
		0.67740	404			
		0.73280	316			
		0.76160	008	0.8264	W	

Table - 27

X-ray results for $Zn_{.15}Cu_{.85}Mn_2O_4$

Cubic		Tetragonal		$1/d^2$obs.	$I_{obs.}$	Lattice parameters
$1/d^2$cal.	hkl	$1/d^2$cal.	hkl			
0.04452	111	0.04180	101	-	-	
0.11872	220	0.1171	112	0.1070	V.W.	
0.16324	311	0.1201	200	0.1190	W	
0.17808	222	0.1359	103	0.1340	W	
0.23744	400	0.1619	211	0.1629	S	Tetragonal:
0.28196	331	0.1672	202	-	-	c = 9.218 Å
0.35616	422	0.1882	004	0.1769	V.V.W.	a = 5.77 Å
0.4007	511, 333	0.2402	220	0.2363	W	c' = 9.218 Å
						a' = 8.179 Å
0.4749	440	0.3240	105	0.3247	W	$\frac{c'}{a'}$ = 1.126
0.5195	531	0.3473	312	0.3535	W	
0.5345	442	0.3761	303	-		Cubic:
0.5936	620	0.40215	321	0.4000	M	a = 8.211 Å
0.6383	533	0.4284	224	0.4322	>W	
0.6531	622	0.4805	400	0.4732	M	
0.7124	444	0.5223	411	-	-	
0.7570	711	0.5275	402	-	-	
0.8313	642	0.5435	206	-	-	
0.8758	731		305			
		0.6006	413	0.6166	W	
			404			
			316			
			008			
				0.8650	W	

Table - 23

X-ray results for $Zn_{.2}Cu_{.8}Mn_2O_4$

Cubic		Tetragonal		$1/d^2$obs.	$I_{obs.}$	Lattice parameters
$1/d^2$cal.	hkl	$1/d^2$cal.	hkl			
0.04422	111	0.04156	101	-		
0.1179	220	0.1066	112	0.1073	W	
0.1621	311	0.1192	200	0.1184	W	
0.1769	222	0.1356	103	0.1340	W	Tetragonal:
0.2358	400	0.16076	211	0.1614	S	c = 9.22 Å
0.2797	331	0.1882	004	-		a = 5.793 Å
0.3518	422	0.2384	220	0.2373	W	c' = 9.22 Å
0.3980	511, 333	0.3074	204	-		a' = 8.231 Å
0.4717	440	0.3238	105	0.3244	W	$\frac{c'}{a'}$ = 1.12
0.5159	531	0.3450	312	-		Cubic :
0.5307	442	0.3740	303	0.3672	W	a = 8.23 Å
0.5896	620	0.3992	321	0.3956	M	
0.6339	533	0.4266	224	0.4343	W	
0.6486	622	0.4768	400	0.4700	M	
0.7074	444	0.5184	411	-		
0.7518	711, 551	0.5238	402	-		
0.8254	642	0.5427	206	-		
0.8698	731, 553	0.5622	305	-		
		0.5960	420, 415	-		
		0.6430	423	0.6377	W	
		0.6649	404			
		0.7215	217, 316			
				0.8501	W	

Table - 23

X-ray results for $Zn_{.25}Cu_{.75}Mn_2O_4$

Cubic		Tetragonal		$1/d^2$obs.	$I_{obs.}$	Lattice parameters
$1/d^2$cal.	hkl	$1/d^2$cal.	hkl			
0.04464	111	0.04215	101	-	-	
0.11904	220	0.10804	112	0.1086	W	
0.1637	311	0.1211	200	0.1191	W	
0.17856	222	0.1371	103	0.1369	>W	
0.2381	400	0.1633	211	0.1650	S	Tetragonal :
0.2828	331	0.1680	202	-	-	c = 9.18 Å
0.3572	422	0.1899	004	0.1823	V.W.	a = 5.747Å
0.4019	511, 333	0.24224	220	0.2399	W	c'= 9.18 Å a'= 8.16 Å
0.4762	440	0.3270	105	0.3237	W	$\frac{c'}{a'}$= 1.125
0.5210	531	0.3503	312	0.3557	W	
	442	0.37935	303	-		Cubic :
0.5954	620	0.4055	321	0.4016	M	a = 8.198Å
0.6396	533	0.43216	224	0.4386	>W	
0.6549	622	0.4845	400	0.4737	M	
0.7144	444	0.5266	411	-	-	
0.7591	711	0.53196	402	-	-	
0.8335	642	0.5485	206	-	-	
0.8782	731	0.5693	305	-	-	
0.9526	800	0.6216	413	0.6356	W	
		0.6744	404	-		
		0.7302	316	0.7277	V.W.	
		0.7597	008			
				0.8711	W	

Table - 32

X-ray results for $Zn_{.5}Cu_{.5}Mn_2O_4$

hkl	obs. density	$1/d^2$obs.	$1/d^2$cal.	Lattice parameters
101	-	-	0.04262	
112	W	0.1119	0.10914	
200	-	-	0.12268	
103	M	0.1380	0.13822	c = 9.15 Å
211	S	0.1660	0.1653	a = 5.71 Å
202			0.1705	c'= 9.15 Å
004	V.W.	0.1866	0.1912	a'= 8.108Å
220	W	0.2450	0.24536	$\frac{c'}{a'}$= 1.128
105	W	0.3245	0.3294	
312	W	0.3557	0.3546	
303	W	0.3856	0.3836	
321	W	0.4093	0.41066	
224	> W	0.4363	0.43656	
400	W	0.4912	0.4907	
411	-	-	0.5333	
402	-	-	0.5385	
206	-	-	0.5529	
305	-	-	0.5748	
413	W	0.6291	0.6289	
404			0.6819	
316			0.7369	
008			0.7649	

Table - 31

Structural data for $Zn_yCu_{1-y}Mn_2O_4$

	Compound	Probable Unit cell formulae	Structure
(1)	$CuMn_2O_4$ [8]	$Cu_8^{1+}[Mn_8^{3+}Mn_8^{4+}]O_{32}^{2-}$	Cubic : a = 8.33 Å
(2)	95% $CuMn_2O_4$ + 5% $ZnMn_2O_4$	Mixture of $ZnMn_2O_4$ - $CuMn_2O_4$ phases	Tetragonal ~30% + Cubic ~70%
(3)	75% $CuMn_2O_4$ + 25% $ZnMn_2O_4$	- do -	Tetragonal ~80% + Cubic ~20%
(4)	50% $CuMn_2O_4$ + 50% $ZnMn_2O_4$	$Cu_4^{1+}Zn_4^{2+}[Mn_{12}^{3+}Mn_4^{4+}]O_{32}^{2-}$	Tetragonal : c = 9.15 Å, a = 5.714 Å, $\frac{c'}{a'}$ = 1.128
(5)	$ZnMn_2O_4$ [8]	$Zn_8[Mn_{16}^{3+}]O_{32}$	Tetragonal : c = 9.24 Å, a = 8.10 Å, $\frac{c'}{a'}$ = 1.14

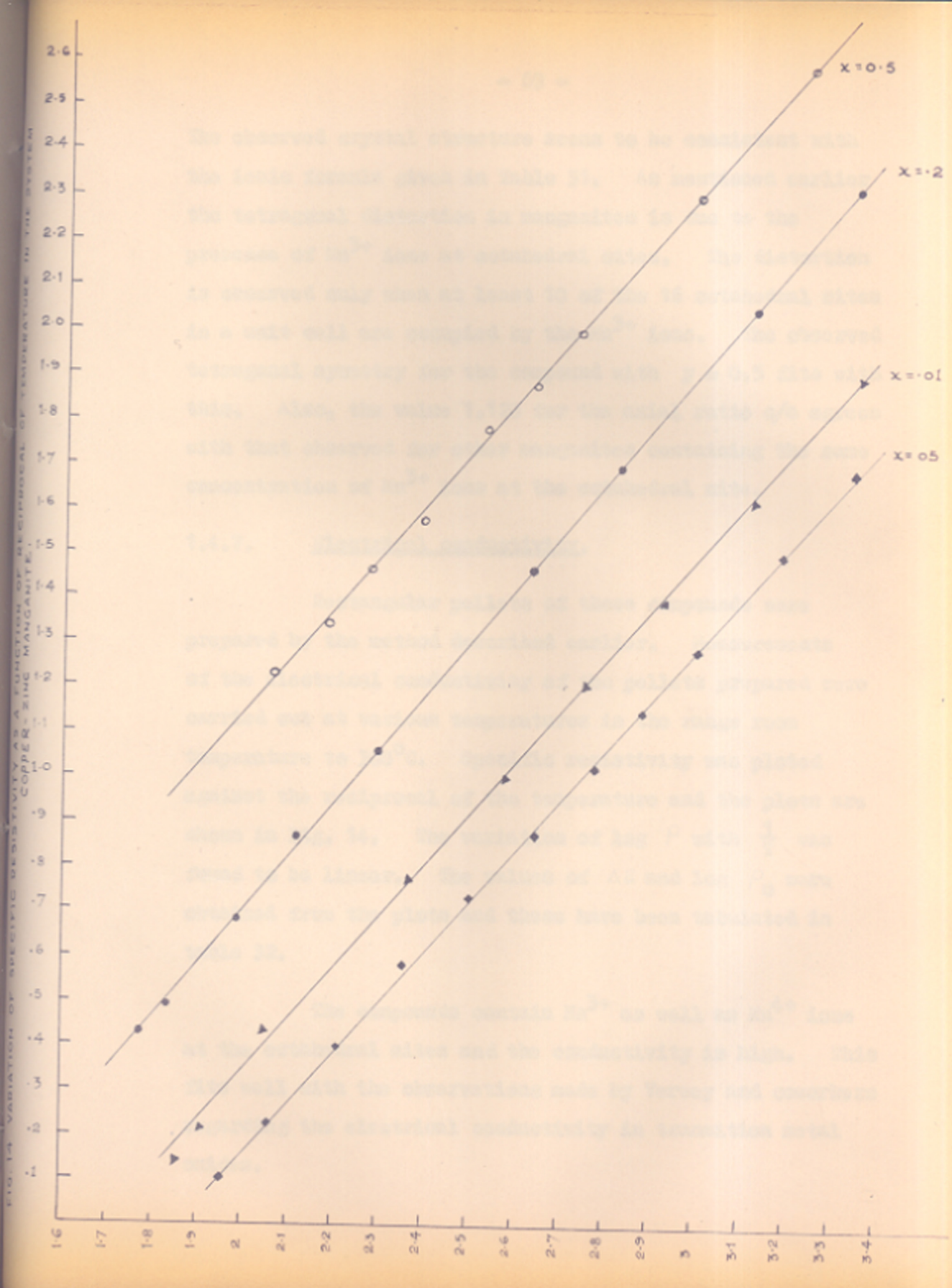
FIG. 1a VARIATION OF SPECIFIC RESISTIVITY AS A FUNCTION OF RECIPROCAL OF TEMPERATURE IN THE SYSTEM COPPER-ZINC MANGANITE.
x=0·5
x=·2
x=·01
x=05
2·6
2·5
2·4
2·3
2·2
2·1
2·0
1·9
1·8
1·7
1·6
1·5
1·4
1·3
1·2
1·1
1·0
·9
·8
·7
·6
·5
·4
·3
·2
·1
1·6
1·7
1·8
1·9
2
2·1
2·2
2·3
2·4
2·5
2·6
2·7
2·8
2·9
3
3·1
3·2
3·3
3·4

The observed crystal structure seems to be consistent with the ionic formula given in Table 31. As mentioned earlier the tetragonal distortion in manganites is due to the presence of Mn^{3+} ions at octahedral sites. The distortion is observed only when at least 10 of the 16 octahedral sites in a unit cell are occupied by the Mn^{3+} ions. The observed tetragonal symmetry for the compound with $y = 0.5$ fits with this. Also, the value 1.128 for the axial ratio c/a agrees with that observed for other manganites containing the same concentration of Mn^{3+} ions at the octahedral site.

1.4.7. Electrical conductivity.

Rectangular pellets of these compounds were prepared by the method described earlier. Measurements of the electrical conductivity of the pellets prepared were carried out at various temperatures in the range room temperature to 300°C. Specific resistivity was ploted against the reciprocal of the temperature and the plots are shown in Fig. 14. The variation of log ρ with $\frac{1}{T}$ was found to be linear. The values of ΔE and log ρ_o were obtained from the plots and these have been tabulated in table 32.

The compounds contain Mn^{3+} as well as Mn^{4+} ions at the octahedral sites and the conductivity is high. This fits well with the observations made by Verwey and coworkers regarding the electrical conductivity in transition metal oxides.

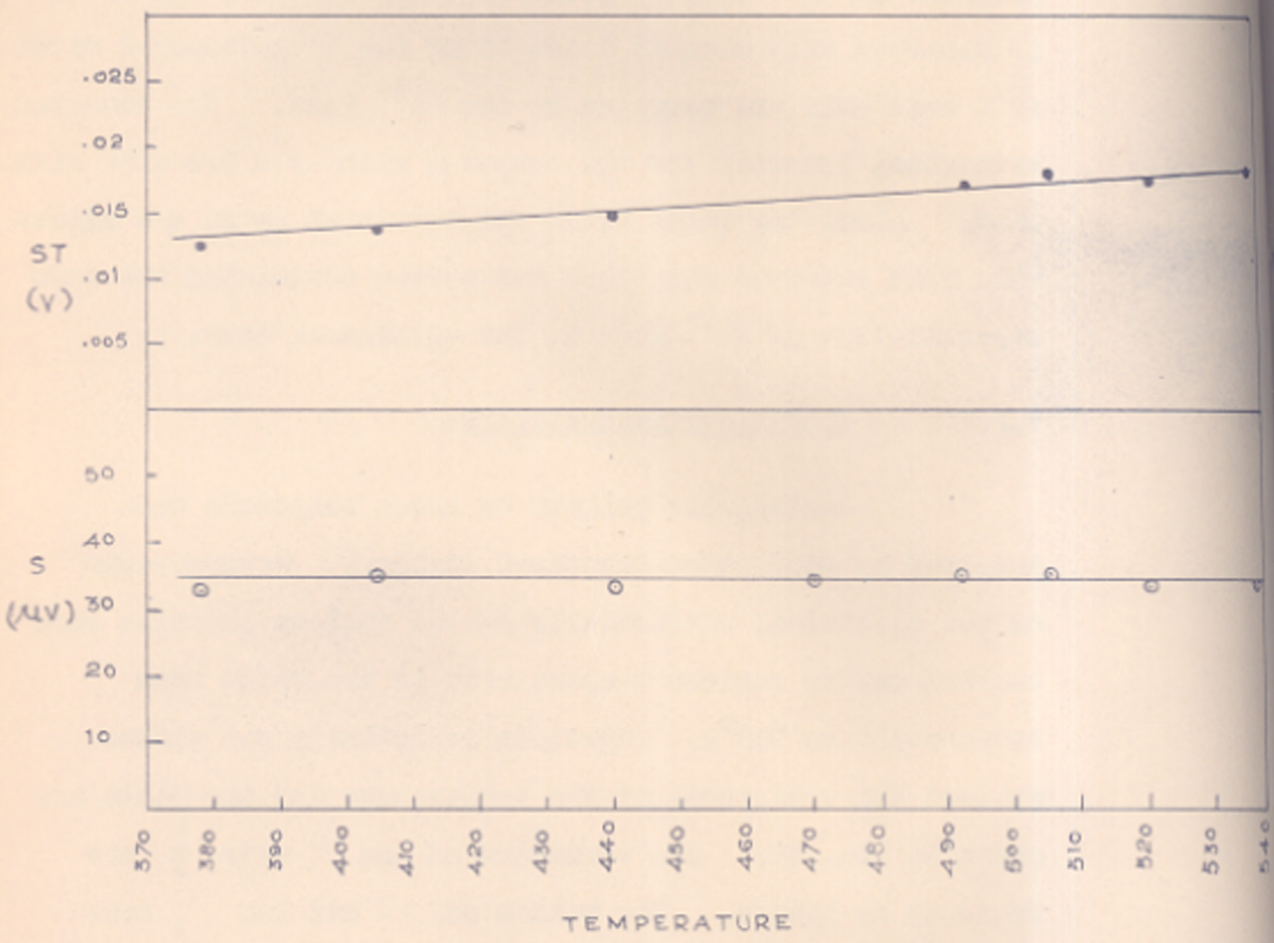

FIG. 15 - VARIATION OF S AND ST AS A FUNCTION OF TEMPERATURE FOR ($Zn_{0.05}$ $Cu_{.95}$ Mn_2O_4)

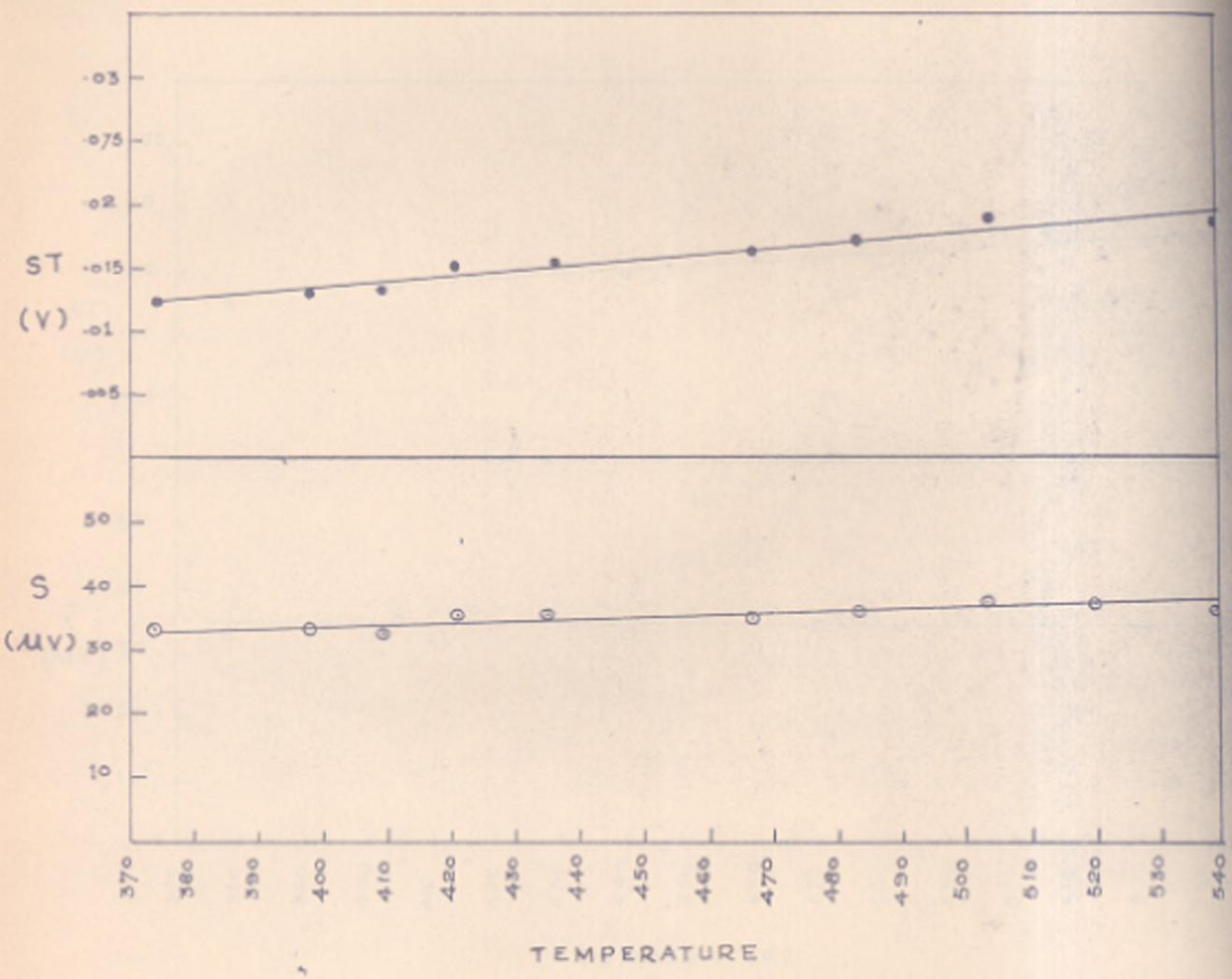

FIG-16- VARIATION OF S AND ST AS A FUNCTION OF TEMPERATURE FOR ($Zn_{\cdot 1}$ $Cu_{\cdot 9}$ Mn_2O_4)

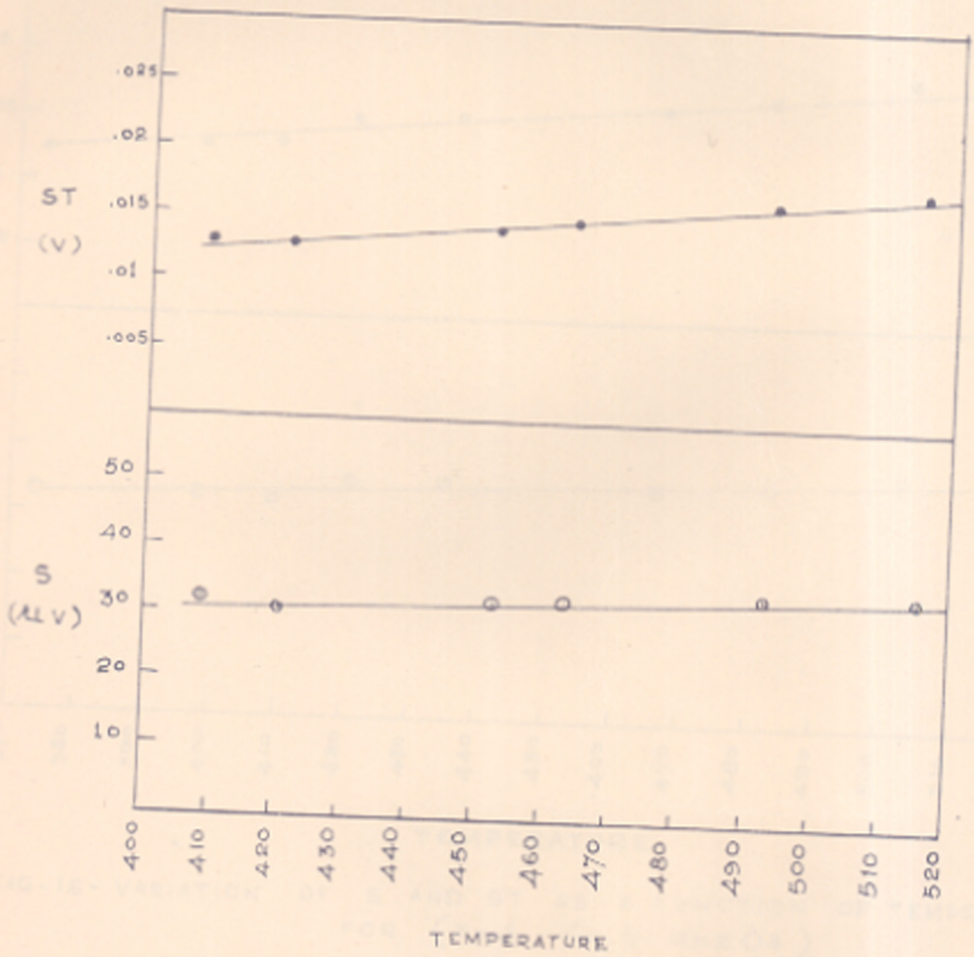

FIG. 17 VARIATION OF S AND ST. AS A FUNCTION OF TEMPERATURE FOR $Zn_{.15}$ $Cu_{.85}$ Mn_2O_4.

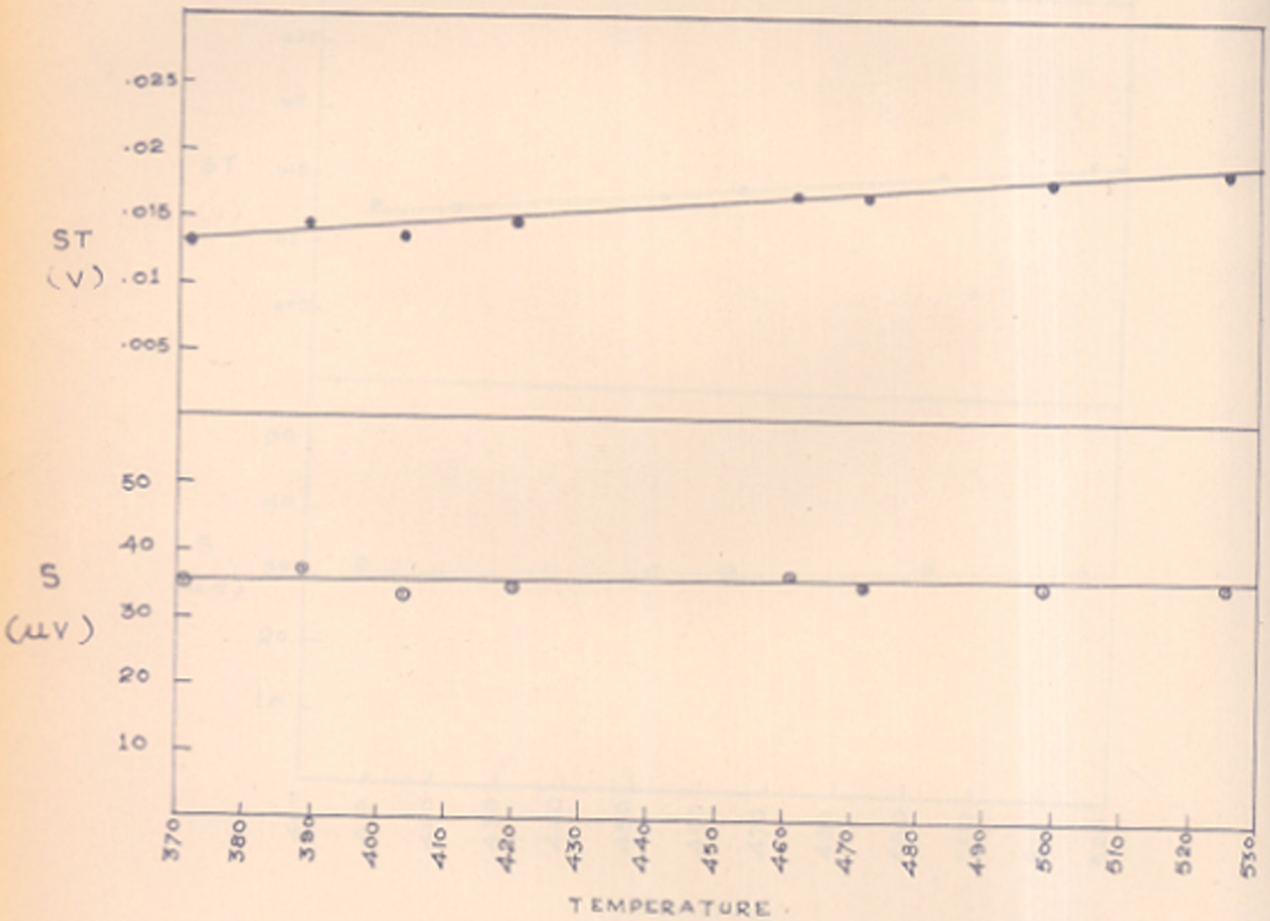

FIG. 18 VARIATION OF S AND ST AS A FUNCTION OF TEMPERATURE FOR $Zn_{.2}Cu_{.18}Mn_2O_4$

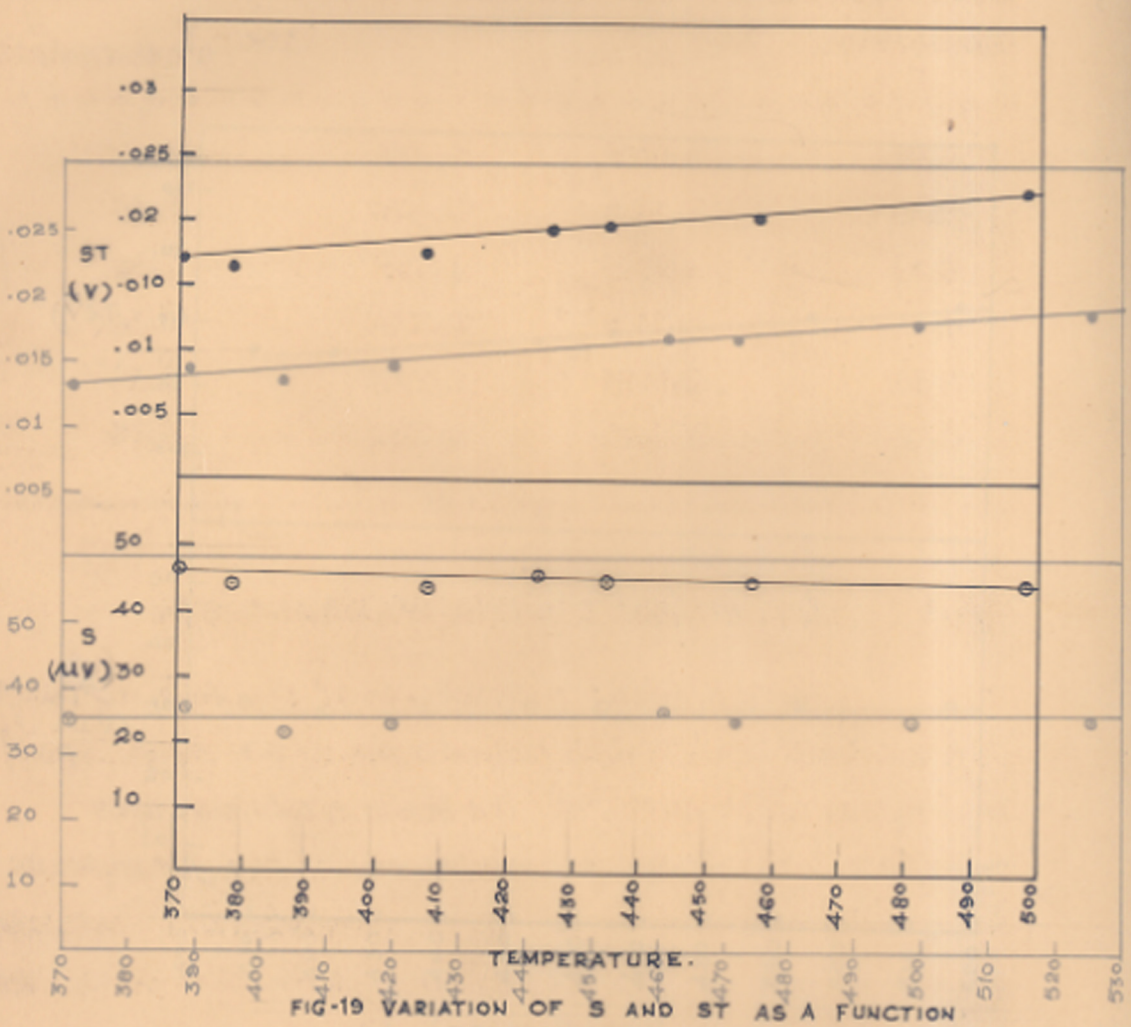

FIG-19 VARIATION OF S AND ST AS A FUNCTION OF TEMPERATURE FOR Zn·25 Cu·75 Mn_2O_4.

FIG. 18 VARIATION OF S AND ST AS A FUNCTION OF TEMPERATURE FOR Zn·2 Cu·18 Mn_2O_4

Table - 12

Conductivity results for $Zn_yCu_{1-y}Mn_2O_4$

Composition y	$\log(\rho_{RT})_{obs.}$	ΔE eV	$(\log \rho_o)_{extrapolated}$
0.05	1.6996	0.2305	$\bar{3}.90$
0.10	1.9019	0.2262	$\bar{3}.93$
0.15	2.3726	0.2694	$\bar{3}.84$
0.20	2.3347	0.2282	$\bar{2}.300$
0.25	2.3160	0.2360	$\bar{2}.36$
0.50	2.6021	0.2354	$\bar{2}.76$

1.4.8. Thermoelectric coefficient measurements.

Thermoelectric coefficients of all these compounds were measured at different temperatures in the range, room temperature to about 250°C. As these substances have relatively small electrical resistances at room temperature and upwards, the measurement of the thermoelectric coefficients did not present any serious problem. Conduction in all these cases was found to be p-type. The values of the thermoelectric coefficient and ST are given in Tables 33 to 37. Plots of thermoelectric coefficient S vs. T, and ST vs. T are shown in Figs. 15-19. It is seen that the thermoelectric coefficient is nearly independent of temperature for all these samples and that it does not change very much from sample to sample.

Table - 33

Thermoelectric coefficients of $Zn_{.05}Cu_{.95}Mn_2O_4$ as a function of temperature

(Type of conduction : p-type)

t_1^oC	t_2^oC	T^oK	$T_{e.m.f.}$ in micro-volts	S microvolts /degree	ST volts per degree x temp.^oK
108	102	378	200	33	0.01247
138	129	404.5	310	35	0.01416
174	160	440	470	33.6	0.01479
230	209	492.5	740	35	0.01724
245	219	505	925	35.5	0.01793
262	232	520	1010	33.4	0.01737
281	250	538.5	1050	34	0.01831

Table - 34

Thermoelectric coefficients of $Zn_{.1}Cu_{.9}Mn_2O_4$ as a function of temperature

(Type of conduction : p-type)

t_1^oC	t_2^oC	T^oK	E e.m.f. in micro-volts	S microvolts /degree	ST volts per degree x temp.^oK
103.5	99	374.3	150	33.5	0.01254
128	122	398	200	33.3	0.01325
140	133	409.5	230	33	0.01351
152	144	421	290	36.25	0.01526
167	157	435	360	36.0	0.01565
201	188	467.5	460	35.4	0.01655
217	203	483	510	36.43	0.01759
222	208	488	525	37.5	0.01830
240	222	503	610	38	0.01912
277	255	539	760	34.5	0.01860

Table - 35

Thermoelectric coefficients of $Zn_{.15}Cu_{.85}Mn_2O_4$ as a function of temperature

(Type of conduction : p-type)

t_1^oC	t_2^oC	T^oK	E e.m.f. in micro-volts	S microvolts /degree	ST volts per degree x temp. ^oK
145	127	409	580	32	0.01308
160	135	420.5	760	30.4	0.01292
194	164	452	940	31.3	0.01415
207	173	463	1100	32.35	0.01498
240	200	493	1340	33.5	0.01650
263	222	515.5	1400	34	0.01753

Table - 36

Thermoelectric coefficients of $Zn_{.2}Cu_{.8}Mn_2O_4$ as a function of temperature

(Type of conduction : p-type)

t_1^oC	t_2^oC	T^oK	$T_{e.m.f.}$ in micro-volts	S microvolts /degree	ST volts per degree x temp. ^oK
100	96	371	140	35	0.01299
118	114	389	150	37.5	0.01458
133	128	403.5	170	34	0.01372
150	144	420	210	35	0.01470
192	184	461	300	37	0.01706
204	194	472	360	36	0.01699
233	219	499	500	35.7	0.01781
260	245	525.5	540	36	0.01892

Table - 37

Thermoelectric coefficients of $Zn_{.25}Cu_{.75}Mn_2O_4$ as a function of temperature

(Type of conduction : p-type)

$t_1^{\circ}C$	$t_2^{\circ}C$	$T^{\circ}K$	$T_{e.m.f.}$ in micro-volts	S microvolts /degree	ST volts per degree x temp. $^{\circ}K$
100	94	370	280	46.6	0.01724
110	101	378.5	400	44	0.01665
140	129	407.5	470	43	0.01752
158	148	426	460	46	0.01960
167	157	435	450	45	0.01957
194	174	457	900	45	0.02056
235	215	498	910	45.5	0.02266

1.5. Discussion.

1.5.1. Zinc lithium manganites.

The results on the semiconducting properties of zinc-lithium manganites throw some light on the mechanism of electrical conduction in spinels containing Mn^{3+} and Mn^{4+} ions at the octahedral sites. The present study, in particular, brings out the interesting variations in the electrical properties as the ratio of the Mn^{3+} to Mn^{4+} ions at the octahedral sites changed systematically. The compounds in this series range from pure zinc manganite where there are only Mn^{3+} ions at the octahedral sites to $Zn^{2+}[Li^{1+}_{.6}Mn^{3+}_{.6}Mn^{4+}_{.8}]O_4$ which contains an excess of Mn^{4+} ions.

As described earlier, the amount of lithium ions actually incorporated in the lattice was determined experimentally by flame-photometric methods and it was found that the total amount of lithium initially taken had gone in the lattice. The incorporation of Li^{1+} ions in the lattice could be either interstitial or substitutional. The following evidences support the latter :

(1) The unit cell volume as determined from the x-ray diffraction data decreases with the increase in the concentration of Li^{1+} ions. (Table 38). Interstitial incorporation is expected to increase the volume.

Table - 38

Unit cell volume for $ZnLi_{2x}Mn_{2-2x}O_4$

Composition	$V^{1/3}$ Å
$Zn[Li_{.1}Mn_{1.9}]O_4$	8.461
$Zn[Li_{.2}Mn_{1.8}]O_4$	8.337
$Zn[Li_{.3}Mn_{1.7}]O_4$	8.258
$Zn[Li_{.4}Mn_{1.6}]O_4$	8.19
$Zn[Li_{0.5}Mn_{1.5}]O_{3.88}$	8.23
$Zn[Li_{0.6}Mn_{1.4}]O_{3.81}$	8.24

(2) The density as determined experimentally using a specific gravity bottle, matches with that calculated for Li^{1+} at substitutional positions (Table 39).

Table - 39

Observed and calculated densities for $ZnLi_{2x}Mn_{2-2x}O_4$

Composition	Density determined	Density calculated
$Zn[Li_{.1}Mn_{1.9}]O_4$	5.15	5.144
$Zn[Li_{.2}Mn_{1.8}]O_4$	5.16	5.165
$Zn[Li_{.3}Mn_{1.7}]O_4$	5.25	5.30
$Zn[Li_{.4}Mn_{1.6}]O_4$	5.35	5.32
$Zn[Li_{.5}Mn_{1.5}]O_{3.88}$	4.97	5.067
$Zn[Li_{.6}Mn_{1.4}]O_{3.81}$	4.82	4.943

If the Li^{1+} ions are present substitutionally in the spinel structure, the ionisation state of some other ions in the lattice must change as the electrical neutrality of the system must be maintained. The following changes are possible.

$$Mn^{3+} \longrightarrow Mn^{4+}; \quad Zn^{2+} \longrightarrow Zn^{3+}; \quad \text{or} \quad O^{2-} \longrightarrow O^{1-}$$

From the known chemistry of these ions it is easy to conclude that out of the three ions Mn^{4+}, Zn^{3+} and O^{1-}, the first is the most stable and hence most likely. Many compounds containing Mn^{4+} ions are well-known whereas the other two ions are not known to exist under normal conditions. This conclusion is also supported by the change in crystal structure from tetragonal to cubic symmetry with the increasing amount of Li^{1+} ion substitution. The tetragonal distortion in such manganites is known to be due to the presence of Mn^{3+} ions at the octahedral sites. The maximum distortion is observed when all the available octahedral sites are occupied by the Mn^{3+} ions and the c'/a' decreases with decreasing concentration of these ions. Below a certain critical concentration of Mn^{3+} ions, the structure changes to the cubic symmetry. The observed variation of c'/a' in the present case follows this pattern showing that the number of Mn^{3+} ions actually decreases with increasing amount of Li^{1+} in the lattice. This obviously supports the conclusion that Mn^{3+} ions change to Mn^{4+} ions.

The actual amount of Mn^{3+} and Mn^{4+} ions in the lattice has been determined experimentally by reduction with oxalic acid and the results are given earlier (refer to table 4). The amount of Mn^{4+} ions increases with increasing concentration of Li^{1+}; however at higher concentrations all the Li^{1+} ions are less effective in producing Mn^{4+} ions as the compound becomes oxygen deficient. This is due to the fact that enough oxygen is not taken up by the system during reaction and sintering. It is likely that the uptake of oxygen is a slow process, and given enough time at elevated temperature, the compounds would become stoichiometric.

The location of Mn^{3+} and Mn^{4+} ions at the octahedral sites is concluded from their known site preference energies. X-ray intensity calculations based on this assumption agree well with the experimental results. Most of the Zn^{2+} ions are found to occupy the tetrahedral sites and Li^{1+} ions share the octahedral sites with the Mn^{3+} ions.

Verwey and coworkers[44b] (1951) have found that electrical conductivity in transition metal oxides is high if the material contains the cations of the same element, but with their valencies differing by unity, situated at similar sites in the crystal. Zinc-lithium manganites do fulfil this condition as Mn^{3+} and Mn^{4+} ions are situated at the octahedral sites of the spinel structure. It is

therefore plausible to assume that in this series, conduction takes place due to electron exchange between octahedral Mn^{3+} and Mn^{4+} ions.

An examination of the spinel structure reveals that the distance between tetrahedral-octahedral or tetrahedral-tetrahedral cations is so large that the overlap between the electronic wave functions on such adjacent pairs will be negligible, and the probability of electron exchange between cations on these sites will be small. Thus the electrical conductivity can only take place by electron exchange amongst the octahedral ions.

Let the total number of manganese ions per unit volume be N and those of Mn^{4+} and Mn^{3+} be n and N-n respectively. Let E be the energy of the conduction level. Thus the fraction $\frac{N-n}{N}$ represents the probability that the states at E are occupied by electrons. In other words N represents the number of available levels at energy E, (N-n) the number of levels occupied by electrons and n gives the number of holes at those levels. The fraction $\frac{N-n}{N}$ must therefore be equal to the Fermi distribution function,

$$\frac{1}{\exp\left(\frac{E-E_F}{kT}\right) + 1}$$

where E_F is the Fermi level. The value of Fermi level E_F is adjusted such that the condition :

$$\frac{1}{\exp\left(\frac{E-E_F}{kT}\right) + 1} = \frac{N-n}{N}$$

is satisfied. Therefore $E_F - E = kT$ in $\frac{N-n}{N}$.

The thermoelectric coefficient S is related to the Fermi energy by the following relationship

$$eST = A + (\epsilon_F - \epsilon) = A + kT\ln\frac{N-n}{n}$$

$$\text{or} \quad S = \left(\frac{A}{eT}\right) + \frac{k}{e}\ln\frac{N-n}{n}$$

where e is the electronic charge. The term A represents the kinetic energy transported by the migrating electrons. The second term of the right hand side of the above equation was easily calculated for all the compounds of the series and the value of $\frac{A}{eT}$ obtained at various temperatures. The results are given in table 40. From these results it is clear that A is not independent of composition as has been assumed earlier[32]. In fact there is a very strong dependence on the composition. In addition $(\frac{A}{eT})$ is nearly independent of temperature or in other words A increases linearly with temperature. The value of A ranges from 1.7 kT for $Zn[Li_{.1}Mn^{3+}_{1.7}Mn^{4+}_{.2}]O_4$ to nearly 0 for $Zn[Li_{0.6}Mn^{3+}_{.58}Mn^{4+}_{.82}]O_4$.

Table - 40

Variation of $\frac{A}{eT}$ as a function of temperature for the series Zinc lithium manganite

x = .05		x = 0.1		x = 0.15		x = 0.2		x = 0.25		x = .3	
Temp.	$\frac{A}{eT}$	Temp.	$\frac{A}{eT}$	Temp.	$\frac{A}{eT}$	Temp.	$\frac{A}{eT}$	Temp.	$\frac{A}{eT}$	Temp.	$\frac{A}{eT}$
570.5	151	504	78	504	65.6	434	35	436	42.06	454	0.15
594	147.5	534.5	76	536	65.86	457	33	455.5	39.62	469	-4.8
611.5	146	574	77.7	556	65.0	472.7	35	523.4	41.5	500	0.15
624	148	587	75	585.5	66.5	494	37	532.5	42.7	534	-2.85
631	146	603	73	618	64	514	35	553	39.7	559.5	-2.85
649	144	615.5	73	639	63	558.7	33	589	41.2	579	-0.53
700	142	650	72	676.5	63.6	611	34	629.5	39.7	601	-4.85
		674	74.4			641.2	36	641	40.2	637	-4.85
						656.5	33			666.7	-4.85

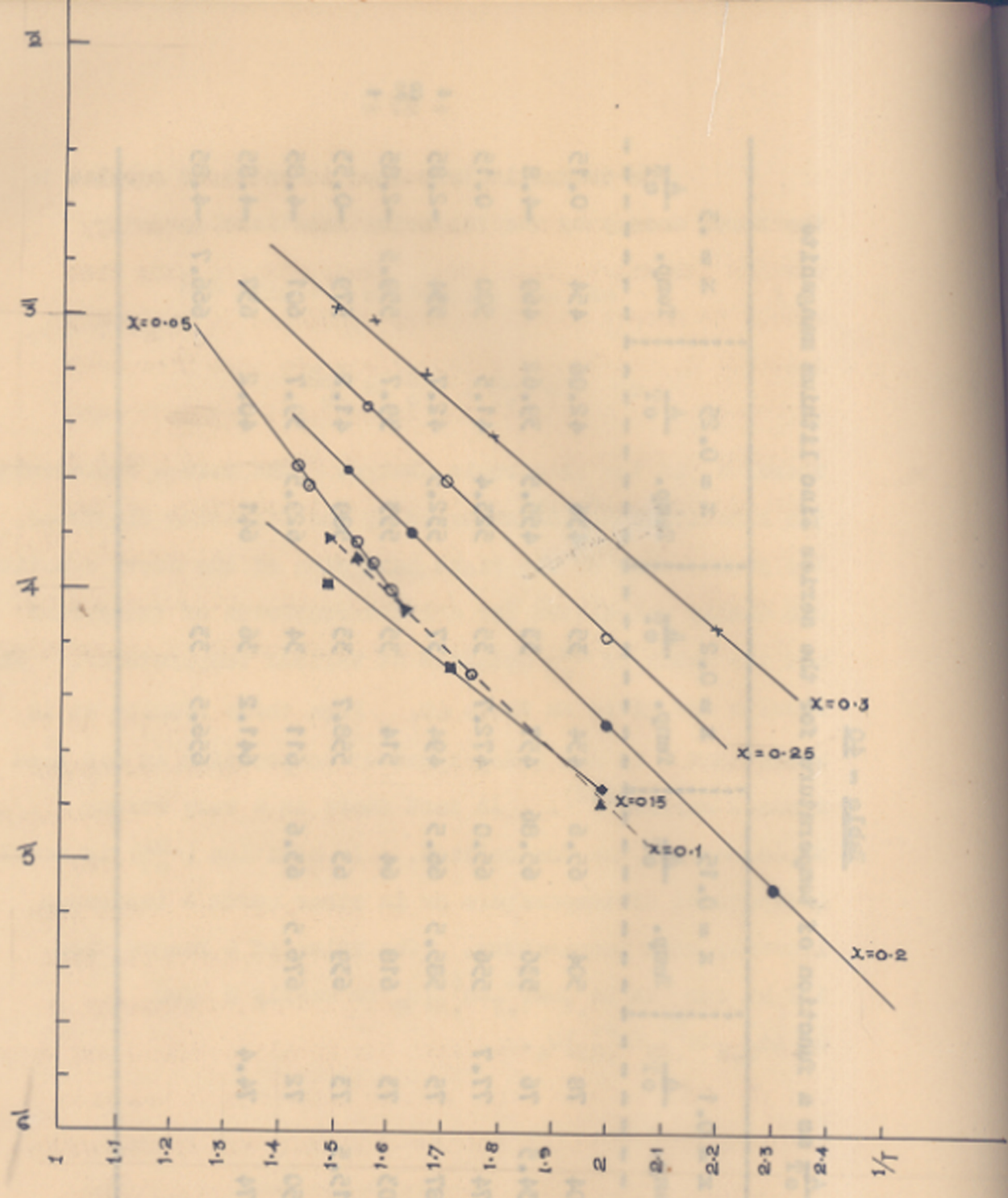

FIG·20·VARIATION OF MOBILITY AS A FUNCTION OF THE RECIPROCAL OF TEMPERATURE.

The conductivity values in sintered samples depend to some extent on imperfections like porosity, surface inhomogeneities etc. These effects vary from sample to sample and it is very difficult to apply any suitable correction. These values are also frequency dependent. The resistivity is known to decrease with increasing frequency and finally to reach a constant value. This dispersion is thought to be due to shorting of the intergranular resistances due to their large capacity[31,47]. The activation energy is, however, fairly reproducible and is truely representative of the nature of the semiconductor.

The electrical conductivity σ is given by the relationship $\sigma = ne\mu$ where 'n' is the number of charge carriers per unit volume and 'μ' the mobility. The number of charge carriers is equal to the number of Mn^{3+} ions when $\varepsilon_F < \varepsilon$, and is equal to the number of Mn^{4+} ions when $\varepsilon_F > \varepsilon$. The mobility at various temperatures can thus be calculated and the results are plotted graphically in Fig. 20. It can be seen that the mobility values are very low ($\sim 10^{-5}$ cm^2/sec volt) at low temperatures but rise exponentially with temperature following the relationship $\mu = \mu_o \exp. - \frac{\Delta E}{kT}$. This type of behaviour is usually observed when the conductivity is by 'd' electrons and the lattice is ionic. Several transition metal oxides are known to exhibit this behaviour. The exponential temperature dependence of mobility is incompatible with the well-known

band picture and arises from the fact that the electron wave functions are localised and there is little overlap between such wave functions centred on adjacent cation sites. If the lattice is polar, the localisation of charge carriers is further increased by self trapping effects as a result of polarisation of the surrounding lattice. For such polarisation to occur it is necessary that the carrier resides at a given site for a period longer than the vibrational period of lattice which is of the order of 10^{-13} sec. Due to very low mobilities (Fig. 20) of the materials under study, the occurrence of self-trapping of this type is to be expected.

The theoretical analysis of the conductivity of such samples on the basis of Heitler-London approach has been done by several investigators[39,40,41,48]. The wave function of the charge carrier is assumed to be localised around a metal ion. Due to an interaction of this localised charge carrier with the lattice, polarisation of the lattice is induced around the charge carrier. This results in a modification of the lattice wave functions and the formation of displaced harmonic oscillators. The total energy of the system is lowered due to the polarisation and the charge carrier gets trapped. The potential due to the other ions however, act as a perturbation which causes the carrier to jump from an ion to its nearest neighbour. The transition probability W depends on temperature in a rather complicated way. Sinha

and Sinha[43] have derived the following expression for the mobility

$$\mu = \left[\lambda^{o}_{nm} T^{-3/2} + \lambda^{a}_{nm} T^{-1/2} + \lambda^{aa}_{nm} T^{1/2} \right] e^{-\Delta E/kT}$$

where λ's are independent of temperature. The probability of such transition W_{nm} in the simplest case i.e. when the transition is not via any intermediate excited state, and the temperature is high (i.e. $kT \gg \hbar\omega$, where ω is Einstein's frequency for the solid), is given by

$$W_{nm} = \frac{P_{nm}^2}{2\hbar} \sqrt{\frac{\pi}{kT \Delta E}} \; e^{-\Delta E/kT}$$

since the mobility μ is given by $\mu = \frac{ed^2 W}{kT}$, we have

$$\mu = \frac{ed^2 P_{nm}^2}{2\hbar kT^{3/2}} \sqrt{\frac{\pi}{\Delta E}} \exp\left(-\frac{\Delta E}{kT}\right)$$

where d represents the distance between a Mn^{3+} ion and a neighbouring Mn^{4+} ion and $P_{nm} = \langle \phi_m | P | \phi_n \rangle$, ϕ_n and ϕ_m are the wave functions for the charge carriers when localised at site n and m respectively and P is the perturbation which is causing the transition, ΔE, the activation energy term and is about half the energy lowering due to self-trapping. Physically this arises from the fact that the energy required to establish a near neighbour coincidence is lower than the actual energy lowering due to self trapping.

Each B site cation in the spinel structure has six nearest neighbour cations. The probability that an electron

from any Mn^{3+} ion will jump to a neighbouring Mn^{4+} ion will be directly proportional to the probability P_f that the neighbouring sites are occupied by Mn^{4+} ions. For a compound represented by the formula $Zn^{2+}[Li^{1+}_{2-p-q}Mn^{4+}_{p}Mn^{3+}_{q}]O_4$, the number of charge carriers per unit volume and the factor P_f are as follows :

Table - 41

	No. of Charge carriers	P_f
$\Delta_F < \delta$	$8q/(a)^2 c'$	$p/2$
$\Delta_F > \delta$	$8p/(a)^2 c'$	$q/2$

In the spinel structure the distance between the nearest octahedral ions is $\frac{a\sqrt{2}}{4}$. In the tetragonal spinel, however, the six neighbours are not equidistant from the central ion. Two are at the distance ($\frac{a\sqrt{2}}{4}$) and the other four are at $\sqrt{\frac{a^2+c^2}{4}}$. However, for simplicity we put d equal to $a\sqrt{2}/4$ for both tetragonal and cubic structures. In that case the conductivity σ is given by the following expression (for both $\Delta_F > \delta$ or $< \delta$).

$$\sigma = \frac{pqe^2\nu^2}{4a\hbar(kT)^{3/2}}\left(\frac{\pi}{\Delta_S}\right)^{\frac{1}{2}} \exp - \frac{\Delta_S}{kT}$$

The values of P_{nn} and ΔE have been calculated for the various compositions from our experimental results and are given in Table 42.

Table - 42

P_{nn} and ΔE values for $ZnLi_{2x}Mn_{2-2x}O_4$

Composition x	P_{nn}	ΔE (eV)
0.05	0.04	0.46
0.10	0.022	0.39
0.15	0.0207	0.364
0.20	0.041	0.389
0.25	0.046	0.368
0.30	0.069	0.365

It is interesting to see that P_{nn} shows a minimum in the transition range where the semiconductivity changes from p to n type or where Fermi level crosses the conduction level. In previous analyses, several authors[31,49,50] have used a phenomenological constant ν which is called the jump frequency. The expression for conductivity in their treatment is as follows :

$$\sigma = \frac{pqe^2\nu}{2n\,kT} \times \exp - \frac{\Delta E}{kT}$$

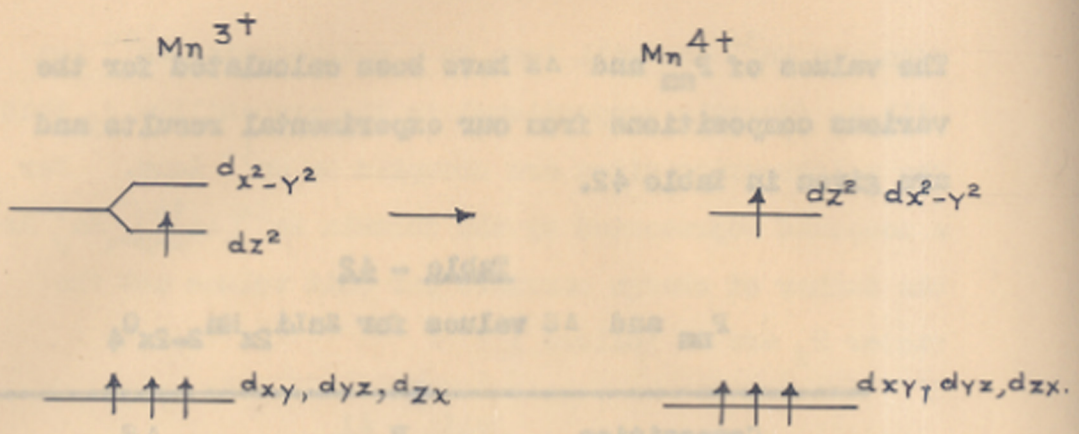
Mn 3+
Mn 4+
dx²-y²
dz²
dz² dx²-y²
dxy, dyz, dzx
dxy, dyz, dzx.

FIG 21.

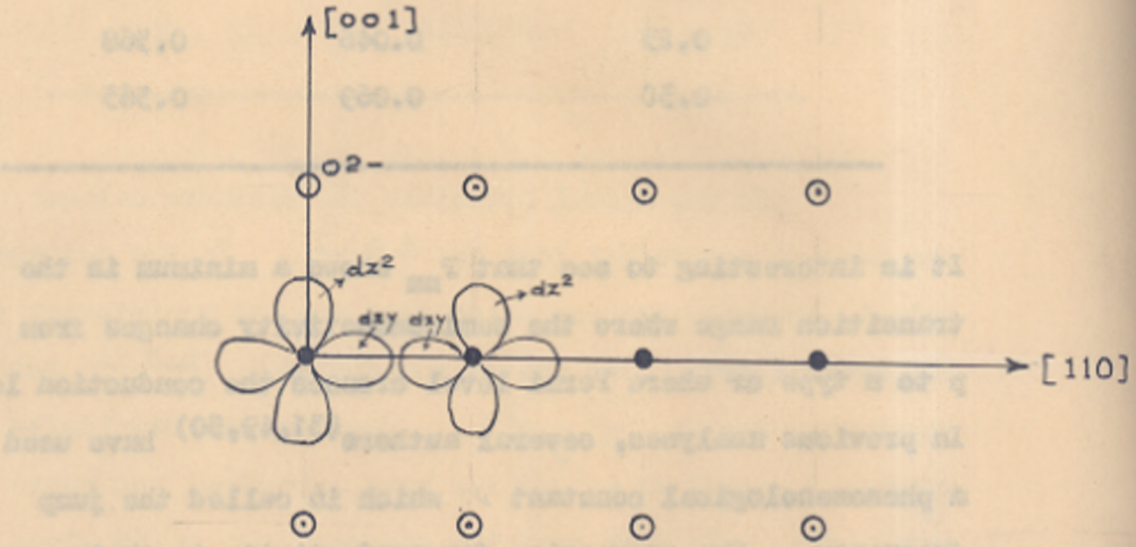
[001]
O2-
dz²
dz²
dxy dxy
[110]

FIG. 22

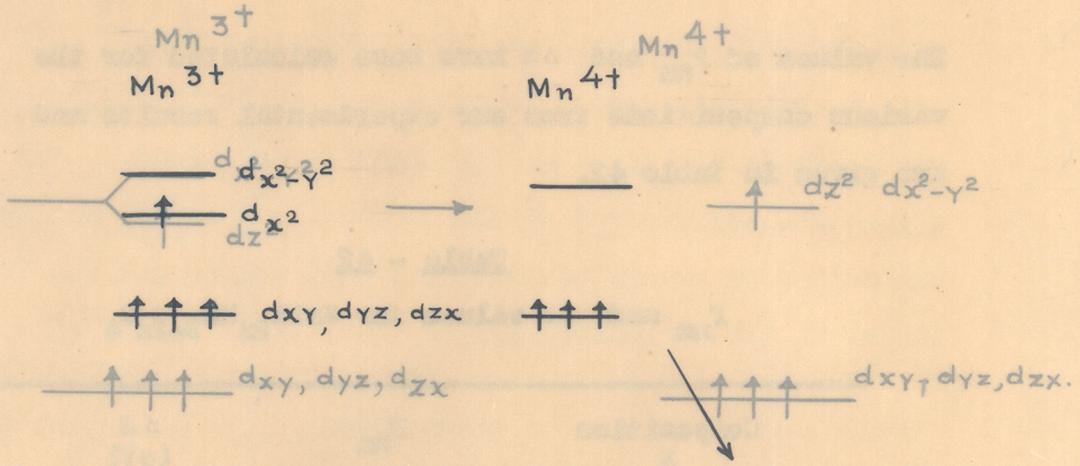

FIG 2.1

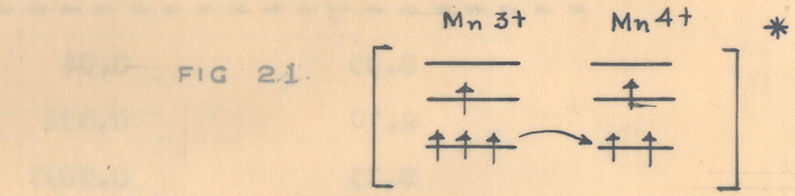

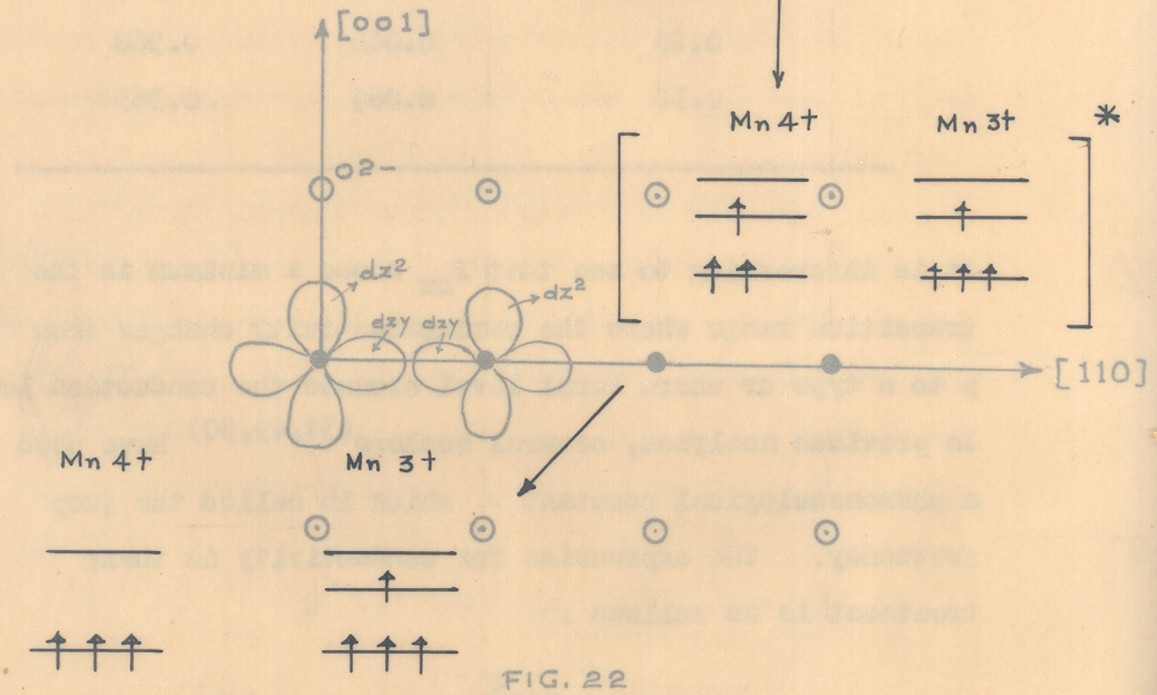

FIG. 22

FIG. 23.

In case of the present systems, the jump frequency as calculated from this formula is of the order of 10^{13}/sec. This appears to be of the same order of magnitude as reported earlier[32].

P_{nm} depends on the overlap between the wave functions localised on the adjacent sites and the activation energy Δ depends on the energy required to establish the near neighbour coincidence. The most straight forward transition which could be responsible for conduction is from the occupied dz^2 orbital of the Mn^{3+} ion to the empty dz^2 orbital of the adjacent Mn^{4+} ion as shown in Fig. 21. However, dz^2 orbitals point towards the oxygen ions and the overlap between the neighbouring dz^2 orbitals would be much smaller than that of the neighbouring dxy orbitals as can be seen from fig. 22. Thus P_{nm} in this case is expected to be at least an order of magnitude lower than in those cases where electron transfer is taking place between the d_{xy} (or any d_γ) levels e.g. in $Fe^{2+} \rightleftharpoons Fe^{3+}$, $Co^{2+} \rightleftharpoons Co^{3+}$, $Ni^{2+} \rightleftharpoons Ni^{3+}$. The jump frequency ($\alpha P_{nm}^2$) should have been hundred times lower, which surely is not the case.

The other possibility is the formation of an intermediate excited state in which one electron of the Mn^{4+} ion occupies the upper dr orbital. The d - d transition is possible as shown in fig. 23. The two configurations marked (*) are activated complexes as in these cases one of the electrons of the Mn^{4+} ion occupies the higher dr orbitals. If the electron transfer is to take place

through the formation of an intermediate activated complex of this type then the activation energy ΔE should at least be equal to the $d\epsilon - dr$ separation. This value is expected to be around 2eV. As the experimentally observed value of the activation energy is much lower, this mechanism of electron transfer seems to be ruled out.

The mechanism suggested by Sinha and Sinha, where crystal field oscillations cause a mixing of the atomic d orbitals with some excited orbitals, appears to overcome many of these above difficulties. The excited orbitals are expected to be less tightly bound than the d orbitals and it is reasonable to expect that there would be a considerable overlap of such wave functions on the adjacent sites. Therefore these excited states will offer an easier path for conduction by the hopping mechanism. This mechanism introduces in the denominator of the pre-exponential factor, a term dependent on the energy separation of the excited orbitals with respect to the ground state and causes a decrease in this factor. It must however be realised that in solids these energies are not large (may be only ~ 5 eV). Furthermore, any decrease due to this energy denominator will be more than compensated by the increase in the appropriate matrix elements due to the increased overlap. In fact a rough estimate of the order of magnitude of various contributions has shown that transitions via such empty orbitals may predominate in suitable cases[43]. The fact

that the mixing of 3d states with higher states does take place in the 3d transition metal oxides is well supported by the optical absorption studies on these compounds.

The activation energy ΔE depends on the energy required to establish the near neighbour coincidence. In the past, it has been assumed that the energy is required only to shift the polarisation from one site to the next. However, there are additional factors which also have to be taken into account. In the present case one has to take into account the energy required to shift the Jahn-Teller distortion. Let us take the ion pair Mn^{3+}-Mn^{4+}. If we assume that the oxygen ions surrounding the Mn^{3+} form a distorted octahedron whereas those surrounding the Mn^{4+} ions form a regular octahedron, then after an electron transfer this arrangement must be exchanged. If we take the energy of the undistorted molecule as zero, the energy lowering due to the Jahn-Teller distortion around Mn^{3+} ion would be given by

$$E = -\alpha Q + \beta Q^2$$

where 'Q' is a normal displacement representing the required distortion. The first term is the energy lowering due to the Jahn-Teller effect and the second is the elastic energy term which opposes distortion. The equilibrium value of $Q(= Q_{eq})$ is obtained from the condition that this total energy must be minimum. Thus,

$$Q_{equ.} = \alpha/2\beta$$

and $$E_{equ.} = -\alpha^2/4\beta$$

For the octahedron around Mn^{4+}, $Q = 0$, and $\mathcal{E} = 0$ as there is no Jahn-Teller distortion. However, in order that an electron transfer take place from the Mn^{3+} to Mn^{4+} ion, an activated complex in which the surroundings of both the ions are identical has got to be formed. The energy of this complex will be approximately

$$\mathcal{E} = -\alpha Q + 2\beta Q^2$$

so that $$Q^* = \alpha/4\beta$$

and $$\mathcal{E}^* = -\alpha^2/8\beta$$

Thus the energy required to form the activated complex

$$\Delta\mathcal{E} = \mathcal{E}^* - \mathcal{E}_{equ.} = \frac{\alpha^2}{8\beta} = \frac{\beta Q_{eq}^2}{2}.$$

It is interesting to note that in the activated complex, the distortion around the Mn^{3+} decreases to half the equilibrium value and the octahedron around the Mn^{4+} ion gets correspondingly distorted so that they both become identical.

On the basis of the present experimental results it is very difficult to establish that there is a contribution to the activation energy due to the Jahn-Teller effect discussed above. However, we do observe that in manganites the activation energy for conduction is always higher than that in the corresponding ferrites. For example, one could

FIG -24 ACTIVATION ENERGY Vs COMPOSITION

(FIG. REPRODUCED FROM THE PAPER BY R.R. HEIKES & W.D. JOHNSTON)

FIG 25 VARIATION OF ACTIVATION ENERGY AS A FUNCTION OF CHARGE CARRIERS.

COMPOSITION X IN Li x T (1-x) O

FIG -24 ACTIVATION ENERGY Vs COMPOSITION

(FIG. REPRODUCED FROM THE PAPER BY R.R. HEIKES & W.D. TOMNSTON)

compare $Zn[Li^{1+}_{.4}Mn^{3+}_{.8}Mn^{4+}_{.8}]O_4$ or $Cu^{1+}[Mn^{3+}Mn^{4+}]O_4$ with $Fe^{3+}[Fe^{3+}Fe^{2+}]O_4$. Here all the compounds have nearly equal number of charge carriers but the activation energies are widely different. Whereas for the two manganites we have the values as .35 eV and .25 eV respectively, for the ferrite we have the value of .05 eV only. Thus there is a difference of at least 0.2 eV which may very well be due to the Jahn-Teller effect discussed above. In case of Li substituted Ni oxides, a similar difference has been observed by Heikes and Johnston. Their results are reproduced in Fig. 24. It can be seen that for any corresponding composition the value of the activation energy for $[Li_xMn_{1-x}O]$ is always higher than that for any other system. Although in lithium substituted MnO the conduction is by the electron exchange between Mn^{2+} and Mn^{3+} ions, the arguments in regard to Jahn-Teller effects are equally applicable.

Another interesting observation is the dependence of ΔE on the composition or on the number of charge carriers. It can be seen from the Fig. 25 that ΔE is high when the number of charge carriers is small and it decreases rapidly as this number increases. Similar observation has been made for almost all oxidic semiconductors. The reasons are not yet clear but possibly the polarisation around one charge carrier is reduced if there are other charge carriers close by.

Zinc copper manganites.

Amongst the substances studied under this series

there is only one homogeneous compounds i.e. $Zn_{.5}Cu_{.5}Mn_2O_4$ apart from pure $CuMn_2O_4$ whose properties have already been reported by Sabane[8].

The thermoelectric coefficient of $Zn_{.5}Cu_{.5}Mn_2O_4$ is $\sim$ 40 uv/ ^oC and is positive indicating that $S_{\frac{1}{2}} > S$ or the number of Mn^{3+} ions at the octahedral site is greater than that of Mn^{4+} ions. Out of the two possible ionic formulae i.e. (i) $Cu^{1+}_{.5}Zn^{2+}_{.5}[Mn^{3+}_{1.5}\ Mn^{4+}_{.5}]O_4$ and

and (ii) $Cu^{2+}_{.5}Zn^{2+}_{.5}[Mn^{3+}]_2O_4$

the first would explain the high electrical conductivity and the positive thermoelectric coefficient of the compound in a very satisfactory way. As explained earlier the thermoelectric coefficient S is related to the number of Mn^{3+} and Mn^{4+} ions by the equation :

$$S = \frac{A}{eT} + k \ln \frac{M-n}{n}$$

where the significance of all the terms are as explained on page 31 . The mobility is low ($\sim 10^{-3}$ cm^2/sec x volt at 375^oK) and rises exponentially with temperature following the relationship $\mu = \mu_o \exp \frac{\Delta E}{kT}$. These results indicate that the mechanism of conductivity in this compound is almost similar to that in zinc-lithium manganites. The value of P_{nm} is equal to 0.02 and that of jump frequency is of the order of 10^{13}/sec. However there are some differences which can be seen by a quantitative comparison amongst them.

For comparison, we take those members where the Mn^{3+} and Mn^{4+} concentrations are as close as possible. One such pair is

$$Cu_{.5}Zn_{.5}[Mn^{3+}_{1.5}\ Mn^{4+}_{.5}]\ O_4^{2-}$$

and $$Zn[Li_{.2}\ Mn^{3+}_{1.4}\ Mn^{4+}_{.4}]\ O_4^{2-}$$

The electrical properties of these two compounds have been compared in the table 43.

Table - 43

Comparison of electrical properties

	$Cu_{.5}Zn_{.5}[Mn^{3+}_{1.5}Mn^{4+}_{.5}]O_4$	$Zn[Li_{.2}Mn^{3+}_{1.4}Mn^{4+}_{.4}]O_4$
Electrical conductivity	p-type	p-type
Activation energy (ΔE)	0.24 eV	0.39 eV
ρ (Room temp.)	$4.0\times10^{2}\ \Omega$	$3.35\times10^{5}\ \Omega$
Structure	Tetragonal	Tetragonal

It is interesting to note here that although the amount of Mn^{3+} and Mn^{4+} ions at the octahedral sites which is supposed to be responsible for electrical conductivity, is about the same, the resistivity at room temperature as well as the activation energy are considerably different. The fact that we have in the second case some Li^{1+} ions at the octahedral site will not by itself be able to explain this amount of difference. The high electrical conductivity

and low activation energy for $Cu_{.5}Zn_{.5}Mn_2O_4$ suggest that there is an additional mode of conductivity for the copper manganite series. One can attribute this to the presence of a small amount of Cu^{2+} ions at tetrahedral sites; thus for $CuMn_2O_4$ the structure could be $Cu^{2+}_{.1}Cu^{1+}_{.9}[Mn^{3+}_{.1}Mn^{4+}_{.9}]O_4$ instead of $Cu^{1+}[Mn^{3+}Mn^{4+}]O_4$. Similarly the structure of $Cu_{.5}Zn_{.5}Mn_2O_4$ could be $Cu^{1+}_{.45}Cu^{2+}_{.05}Zn^{2+}_{.5}[Mn^{3+}_{1.55}Mn^{4+}_{.45}]O_4$. Thus there would be conduction not only by electron exchange between Mn^{3+} and Mn^{4+} ions but also by such exchanges between Cu^{1+} and Cu^{2+} ions. Another explanation is that in this series the conduction is not only by 'd' electron hopping but there is also some contribution from the band type conductivity.

+ + + +

PART - II

MAGNETIC PROPERTIES

OF

ZINC LITHIUM MANGANITES

AND

ZINC COPPER MANGANITES

2.1. Introduction.

In this section, the work carried out on the magnetic properties of the manganites will be reviewed.

Honda and Sonne[51] (1944) measured the magnetic susceptibility of Mn_3O_4 at 20°C and found the value to be 55.8×10^{-6}. This measurement was extended by Moore, Merylinn and Selwood[52] (1952) who got χ values at three different temperatures i.e. $\chi_{298°K} = 54.2 \times 10^{-6}$; $\chi_{193°K} = 66.6 \times 10^{-6}$; $\chi_{93°K} = 126 \times 10^{-6}$. Borovik, Romanov and Orlova[53] (1957) carried out this study for the temperature range of 20° to 300°K, and observed that Mn_3O_4 becomes ferromagnetic below 42.5°K and the temperature dependence of the magnetic susceptibility above the Curie temperature is well described by the formula

$$\frac{1}{\chi} = \frac{T}{C} + \frac{1}{\chi_0} - \frac{\sigma}{T-\theta}$$

derived by Neel to explain the magnetic properties of ferrites. The ferromagnetic properties of ferrites were successfully explained by Neel[54] (1948) by assuming that all the tetrahedral spins are parallel to one another as are the octahedral spins but these two spins are mutually antiparallel. This is the result of a stronger negative exchange interaction (J_{AB}) between A (tetrahedral) and B (octahedral) ions as compared to that between A and A (J_{AA}) or between B and B (J_{BB}).

In regard to manganites, however, there are many experimental results where a straightforward application of Neel's model does not give the correct result. For example, it was found that Mn_3O_4 has a lower saturation magnetisation than that predicted by the Neel model. Jacob[55] (1959) attempted to explain this on the basis of Yafet and Kittel's theory. Y and K[56] (1952) had shown by taking into account the existence of six sublattices in the spinel structure that for large antiferromagnetic B-B interaction a triangular arrangement was more stable than the Neel's arrangement. Here, the spins on one site fall into two similar sublattices, each sublattice being ferromagnetically saturated. The magnetisations of the two sublattices, however, are at angle to each other and their resultant is antiparallel to the magnetisation of the spins on the other site.

Jacob[55] (1959) studied compounds of the general formula $(M_xMn_{1-x})Mn_2O_4$ where M is Co, Zn and Mg. The magnetisation on these was measured at 4.2^oK, using pulsed fields upto 140 kilo-oersteds. A field-dependent susceptibility has been observed in these compounds. This observation supported the triangular model of Yafet and Kittel and directly measured the strength of B-B interaction. The spontaneous moment of Mn_3O_4 has been observed as 1.56 ± 0.04 Bohr magneton per molecule with the B-site moments subdivided into groups at angles.

Recently, Jacob and Kouvel[57] (1961) have extended the magnetic studies on these mixed manganites. They have observed a unidirectional anisotropy which was detected by the observation of hysteresis loops displaced along the field axis when the materials were cooled to low temperatures in magnetic fields of several kilo-oersteds. Further, the unidirectional behaviour is stable to reverse field pulses of 140 Koe. An exchange anisotropy model is proposed involving interactions between ferrimagnetic and nearly antiferromagnetic regions brought about by the random distribution of the diamagnetic ions among the tetrahedral sites.

Dwight and Menyuk[58] (1960) investigated the magnetic properties of single crystals of Mn_3O_4 between 4.2^oK and 41.9^oK (Curie temperature). Their results showed that although the concept of canted spin appeared to be essentially correct, the Yafet-Kittel theory was over-simplified and the conclusions based on this did not agree quantitatively with their experimental results.

Kaplan[59] (1960) has shown theoretically that the Yafet Kittel arrangements are not stable in cubic spinels. Such arrangements can however get stabilised in the presence of tetragonal distortion. He also showed that it is possible to have arrangements in which there are non-zero angles between those on B sites and this is contrary to the Yafet and Kittel's results.

Lyons, Kaplan, Dwight and Menyuk[60] (1961) have shown that for B-B interactions which are sufficiently large to destabilise the Neel's configuration in the cubic spinels a spiral spin arrangement has lower energy than Neel's or Y.K's. They expect the spiral to be the ground state for $8/9 < u < 1.298$ where $u = (4J_{BB}S_B)/(3J_{AB}S_A)$, S_A and S_B being the spin magnitudes at the A and B sites respectively.

Menyuk, Dwight, Lyons and Kaplan[61] (1962) have extended this study to the tetragonal spinels and have given diagrams in a space described by the ratios of various exchange interactions showing stability regions of Neel, Y.K. and the collinear antiferromagnetic spin configurations.

Wickham and Croft[26] (1958) studied several spinels containing manganese. A complete range of solid solutions in the system $Co_{3-x}Mn_xO_4$ was prepared and crystallographic and magnetic properties of these were studied. The values for the saturation magnetic moment were measured at 4.2°K. The cation distribution (for $0 \leq x \leq 2.0$) has been written as $Co^{2+}[Co^{3+}_{2-x}Mn^{3+}_x]\ O_4$. Although, the magnetic moments for these compounds, has been thought to arise as a result of indirect Neel type coupling between the Co^{2+} ions at tetrahedral sites (A-sites) and Mn^{3+} ions on the octahedral sites (B-sites) the possibility of the existence of triangular coupling has been overlooked and cannot be ruled out. The number of Mn^{3+} ions on the octahedral sites increases through

the composition range $0 \leq x \leq 1.2$ and the number of A–B interactions increases producing a constantly rising Curie temperature which reaches a maximum of 191°K at $x = 1.2$. An abrupt change in the magnetisation curve occurs for this value of x. An appreciable magnetic moment appears again for values of $x > 2.1$ reaching the maximum of 1.4 Bohr magneton for pure Mn_3O_4.

Sabane[3] (1960) has carried out the paramagnetic susceptibility measurements at different temperatures for $CdMn_2O_4$, $ZnMn_2O_4$, $MgMn_2O_4$, Mn_3O_4, $CoMn_2O_4$, $NiMn_2O_4$ and $CuMn_2O_4$. The variation of paramagnetic susceptibility of $CdMn_2O_4$ with temperature is according to the Curie–Weiss law. $ZnMn_2O_4$ exhibits a temperature independent susceptibility. The susceptibility variation for the other compounds is similar to that of a ferrimagnetic material above its Curie temperature (of Neel's equation). For $MgMn_2O_4$ this was interpreted as due to a partially inverse structure of the compound in which some Mn^{3+} ions had moved to the tetrahedral sites and an equal amount of Mg^{2+} ions to the octahedral sites. The ferrimagnetism in the rest of the compounds was explained on the basis of the Neel's theory of ferrimagnetism and the Yafet-Kittel's modification.

A theoretical study on antiferromagnetism in some normal spinels (cubic or tetragonally distorted) has been done by Sinha and Sinha[62] (1962). The normal spinels

selected were such that the cations located at tetrahedral sites are diamagnetic while those at octahedral sites are paramagnetic. The molecular field approximation has been used. They have found out that the most stable arrangement is one in which each $\langle 110 \rangle$ and $\langle 1\bar{1}0 \rangle$ row is antiferromagnetically ordered with the spin vectors pointing along these directions. The arrangement predicts temperature independent magnetic susceptibility below the transition temperature for all fields. Reference is made to experimental confirmation of this in certain spinels.

Some manganites exhibit a different type of exchange interaction which is now commonly known as 'double exchange'.

Magnetic behaviour of $LaMnO_3$-$CaMnO_3$ and of $LaMnO_3$-$SrMnO_3$ were studied by G.H.Jonker and J.H. Van Santen[5] (1950). These compounds have perovskite structure and are ferromagnetic and conducting. They attributed this behaviour to strong positive $Mn^{3+} - Mn^{4+}$ exchange interaction combined with a weak $Mn^{3+} - Mn^{3+}$ interaction and a -ve $Mn^{4+} - Mn^{4+}$ interaction. The $Mn^{3+} - Mn^{4+}$ interaction was presumed to be of the indirect exchange type and was thought to be the first example of a +ve exchange interaction in oxidic substances.

C.Zener[6] (1951) however, interpreted the electrical and magnetic properties as arising from the coupling of the incomplete d shells due to electron exchange

via O^{2-} ions. In $LaMnO_3$, if some of the La^{3+} ions are replaced by Ca^{2+} ions, it is necessary that the corresponding number of Mn^{3+} ions change to Mn^{4+} ions. Here, these two manganese ions are separated by a O^{2-} ion. Zener investigated the problem of electron transfer from the Mn^{3+} ion to the Mn^{4+} through the oxygen ion. The wave function before and after the transfer can be represented by Ψ_1 and Ψ_2.

$$\Psi_1 : Mn^{3+}\ O^{2-}\ Mn^{4+}$$

$$\Psi_2 : Mn^{4+}\ O^{2-}\ Mn^{3-}$$

It was shown that the exchange energy ϵ, given by

$$\epsilon = \int \Psi_1^a (H - \epsilon_o)\ \Psi_2\ d\tau$$

where H is the Hamiltonian of the whole system and ϵ_o is the energy associated with the initial state Ψ_1 and Ψ_2, is non-vanishing only if the spins of the two d-shells are parallel. This indirect ferromagnetic coupling through the oxygen ion was called double exchange. Such coupling arises as the system is inherently degenerate due to the presence Mn ions of two different charges. It can also be seen that this type of exchange causes high conductivity. Zener has also established the following quantitative relation between the electrical conductivity (σ) and ferromagnetic Curie temperature (Tc) :

$$\sigma \simeq \frac{xe^2}{ah} \left(\frac{Tc}{T} \right)$$

where x is the fraction of the Mn ions which have a 4+ charge

and 'a' is the distance between the Mn^{3+} and Mn^{4+} ions involved in the electron exchange. The agreement with Jonker and Van Santens' experimental results was found to be good.

R.R.Heikes, T.R.McGuire and R.J.Happel[7] (1961) have studied the magnetic structure of lithium substituted manganese selenide. Paramagnetic susceptibility has been measured at various temperatures and from the results obtained they conclude that at low temperatures, the hole which is introduced by the Li^+ is loosely bound to the Li^+ itself. In the region of the Li ion, double exchange causes local distortions of the spin system which they refer to as clusters. As the Li concentration is increased the clusters overlap sufficiently so that a magnetic field induces an appreciable magnetic moment. At higher concentrations of lithium they observe the spontaneous magnetisation below 110°K. As the temperature is lowered through 70°K the spontaneous moment disappears and antiferromagnetism is found.

P.G. De Gennes[63] (1960) has theoretically studied the effects of double exchange in magnetic compounds of mixed valency. He has shown that this type of electron exchange should always give rise to a distortion of the ground state spin arrangement. If the Zener carriers are mobile the distortion would correspond to a uniform canting of the spin sublattices. The bound carriers, on the other hand, were expected to give a non-homogeneous distortion, but the

average effects would be the same as above. It was found that the canted arrangements would be stable upto a temperature T. Above this temperature the systems were expected to change to either antiferromagnetic or ferromagnetic state depending upon the relative amounts of the mobile electrons.

The magnetic behaviour of some chromites where oxygen ion has been replaced by S, Se or Te has been studied by Lotgering (1964). $CuCr_2X_4$ where X = S, Se, Te and $ZnCr_2Se_4$ were investigated. These compounds exhibited the spinel structure. Copper compounds showed strongly ferromagnetic properties and were found to be highly conducting, while $ZnCr_2Se_4$ was found to be semiconducting and did not show any ferromagnetic properties. According to him the ferromagnetic properties in copper compounds were due to double exchange interaction.

In what follows, we discuss the results of our studies on the paramagnetic susceptibility of zinc lithium manganites and zinc copper manganites.

+ + + +

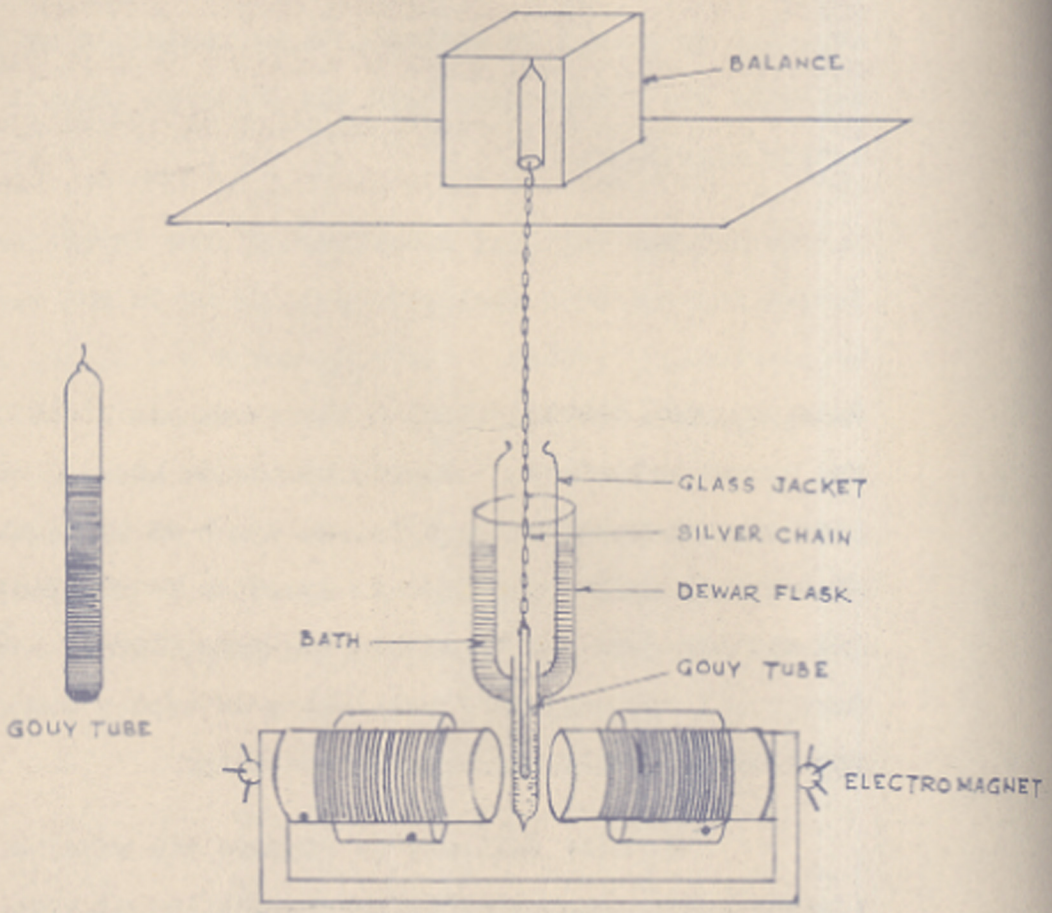

FIG. 26 GOUY METHOD FOR SUSCEPTIBILITY MEASUREMENTS.

2.2. Experimental technique.

The Gouy method for the susceptibility measurements was followed. If a cylindrical sample of matter is suspended between the poles of a magnet so that one end of the sample is in a region of large field strength and the other in a region of negligible field, then the force acting on the sample,

$$f = \frac{1}{2} KH^2A$$

where K = vol. susceptibility, H = magnetic field applied and A = Area of crossection of the sample. f is conveniently measured by suspending the sample from the balance, then, $f = g \times \Delta W = \frac{1}{2} KH^2A$, g = gravitational constant. Hence, to measure K, it is necessary to produce a steady magnetic field and to measure the change in weight of the substance after the application of field.

A small flat face electromagnet (Fig. 26) with a gap between the magnetic pole pieces of about 3.8 cms was used. The magnet was fed through a continuously variable stabilised supply of 0-160 volts D.C. and 0-10 amperes current. A steady magnetic field of about 5000 oersteds was obtained by passing a current of 5 amps. through the coils of the electromagnet. This field was used at all temperatures.

The change in weight was measured by a Metler-make single pan micro balance which could read upto 0.01 milligram. This was found to be satisfactory for diamagnetic compounds also.

A cylindrical pyrex specimen tube, 20 cms. in length and with a uniform internal diameter of 3 mm was chosen. This tube was filled with the specimen under study upto a fixed mark and suspended from the pan of the microbalance to the centre of the magnetic pole pieces. A silver chain was used for suspending the tube. As mentioned previously, the bottom of the specimen tube was kept at the centre of the large uniform magnetic field, and the other end of the sample was in the region of negligible field. The specimen tube was surrounded by a cylindrical pyrex glass tube, used as a glass chamber, which again was fixed in the specially designed double walled pyrex Dewar flask arranged in the centre of the magnetic pole pieces. Dry nitrogen gas was circulated through the glass chamber so that the susceptibility of the medium was negligible.

The susceptibility was measured at about 93°K, 194.5°K, 273°K, 298°K and 330°K. The desired temperature was obtained by using suitable baths. Sufficient time was allowed for the attainment of equilibrium at a given temperature. The temperatures were measured by using a calibrated copper-constantan thermocouple.

As mentioned earlier, the force f acting on a sample in the magnetic field is $f = \frac{1}{2} KH^2A = g \cdot \Delta W$, from which the relation

$$\frac{\chi_1 w_1}{\chi_2 w_2} = \frac{\Delta w_1}{\Delta w_2}$$

can be easily obtained where,

χ_1 = magnetic susceptibility per gm. of sub.1;

χ_2 = magnetic susceptibility per gm. of sub.2;

w_1 = wt. of the subs. 1;

w_2 = wt. of the subs. 2;

Δw_1 = apparent change in wt. of sub. 1;

Δw_2 = apparent change in wt. of sub. 2.

Hence, $$\chi_2 = [\chi_1 \frac{w_1}{\Delta w_1}] [\frac{\Delta w_2}{w_2}]$$

i.e. ifthe magnetic susceptibilities of the two compounds are measured under identical conditions, and the value of χ for one of the compounds is known, then χ_2 can be easily obtained from the above relation. x .

If , $$\frac{\chi_1 w_1}{\Delta w_1} = A, \quad \chi_2 = A \frac{\Delta w_2}{w_2}$$

A is denoted as the tube constant for the magnetic set up.

The magnetic balance was calibrated with the aid of Analar grade copper sulphate $CuSO_4, 5H_2O$. The accepted value of magnetic susceptibility for copper sulphate is χ gm. = 6.24×10^{-6} at 300^0K.

By using this constant the magnetic susceptibility of Mn_3O_4 (specpure) was determined at various temperatures. The values for Mn_3O_4 at different temperatures were in agreement with those reported by Moore, Merilian, and Selwood (1952). These values were accepted as secondary

standards and the mean specimen tube constant A for all temperatures between 93°K to 350°K was found to be A = 13.52×10^{-4}. The specimen tube was kept the same throughout the measurements of the susceptibility of the compounds under investigation. The magnetic susceptibility measurements on conductivity water gave an additional check on the value of the tube constant.

Thus, the values for $\chi_{gm.}$ of the unknown substances were obtained by knowing the change in weight of the unknown sample under identical conditions.

+ + + +

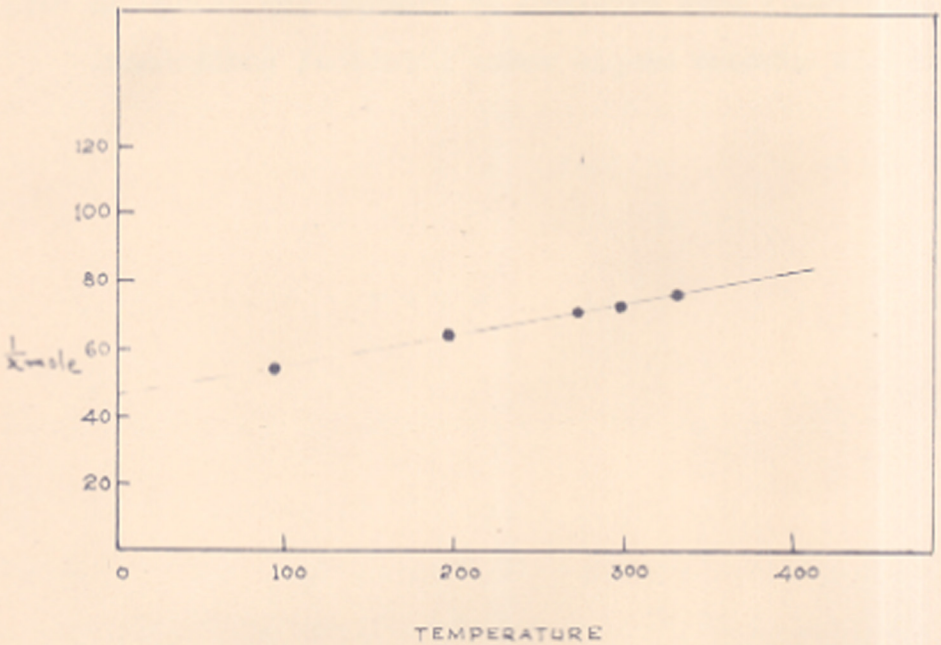

FIG 27· VARIATION OF $\frac{1}{\chi}$ mole AS A FUNCTION OF TEMPERATURE FOR $Zn\ Li_{.1}\ Mn_{1.9}\ O_4$

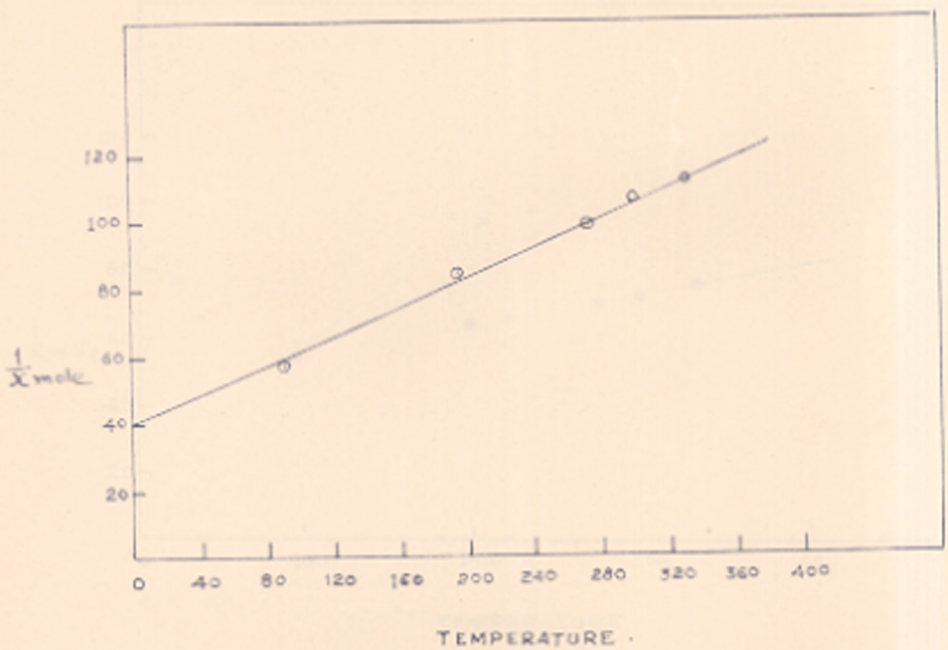

FIG 28. VARIATION OF $\frac{1}{\chi}$ mole AS A FUNCTION OF TEMPERATURE FOR $Zn\ Li_{.2}\ Mn_{1.8}\ O4$

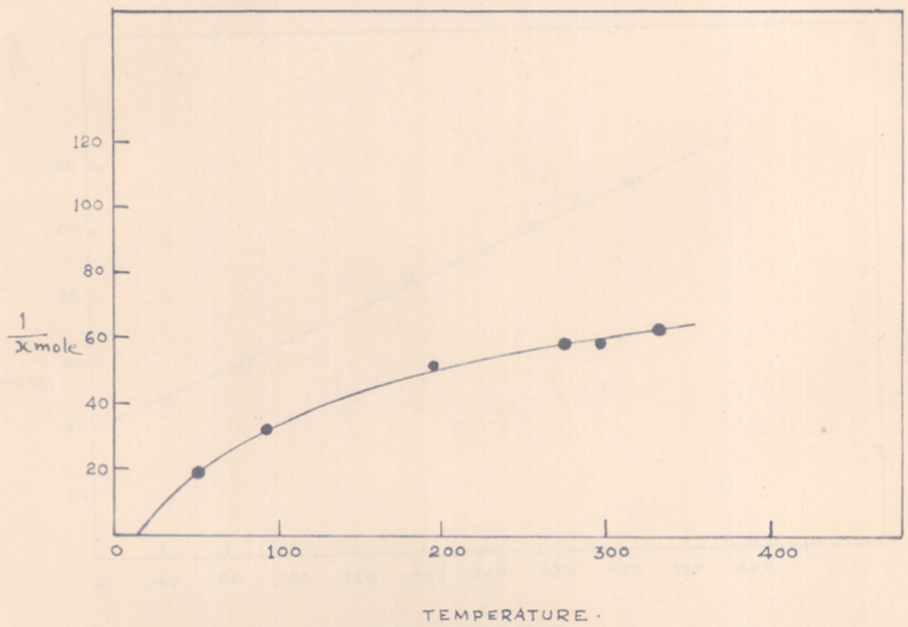

FIG. 29 VARIATION OF $\frac{1}{x}$ mole AS A FUNCTION OF TEMPERATURE FOR $Zn\ Li_{.3}\ Mn_{1.7}\ O4$

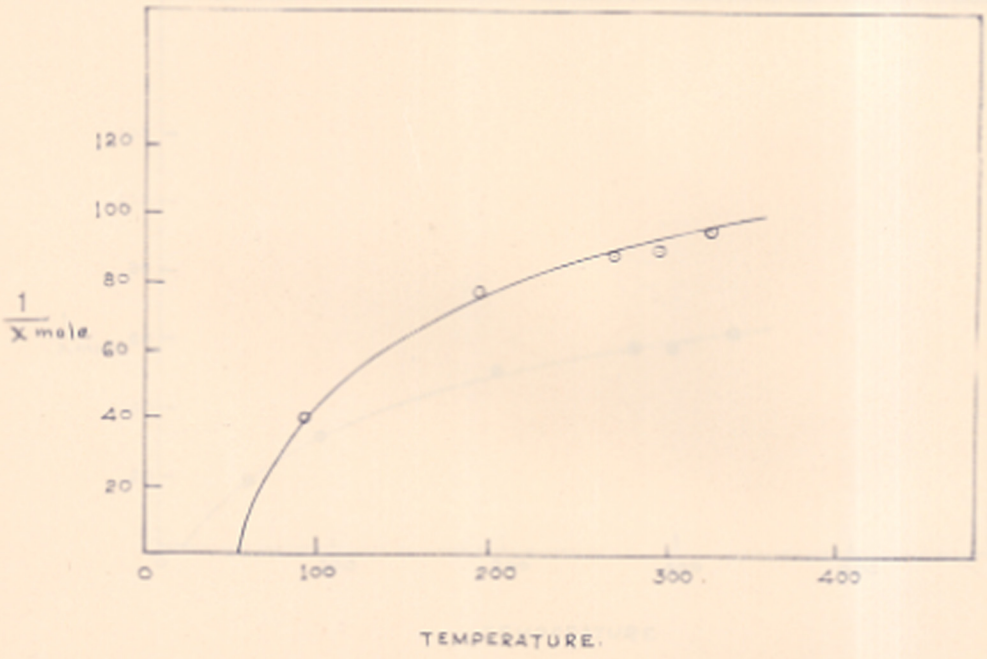

FIG. 30. VARIATION OF $\frac{1}{X}$ mole AS A FUNCTION OF TEMPERATURE FOR $Zn\ Li_{.4}\ Mn_{1.6}\ O_4$

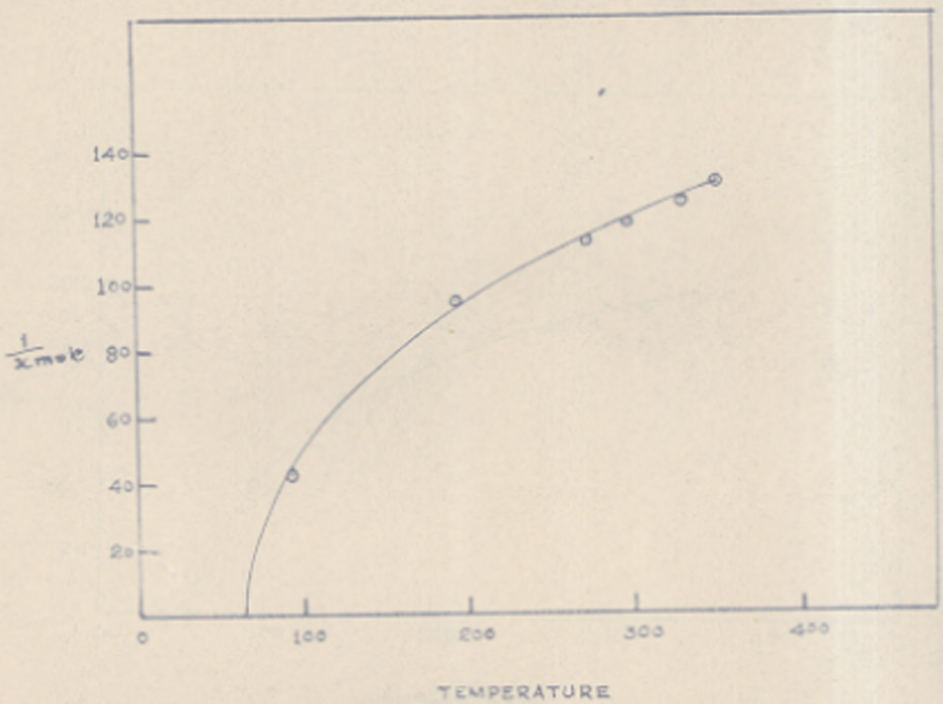

FIG. 31 VARIATION OF $\frac{1}{\chi}$mole AS A FUNCTION OF TEMPERATURE FOR $Zn\ Li_{.5}\ Mn_{1.5}\ O_{3.88}$

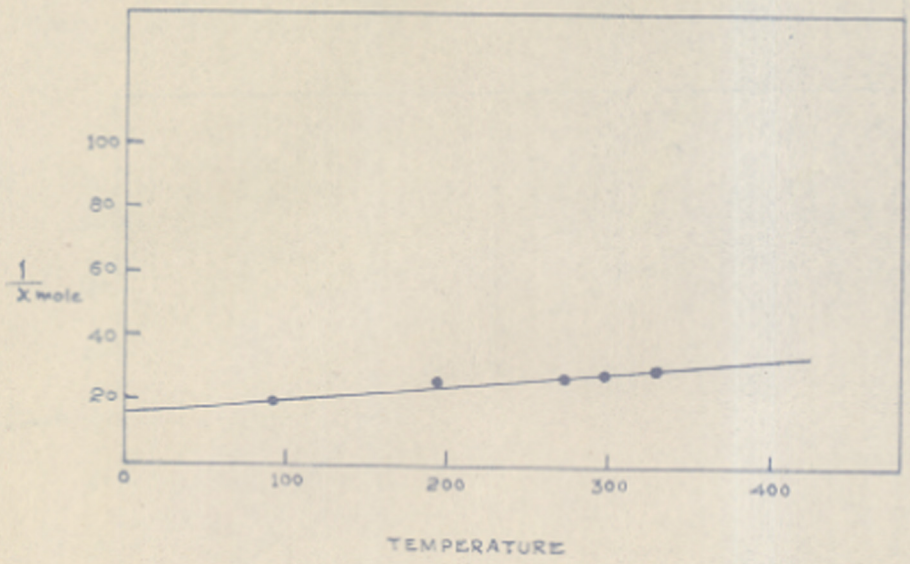

FIG. 32 VARIATION OF $\frac{1}{\chi_{mole}}$ AS A FUNCTION OF TEMPERATURE FOR $Zn\ Li_{.6}\ Mn_{1.4}\ O_{3.82}$

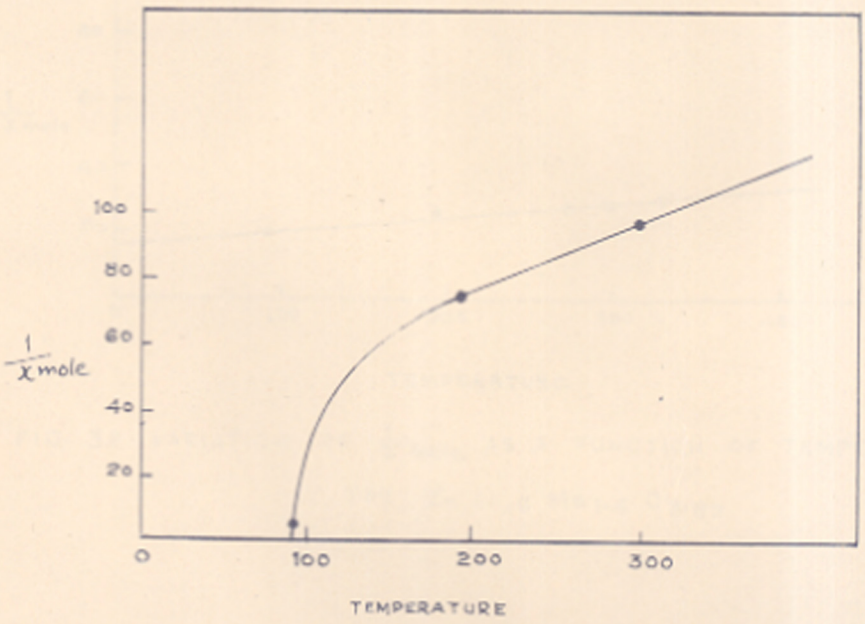

FIG. 31 VARIATION OF $\frac{1}{\chi}$ mole AS A FUNCTION OF ABSOLUTE TEMPERATURE FOR THE COMPOUND $(Cu_{.95}\ Zn_{.05})\ Mn_2\ O_4$.

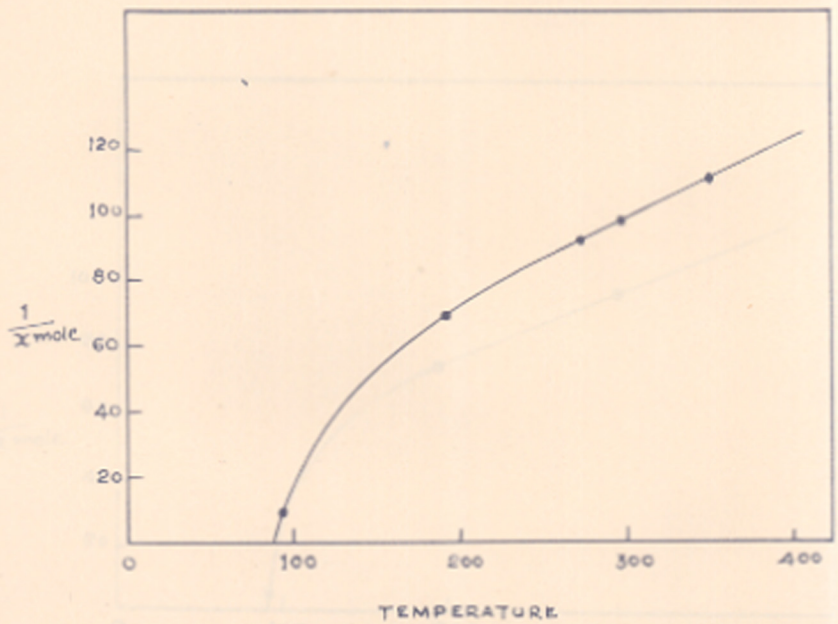

FIG- 32 - VARIATION OF $\frac{1}{\chi}$ mole AS A FUNCTION OF AN ABSOLUTE TEMPERATURE FOR THE COMPOUND $(Zn_{.1}\ Cu_{.9})\ Mn_2O_4$.

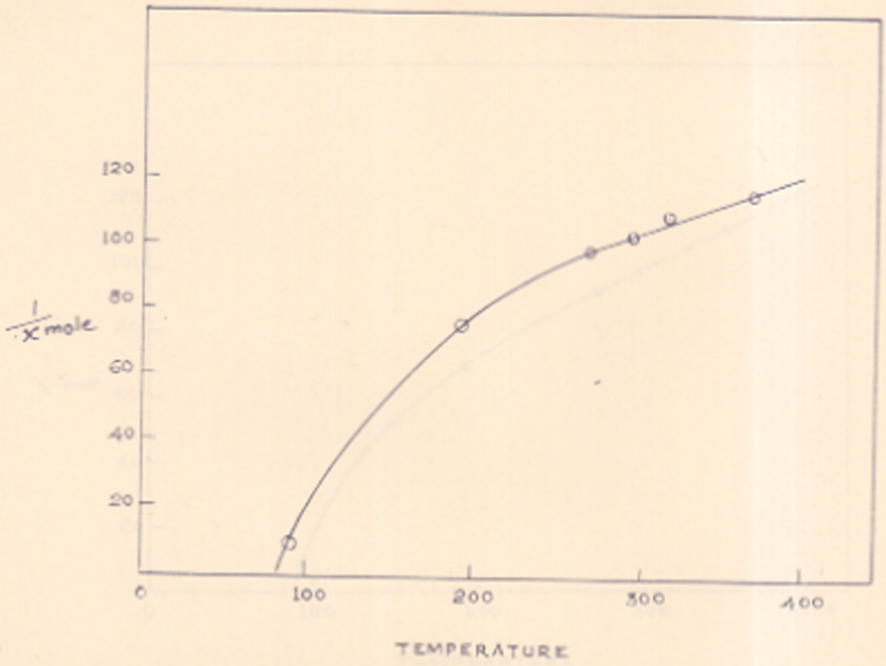

FIG 33- VARIATION OF $\frac{1}{\chi}$ mole AS A FUNCTION OF THE TEMPERATURE FOR $(Cu_{.85}Zn_{.15})Mn_2O_4$

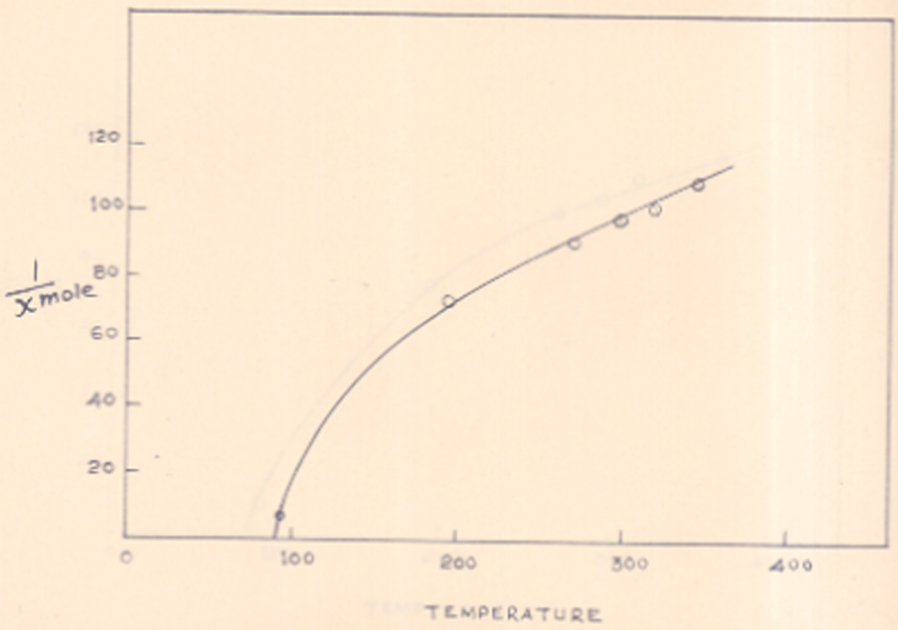

FIG 34 - VARIATION OF $\frac{1}{\chi \text{ mole}}$ VS. $T^{\circ}K$ FOR THE COMPOUND $(Cu_{.8}\ Zn_{.2})\ Mn_2\ O_4$

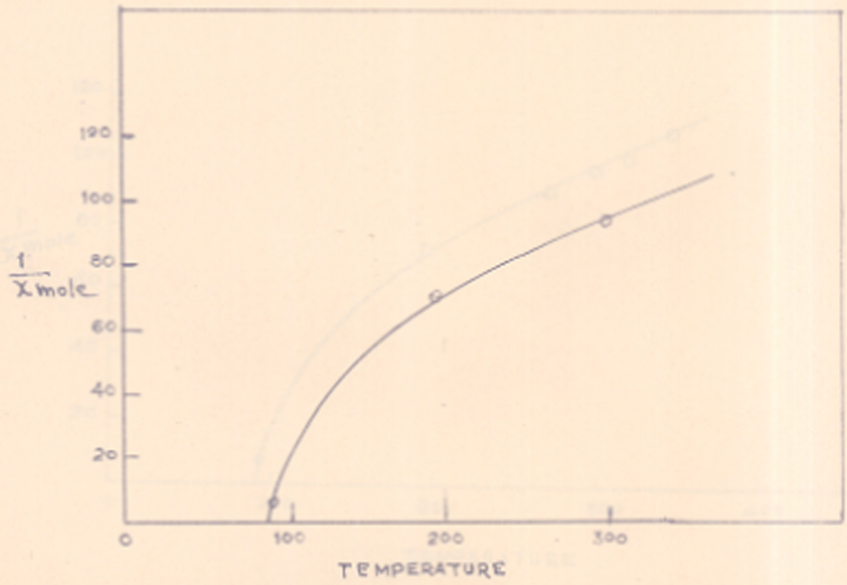

FIG. 35 - VARIATION OF $\frac{1}{\chi}$ mole AS A FUNCTION OF AN ABSOLUTE TEMPERATURE FOR THE COMPOUND $(Cu_{.75}Zn_{.25})Mn_2O_4$

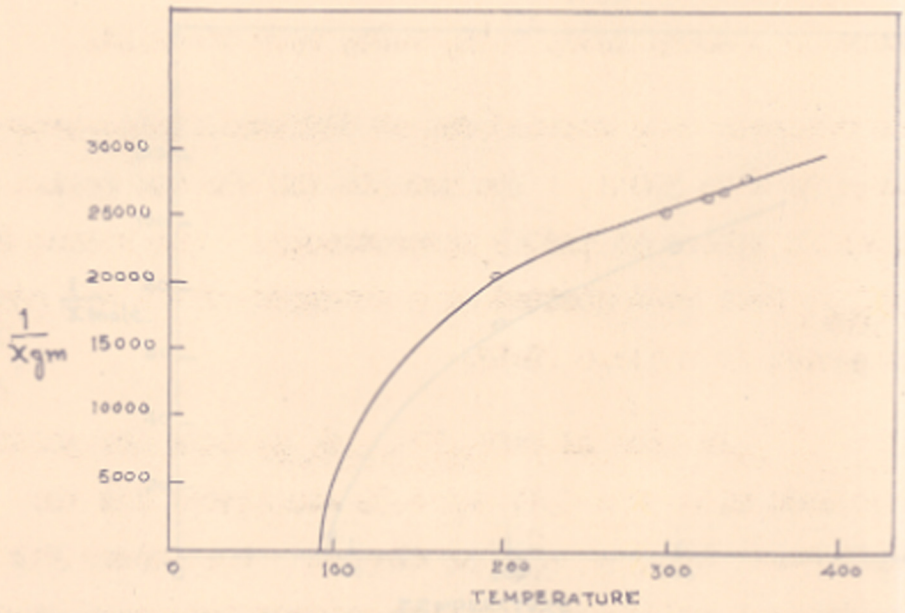

FIG. 36 VARIATION OF $\frac{1}{\chi_{gm}}$ VS T FOR THE COMPOUND $(Cu_{.5}\ Zn_{.5})Mn_2O_4$

2.3. Experimental Results.

The paramagnetic susceptibilities of the following series of compounds were measured by the Gouy method :

(i) $ZnLi_{2x}Mn_{2-2x}O_4$

where x = 0.05, 0.10, 0.15, 0.20, 0.25 and 0.30.

(ii) $Zn_yCu_{1-y}Mn_2O_4$

where y = 0.05, 0.10, 0.15, 0.20, 0.25 and 0.50.

Measurements were carried out at different temperatures in the range 90°K to 350°K. The results for the two series are given in Tables 44 and 45 respectively. The values of $1/\chi_{Mol.}$ have been plotted as a function of T°K and are presented in figures 27-38.

In case of $ZnLi_{2x}Mn_{2-2x}O_4$ series, the plots for compounds with x = 0.05 and 0.10 are linear and the Curie-Weiss law $\chi = \frac{C}{T+\theta}$ is obeyed. The values for the constants C and θ for these two systems have been calculated from the graph and are given in Table 44. The $\frac{1}{\chi}$ - T plots for compounds with x = 0.15, 0.2 and 0.25 seem to obey the equation

$$\frac{1}{\chi} = \frac{T}{C} + \frac{1}{\chi_0} - \frac{\sigma}{T-\theta}$$

given by Neel for the paramagnetic susceptibility of ferrimagnetic substances above the Curie temperature.

Here C, $\frac{1}{\chi_0}$, σ, θ are constants related to various magnetic interactions and concentration of cations over A and B sites. These constants were calculated as follows : At high temperatures the last term i.e. $\frac{\sigma}{T-\theta}$ becomes very small and so

$$\frac{1}{\chi} = \frac{T}{C} + \frac{1}{\chi_0}$$

$\frac{1}{\chi_0}$ and C were therefore obtained from the extrapolated intercept and the slope of the curve in the high temperature limit. Making use of these values of C, χ_0 and the experimentally observed values of χ at low temperatures, the constants σ and θ were obtained. These values were used to refine the values of C and χ_0 and the process of successive refinement was continued till the best match with the experimental values was obtained. The values of the constants thus calculated for the systems x = 0.15, 0.20 and 0.25 are included in Table 44. The theoretical values according to Neel's equation using the above constants are given by graph while the experimental points are the full circles on the graph. It can be seen that the agreement is quite good. The compound x = 0.30 shows a nearly temperature-independent susceptibility. The C and θ values for this system are 24 and 388 respectively.

In case of $Zn_yCu_{1-y}Mn_2O_4$ series all the compounds which have been studied exhibit the Neel-type variation. Here also the various constants have been calculated by the

method discussed above and are presented in Table 45. In the figures the calculated values are shown by full lines and experimental values by circles. The agreement is good. However it must be realised that the results for systems with Y = .05 - .25 are of limited significance as they consist of mixed phases. The systematic variation of the constants is to be expected because of the progressive dilution of the ferrimagnetic phase. However, the two end members i.e. pure $CuMn_2O_4$ and $Zn_{.5}Cu_{.5}Mn_2O_4$ are homogeneous and ferrimagnetic, and so a study of their properties is quite interesting. The results are discussed in the next chapter.

Table - 44

Paramagnetic susceptibility results for zinc lithium manganites

Comp. / Temp.	Values of $1/\chi_{molar}$ 93°K	194.5°K	273°K	298°K	330°K	Constants
$ZnLi_{0.1}Mn_{1.9}O_4$	54.25	67.66	71.8	75.55	75.5	θ = +500 C = 10.9
$ZnLi_{.2}Mn_{1.8}O_4$	56.96	85.98	97.5	106.4	110.8	θ = +185 C = 4.6
$ZnLi_{.3}Mn_{1.7}O_4$	32.29	52.36	58.4	59.21	63.2	θ = - 70 C = 20 $\frac{1}{\chi_o}$ = 59.5 σ = 5200
$ZnLi_{.4}Mn_{1.6}O_4$	41.45	79.27	88.45	89.33	94.0	θ = 6.5 C = 10 $\frac{1}{\chi_o}$ = 75.5 σ = 3750
$ZnLi_{.5}Mn_{1.5}O_{3.88}$	44.42	96.94	113.7	119.3	126.7	θ = 35 C = 4.6 $\frac{1}{\chi_o}$ = 62.5 σ = 2250
$ZnLi_{.6}Mn_{1.4}O_{3.81}$	20.09	26.75	28	28.26	29.88	θ = 388 C = 24

Table - 45

Paramagnetic susceptibility results for zinc copper manganites

Comp.	values of $1/\chi_{moles}$						Constants			
	Temp. 93°K	194°K	273°K	298°K	323°K	350°K	θ	C	$\frac{1}{\chi_o}$	σ
0.05	2.85	73.64		94.58			80	5.5	44.4	760
0.1	9.42	71.53	91.26	97.79		111.6	50	5	48.6	2502
0.15	8.31	74.82	97.7	102.3	108.1	114.7	60	5.1	53.06	2078
0.2	7.43	75.15	92.17	99.28	102.0	109.8	50	5.2	52.76	2122
0.25	4.616	70.89		90.99			68	5.3	43.0	1400
0.5	16.31	88.82	104.2	108.9	112.7	118.8	60	5.6	64.5	2100

2.4. Discussions.

2.4.1. Zinc-Lithium manganites.

Pure zinc manganite[8,33] shows a temperature independent magnetic susceptibility in the temperature range 100-200°K and above 200°K it has a Curie-Weiss type behaviour. These results have been analysed theoretically by Sinha and Sinha (1962) and they concluded that zinc manganite is anti-ferromagnetic in this temperature range. The most stable arrangement was found to be one in which each $\langle 110 \rangle$ and $\langle 1\bar{1}0 \rangle$ row is antiferromagnetically ordered with spin vectors pointing in this direction. This arrangement could explain the temperature independent susceptibility.

Zinc lithium manganites with low concentrations of Li^{1+} ions (i.e. for $x \leqslant 0.10$) appear to be paramagnetic and the slopes for $\frac{1}{\chi}$ vs T plots increase with increasing concentration of Li^{1+} ions; From a temperature independent susceptibility for pure zinc manganite the plot changes to a Curie Weiss straight line for the composition $x = 0.1$. The C value for $x = 0.1$ is 4.6 and the calculated value for this composition is 5.0 assuming the molecular formula as $Zn[Li^{1+}_{.2}\ Mn^{3+}_{1.6}\ Mn^{4+}_{.2}]\ O_4$. The agreement is fair. However, no transition to antiferromagnetic phase has been observed in the temperature range of our investigations.

The $\frac{1}{\chi}$ vs T plots for compositions in the range $0.15 \leqslant x \leqslant 0.25$ are not linear but are curved concave

towards the temperature axis. This is indicative of a transition to ferromagnetic phase at lower temperatures. The extrapolated values of the Curie temperature are 64°K, 54°K, 18°K for the compositions x = 0.25, 0.2 and 0.15 respectively. The existence of the ferromagnetic phase is very interesting, as a straightforward application of Neel's theory does not predict a ferromagnetic behaviour for these compounds. Since all the tetrahedral sites are occupied by Zn^{2+} ions which are diamagnetic, the negative B-B interaction would predominate leading to antiferromagnetic ordering at low temperatures. The fact that we have some Li^{1+} and Mn^{4+} ions at the octahedral sites does not change the situation if these ions are distributed at random over the two sublattices. The net magnetic moments of the two sublattices will still be equal and opposite, although each one is reduced in magnitude due to the presence of Li^{1+} and Mn^{4+}.

The presence of Mn^{3+} and Mn^{4+} ions at the octahedral sites suggests the possibility of an interaction of the type, first observed by Jonker in $(LaCa)MnO_3$[5]. As mentioned earlier, the theoretical foundation for this type of interaction which has been named as "double exchange", has been laid by Zener. He has shown that there exists a possibility of ferromagnetic coupling in crystals containing an ion in two different valence states. The theoretical work has been extended by Anderson and Hasegawa[64] (1955), and

more recently by P.G.DeGennes[63] (1960). Although the majority of the compounds where this type of coupling has been observed belong either to the perovskite structure or to the NaCl structure, recently Lotgering has observed such coupling in $CuCr_2X_4$ where X is S, Se or Te which have the 'spinel' structure. The experimental results indicate the presence of Cr^{3+} and Cr^{4+} at the octahedral sites and a ferromagnetic ordering of their spins due to double exchange. However, in case of zinc-lithium manganites, there are a few results which do not fit in with the behaviour expected for compounds showing double exchange interactions. This type of interaction is known to give rise to metallic type of conductivity. $La_xCa_{1-x}MnO_3$, $Li_xMn_{1-x}Se$, and $CuCr_2X_4$ (X = S, Se or Te) show the metallic type of conductivity. Conductivity of these compounds is high at room temperature and decreases with increasing temperature following $\frac{1}{T}$ relationship. If one substitutes 10% La in $LaMnO_3$ by Ca, the room temperature conductivity is increased by two orders of magnitude. $CuCr_2Se_4$ has a very high room temperature conductivity ($\sigma \simeq 10^4$ mho/cm) and a small negative temperature coefficient of conductivity. On the other hand $ZnCr_2Se_4$ which has a much smaller conductivity and a positive temperature coefficient of conductivity is not ferromagnetic and does not show double exchange. Similar behaviour is observed in lithium substituted transition metal oxides studied by Johnston and Heikes[31]. All the compounds showed semi-conductivity

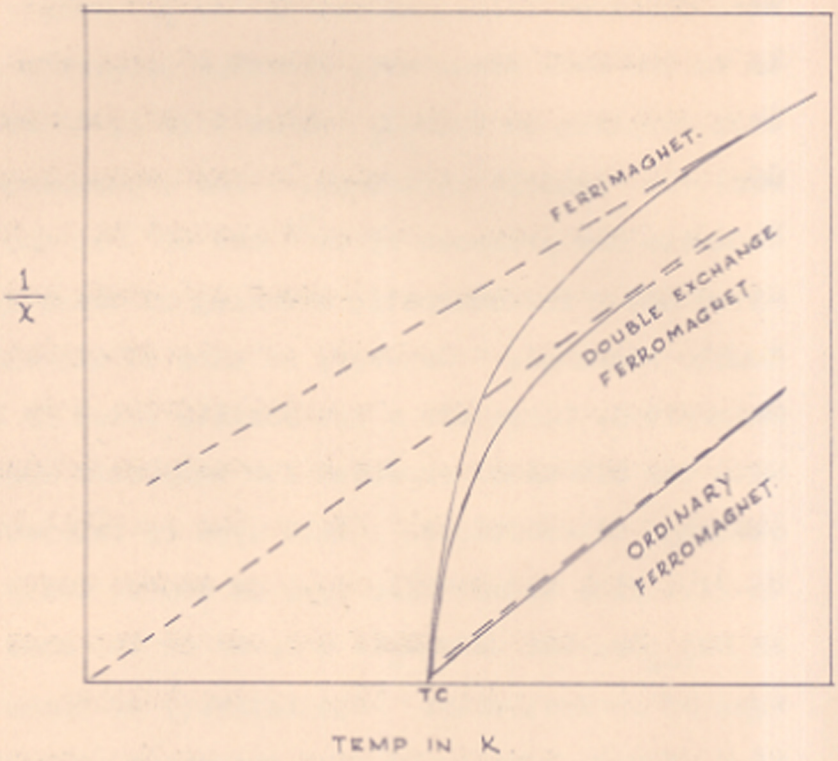

FIG-39 QUALITATIVE SUSCEPTIBILITY CURVES FOR FERRIMAGNET, FERROMAGNET, AND DOUBLE EXCHANGE FERROMAGNET.

rather than metallic conductivity and they did not show any ferromagnetism. Thus it appears established that the double exchange interaction always leads to metallic type conductivity. The absence of this type of conductivity therefore excludes the possibility of the existence of double exchange in the zinc lithium manganites. Furthermore, $LiMn_2O_4$ whose most probable structure is $Li[Mn^{3+}Mn^{4+}]O_4$ has been synthesised by Wickham and Croft and later by Lopatin but the compound is not ferromagnetic and is a semiconductor. From the ionic formula this compound would appear as ideal for the existence of double exchange. Its absence can be only due to the possibility that in the oxide spinel the double exchange cannot occur because the lattice is polar ; hence the charge carriers are trapped due to induced polarisation of the lattice. The replacement of oxygen by sulphur or selenium in the spinel lattice decreases the extent of electron trapping, rendering the double exchange possible.

The $\frac{1}{\chi}$ - T plot also is not as is expected from compounds showing double exchange. The backward extrapolation of the high temperature part of the plot meets the temperature axis at negative T. This does not match either with the theoretical results of Anderson and Hasegawa (see fig. 39 reproduced from their paper) or the experimental results on $LaCaMnO_3$ and $CuCr_2X_4$. Anderson and Hasegawa predict that the extrapolation of the high temperature curve passes through the origin (i.e. T = o). The experimental

results on $LaCaMnO_3$ and $CuCr_2X_4$ show linear $\frac{1}{\chi}$ - T plots meeting the temperature axis at positive temperature values.

On the basis of these considerations the existence of double exchange interactions in zinc lithium manganites may be ruled out.

One plausible explanation of the observed behaviour is that a small fraction (say $\sim$ 5%) of the paramagnetic ions i.e. Mn^{3+} or Mn^{4+} are present at the tetrahedral sites. It is not possible to determine the cation distribution by X-ray analysis to an accuracy sufficient to rule out the possibility of this small extent of migration. This arises from the fact that differences in the X-ray scattering power of Zn and Mn ions is very small. Although the Zn^{2+} ions are known to have a larger preference for the tetrahedral sites as compared to Mn^{3+} or Mn^{4+} ions, it is quite likely that some disorder is introduced at the high temperatures used for preparation of the samples which can remain quenched even at room temperature. In that case the observed behaviour can arise from the ferrimagnetic arrangement due to the negative A-B interaction. That about 5% magnetic ions at tetrahedral sites are adequate to produce observable ferromagnetism can be seen from the results on $ZnMgFe_2O_4$ solid solutions[65]. Sabane[8] and Miyahara and Muramori[66] (1960) have found that $MgMn_2O_4$, when quenched from high temperatures shows a small ferromagnetism and this has been attributed to a partial migration of Mn^{3+} ions from the octahedral to tetrahedral sites.

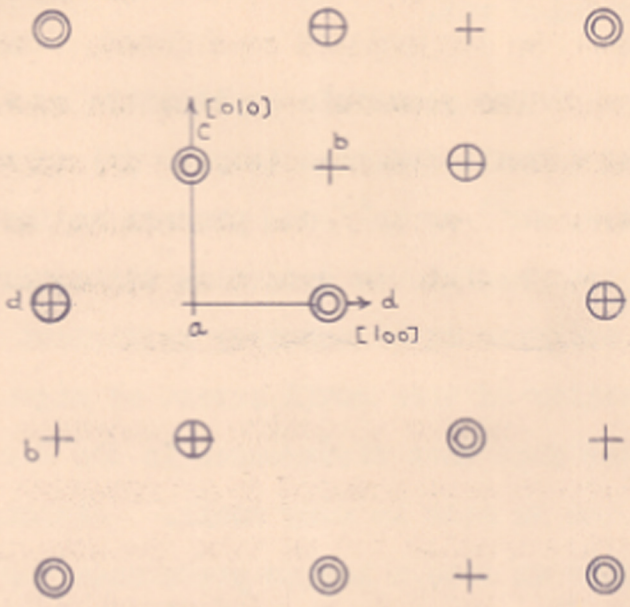

FIG-40 THE OCTAHEDRAL METAL IONS AND THE OXYGEN. IONS IN THE SPINEL STRUCTURE

◎ ABOVE THE PLANE OF THE DIAGRAM.

\+ IN THE PLANE OF THE DIAGRAM

⊕ BELOW THE PLANE OF THE DIAGRAM.

This type of migration seems to explain the observed behaviour of the zinc lithium manganites very well. Particularly the temperature variation of the magnetic susceptibility is exactly what one would expect for the ferrimagnetic compounds. The only apparent difficulty is about the composition dependence. The fact that ferromagnetism appears only when the numbers of Mn^{3+} and Mn^{4+} at octahedral sites are equal or in other words manganese ions do not migrate to the tetrahedral sites when $x < 0.15$ or $x > 0.25$, does not find a straightforward explanation on the basis of the above picture.

Another plausible explanation could be the formation of some ordered superstructure at low temperatures. As an illustration let us take the composition $Zn[Li_{.5}Mn^{4+}_{1.0}Mn^{3+}_{.5}]O_4$. Following Yafet and Kittel we subdivide the B sites into four sublattices a, b, c, d. If we take one ion from each sublattice they form a tetrahedron as shown in fig. 40. The other ions in the figure are oxygen ions. Li^{1+} ion at any one site of a lattice (say a) acts as an effective charge carrier of - 2e and is able to attract two holes (Mn^{4+} ions) to form bound states and the arrangement having minimum electrostatic energy is one in which all the Li^{1+} ions are arranged on the sublattice "a" and all the Mn^{4+} ions on the sublattice 'b' and 'c' and the Mn^{3+} ions on 'd' (as Li^{1+}, Mn^{4+}, Mn^{3+} = 1 : 2 : 1 for the composition $Zn[Li^{1+}_{.5}Mn^{4+}_{1.0}Mn^{3+}_{.5}]O_4$).

We have three sublattices b, c, d occupied by the magnetic ions. If the interactions γ_{bc}, γ_{cd} and γ_{bd} are assumed to be much larger than the interactions of the type γ_{bb}, γ_{cc}, γ_{dd}, the molecular fields acting on the lattices b, c, d can be written as :

$$\underline{H}_b = \gamma_{bc} \underline{M}_c + \gamma_{bd} \underline{M}_d$$

$$\underline{H}_c = \gamma_{cd} \underline{M}_d + \gamma_{bc} \underline{M}_b$$

$$\underline{H}_d = \gamma_{bd} \underline{M}_b + \gamma_{cd} \underline{M}_c$$

and the interaction energy E is given by

$$E = -\frac{1}{2} \sum \underline{H}_i \underline{M}_i$$

$$= - \left[\gamma_{bc} \underline{M}_b \cdot \underline{M}_c + \gamma_{bd} \underline{M}_b \cdot \underline{M}_d + \gamma_{cd} \underline{M}_c \cdot \underline{M}_d \right]$$

If $M_b : M_c : M_d = 3 : 3 : 4$, $\gamma_{bd} = \gamma_{cd}$ and

α is the angle between $\underline{M}_b$ and $\underline{M}_c$

β is the angle between $\underline{M}_b$ and $\underline{M}_d$ and

γ is the angle between $\underline{M}_c$ and $\underline{M}_d$.

$$E = - K \left[\gamma_{bc} \cos \alpha + \frac{4}{3} \gamma_{bd} (\cos \beta + \cos \gamma) \right]$$

where K is a constant.

$$= + K \left[a \cos \alpha + b (\cos \beta + \cos \gamma) \right]$$

where $a = \gamma_{bc}$ and $b = \frac{4}{3} \gamma_{bd}$.

Two cases arise : (i) there is no anisotropy energy i.e. the

spins are free to align in any direction; (ii) there is a large anisotropy energy and there are only certain preferred directions of magnetisation. The first case leads to a triangular spin arrangement with no net magnetisation. However for the second case, the lowest energy configuration will be ferrimagnetic. Let us take for example, a case where the (100) directions are easy directions of magnetisation. In this case for $a < b$, the minimum energy is obtained when M_b and M_c are parallel to one another and antiparallel to M_a, for $a > b$ the minimum energy is obtained when M_a and M_c are parallel to one another but antiparallel to M_b. Both arrangements lead to a resultant magnetic moment and the compound should be ferrimagnetic. On the other hand, if the (110) directions are easy directions for magnetisation, the triangular arrangement of the type shown in Fig. 41 has the lowest energy. This arrangement also gives rise to a net magnetic moment of one Bohr magneton. We have not discussed all the possibilities but the above considerations are adequate to show that it is possible to get a ferrimagnetic structure if the ions at the octahedral site get ordered. It is however not possible to decide as to which type of arrangement is actually prevalent in the present system.

At low lithium concentrations this type of ordering will not be possible because the number of these ions will be too small to form a continuous chain over one sub-lattice. At higher concentrations the amount of Mn^{3+} ions

will become small and the same difficulty will arise. This type of ordering is therefore, expected to be present only in the compositions close to $Zn[Li_{.5}Mn^{4+}_{1.0}Mn^{3+}_{.5}]O_4$, and in fact this is what is actually observed.

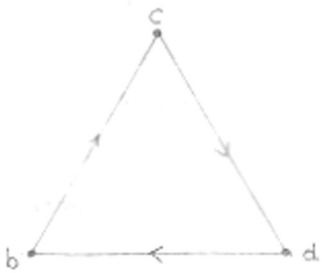

FIG - 41

2.4.2. Zinc-Copper manganites.

In this series there is only one compound which is homogeneous and single phased i.e. $Cu_{.5}Zn_{.5}Mn_2O_4$. We will confine our discussion to this compound and shall examine its properties in relation to those of pure copper manganite studied by Sabano (1960) and Baltser and Lopatin (1964).

Both these compounds obey the Neel's equation

$$\frac{1}{\chi} = \frac{T}{C} + \frac{1}{\chi_0} - \frac{\sigma}{T-\theta}$$

This is indicative of the fact that they are ferrimagnetic at low temperature. For copper manganite this is already confirmed experimentally. The Curie constants (for these

two substances as experimentally determined are given in Table 46 together with the calculated values (spin only) for the various possible ionic formulae. The Curie constants were calculated by the formula :

$$C_A = n(n+2)\frac{N_o \beta^2}{3K}$$

where K = Boltzmann constant;

N_o = Avagadro's number;

β = Bohr magneton

and n = no. of free spins on an ion.

The C_A values are additive so the C_M can be obtained by adding the C_A values for the various ions constituting the molecule.

Table - 46

Composition	Measured C_M	Spin only C_M	
		$Cu^{2+} + Mn^{3+}$	$Cu^{1+} + Mn^{4+}$
$CuMn_2O_4$	5.63	6.38	4.88
$Cu_{.5}Zn_{.5}Mn_2O_4$	5.60	6.19	5.44

In case of copper manganite the agreement is not good for either of the two structures and the experimental results are suggestive of some intermediate formula. The composition $Cu^{1+}_{.5}Cu^{2+}_{.5}[Mn^{3+}_{1.5}Mn^{4+}_{.5}]$ would give the calculated

value of C_N = 5.6 which would match exactly with the experimental results. In fact the ionic arrangement would also explain the high electrical conductivity of the material. However, the cubic symmetry would become anomalous. There would be about 12 Mn^{3+} ions per unit cell at the octahedral sites. This would be greater than the critical number ($\sim$9.0) required to bring about the tetragonal distortion (Irani, Sinha and Biswas[27]). The formula $Cu_x^{2+}Cu_{1-x}^{1+}[Mn_{1+x}^{3+}Mn_{1-x}^{4+}]O_4$ with $0.1 \leqslant x \leqslant 0.2$ would appear more appropriate. This would be consistent with the structural and electrical properties. The C_N value would be 5.0 - 5.2 which would be only slightly lower than the experimental value. Pallot and Maroni[67] have found in the case of ferrites that the observed C is lower than the calculated C as can be seen from the following table.

Table - 47

Ferrite	$\frac{1}{\lambda_0}$	σ	θ^0K	Range of validity deg.	C' cal.	C obs.
Fe_2O_3.FeO	103.2	15,100	777	700-1100	11.9	14.2
Fe_2O_3.CoO	111.9	11,550	744	700-1200	11.8	13.9
Fe_2O_3.NiO	191.8	7,750	863	800-1200	10.0	19.5

This discrepancy has been attributed to a thermal variation of molecular field coefficients caused by a progressive increase in interatomic distance (thermal expansion). Neel states that this effect plays an important role in the interpretation of the magnetic properties of ferrites.

Similar discrepancy between the observed and calculated C has also been observed in our own results discussed earlier in connection with zinc lithium manganite. The calculated and observed values of C of the ferrimagnetic compounds are given in Table 48.

Table - 48

Ionic Formula	$C_{obs.}$	$C_{cal.}$
$Zn[Li_{.3}Mn^{3+}_{1.1}Mn^{4+}_{.6}]O_4$	20	4.43
$Zn[Li_{.4}Mn^{3+}_{.8}Mn^{4+}_{.8}]O_4$	10	3.9
$Zn[Li_{.5}Mn^{3+}_{.74}Mn^{4+}_{.76}]O_4$	4.6	3.65

In addition to the reasons given by Neel there may be some other factors which are responsible for high C in case of zinc lithium manganites. Cluster formation of a few magnetic ions may be one of the reasons for this high value.

On the basis of the above ionic structure for copper manganite it is easy to explain the magnetic properties of zinc-copper manganite. If it is assumed that the same ratio of Cu^{1+} : Cu^{2+} is maintained then the ionic formula for $Cu_{.5}Zn_{.5}Mn_2O_4$ would be :

$$Zn_{.5}Cu^{2+}_{0.10-0.05}Cu^{1+}_{0.40-0.45}[Mn^{3+}_{1.10-1.05}Mn^{4+}_{0.90-0.95}]O_4 .$$

This arrangement would be consistent with the ferrimagnetic behaviour of the compound. About 5-10% of the tetrahedral sites would be occupied by the paramagnetic Cu^{2+} ions which would be adequate to cause ferrimagnetism as has already been shown earlier. The calculated value of the Curie constant C on the basis of this formula is approximately 5.5 which is in good agreement with the experimental value.

+ + + +

PART - III

JAHN-TELLER DISTORTION

IN

MIXED MANGANITES

3.1. Introduction.

The distortions from cubic symmetry which occur in certain transition metal oxides particularly those with the spinel structure (see page 8), has attracted the attention of a number of investigators.

Goodenough and Loeb[68] (1955) explained the tetragonal distortion in oxidic spinels as arising due to the tendency of octahedral ions to form square, coplanar, covalent bonds. A cation forming hybridized dsp^2 orbitals which point to the four corners of a square would prefer an octahedral interstice because the geometrical considerations indicate that such bonds can easily be formed in any of the three biaxial planes of such a site. At high temperatures, there can be a resonance of the covalent bonds in these biaxial planes, and the interstice can exhibit a cubic symmetry. Below the transition temperature the covalent bonds are frozen into one of the above three planes, so that now the octahedral cation is bound to its six neighbouring anions by four coplanar covalent bonds and two linear electrovalent bonds. Since the lengths of the former are shorter than those of the latter, the spinel gets distorted to a tetragonal symmetry with the axial ratio $c/a > 1$.

Dunitz and Orgel[69] (1957) have discussed these distortions in terms of the crystal field theory. When a transition metal cation is situated at the octahedral site, the five d orbitals no longer have the same energy

but are split into two energy groups, a lower triplet t_{2g} and an upper doublet e_g. The electrostatic repulsion between the d electrons and the surrounding negative ions cause the splitting. The doubly degenerate e_g orbitals ($d_{x^2-y^2}$, d_{z^2}) point towards the surrounding octahedral ions and are thus energetically destabilised, while the triply degenerate t_{2g} orbitals (d_{xy}, d_{yz}, d_{zx}) point between the surrounding ions, where the field is least and are therefore more stabilised.

In case of a tetrahedrally located cation the set of d orbitals splits into a lower doublet e and an upper triplet t_2 orbitals. The electrostatic repulsion between the d electrons and the four negative ions placed at the corners of a regular tetrahedron causes the splitting.

Dunitz and Orgel have pointed out that in many cases distortions are related in a simple fashion to the electronic configuration of the cation and may be considered to arise as a result of a Jahn-Teller distortion.

Jahn and Teller[70] (1937) have shown that if the electronic state of a non-linear molecule is degenerate the system is unstable and distortion to a lower energy state takes place. Jahn-Teller's theory may be illustrated by taking a particular example, that of Cu^{2+} ion. If the Cu^{2+} ion is situated at the octahedral site the d electron configuration of the ion is $(t_{2g})^6 (eg)^3$. It gives rise to a doubly degenerate ground state since two assignments

of the e_g electrons, $(d_{z^2})^2 (d_{x^2-y^2})^1$ and $(d_{z^2})^1 (d_{x^2-y^2})^2$ are possible. Hence the regular octahedral arrangement, according to the Jahn-Teller theorem, is unstable. The system could be energetically stabilized if a distortion from regular octahedral symmetry takes place. There are various possible distortions which could remove the degeneracy. However, in case of Cu^{2+} and Mn^{3+}, the tetragonal distortion of $c/a > 1$ is most commonly observed.

Opik and Pryce[71] (1957) and Liehr and Ballhause[72] (1958) have studied in details the conditions which stabilise a particular distortion in preference to others.

The magnitude of Jahn-Teller distortions depends on the bonding and anti-bonding power of the degenerate electrons. It varies from one transition metal ion to another according to the electronic configuration. It has been pointed out by Dunitz and Orgel that the maximum distortion is to be expected when degeneracy exists in anti-bonding orbitals. In octahedral coordination the t_{2g} orbitals are relatively non-bonding and consequently cause very small distortions. Van Vleck[73] (1939) has studied the distortions caused by d^1 and d^2 electrons and his results confirm the small distortions due to electrons from the t_{2g} non-bonding orbitals. It has been predicted by Dunitz and Orgel that configurations $(t_{2g})^3 (eg)^1$ and $(t_{2g})^6 (eg)^3$ produced by d^4 and d^9 electrons respectively

are degenerate with respect to strongly antibonding eg orbitals and should produce larger distortions.

The experimental results on manganites containing Mn^{3+} (d^4) ions at octahedral sites, confirm the above predictions given by Dunitz and Orgel. The table 49 gives the d electron configurations of the various ions at the octahedral and tetrahedral sites and the type of Jahn-Teller distortion expected.

Table - 49

Jahn-Teller distortions for d electrons

Ions	No. of d electrons	Octahedral configuration	Distortion	Tetrahedral configuration	Distortion
Ti^{3+}	1	t_{2g}	small	e	small
V^{3+}	2	$(t_{2g})^2$	small	$(e)^2$	0
V^{2+}, Cr^{3+}, Mo^{3+}	3	$(t_{2g})^3$	0	$(e)^2 t_{2g}$	large c/a > 1
Cr^{2+}, Mn^{3+}	4	$(t_{2g})^3(eg)^1$	large c/a > 1	$(e^2)(t_{2g})^2$	large c/a < 1
Mn^{2+}, Fe^{3+}	5	$(t_{2g})^3(eg)^2$	0	$(e)^2(t_{2g})$	0
Fe^{2+}, Co^{3+}	6	$(t_{2g})^4(eg)^2$	small	$(e)^3(t_{2g})^3$	small
Rh^{3+}, Co^{2+}	7	$(t_{2g})^5(eg)^2$	small	$(e)^4(t_{2g})^3$	0
Ni^{2+}	8	$(t_{2g})^6(eg)^2$	0	$(e)^4(t_{2g})^4$	large c/a > 1
Cu^{2+}	9	$(t_{2g})^6(eg)^3$	large c/a > 1	$(e)^4(t_2)^5$	large c/a < 1

The deviation of the number of oxidic spinels from the cubic symmetry could thus be explained on the basis of the predictions given by Dunitz and Orgel in the above table.

Bertaut, Bochirol and Weil[74] (1950) have observed that $CuFe_2O_4$ is tetragonally distorted at room temperature and above, and transforms to the cubic symmetry at 68°C. Prince and Treuting[75] (1956) and Miyahara and Ohinishi[76] (1956) determined the structure of $CuFe_2O_4$ and they found it to be inverse.

Structural properties of $CuCr_2O_4$ were studied by McGuire, Howard and Smart[77] (1952) and they observed it to be tetragonally distorted with $c/a \simeq 1.1$ which has been corrected by Prince[78] (1957). Dunitz and Orgel have explained the distortion on the basis of Crystal field theory and Jahn-Teller distortion. The compound is normal and hence Cu^{2+} ions with d^9 configuration and placed at tetrahedral sites cause large distortion with $c/a < 1$.

Nickel chromite was also found to be tetragonally distorted by Lotgering[79] (1956). The transformation from tetragonal to cubic symmetry has been observed by him at 310°C. Romeijn[21] (1953) found this compound to be a "normal" spinel so that Ni^{2+} ions almost exclusively occupy tetrahedral sites. Dunitz and Orgel have explained this tetragonal distortion as the distortion caused by the presence of Ni^{2+} ions with d^8 configuration at the tetrahedral sites. No other

example of tetrahedrally coordinated Ni^{2+} has so far been established with certainty by diffraction methods.

A large number of manganites crystallising with spinel structure have been investigated by several investigators. Mason[15] (1947) has observed that both Mn_3O_4 and $ZnMn_2O_4$ are tetragonally distorted spinels. The crystal structure of the several manganites has been given by Sinha, Sanjana and Biswas[10] (1957). The manganites studied by them were $CdMn_2O_4$, $MnMn_2O_4$, $MgMn_2O_4$, $ZnMn_2O_4$, $Co_xMn_{1-x}[Co_{1-x}Mn_{1+x}]O_4$, $Fe_xMn_{1-x}[Fe_{1-x}Mn_{1+x}]O_4$, $CuMn_2O_4$ and $Mn[NiMn]O_4$. They observed that $CdMn_2O_4$, $Mn[Mn_2]O_4$ $Mg[Mn_2]O_4$, $ZnMn_2O_4$ are "normal" and tetragonally distorted spinels. Further the variation of the tetragonal distortion with temperature has been studied by Irani, Sinha and Biswas[27] (1960). According to them, the distortion in the manganites of Mn^{2+}, Mg^{2+}, Zn^{2+} and Co^{2+}, which are "normal" spinels, is due to the location of Mn^{3+} ions at the octahedral sites and the transformation from tetragonal to cubic symmetry at elevated temperatures due to the randomization of direction of the individual distorted octahedral.

$CuMn_2O_4$ and $NiMn_2O_4$ have been found to have cubic spinel structure (Sinha, Sanjana and Biswas[10] 1957). $NiMn_2O_4$ is "inverse" and the number of Mn^{3+} ions at the octahedral sites is less than that required to give the cooperative tetragonal distortion. On the other hand copper manganite is "normal" and the cubic structure is

not so easy to explain. One would expect that if the structure is $Cu^{2+}[Mn_2^{3+}]O_4$, it should exhibit tetragonally distorted structure as the distorting Mn^{3+} ions are present at the octahedral sites. The observed cubic symmetry has been explained by Sinha, Sanjana and Biswas[10] (1957) by assigning the structure $Cu^{1+}[Mn^{3+}Mn^{4+}]O_4$ to the compound. The number of Mn^{3+} ions is then less than that required to give the cooperative distortion. Miyahara[80] (1962) on the other hand, has explained the cubic structure as due to the opposing influences of the tetrahedral Cu^{2+} and octahedral Mn^{3+} ions. The former tends to distort with $c/a < 1$ and the latter with $c/a > 1$. The two effects balance exactly and no distortion is therefore observed. The results on the electrical and magnetic properties of copper-zinc manganites discussed in the earlier two sections suggest that the most appropriate formula for copper manganite would be $Cu_x^{2+}Cu_{1-x}^{1+}[Mn_{1+x}^{3+}\ Mn_{1-x}^{4+}]O_4$ with $0.1 \leq x \leq 0.2$.

We have synthesised some new compounds to study the Jahn-Teller distortion when two different distorting cations are present in the structure. In the following section we present the results on their structural and electrical properties.

+ + + +

3.2. Results and Discussions.

3.2.1 Copper-Ferrite manganite [$CuFeMn_2O_4$]

This compound was formed by heating a well-ground mixture of CuO, Fe_2O_3 and Mn_2O_3 (all A.R.) in appropriate proportions at 950°C, for about 55 hours in air. The sample was taken out from the furnace and allowed to cool in air. X-ray powder diffraction pattern was taken for this compound on a 14 cms Debye-Scherrer camera using Mo-K_α radiation. The compound was found to be homogeneous and exhibited a cubic spinel structure. Lattice constant 'a' was computed using high angle reflections by the standard method and is given together with the observed and calculated values of $1/d^2$ in the Table 50.

The diffraction intensities of various reflections have been calculated for two models (i) in which copper ions are at the tetrahedral sites and (ii) in which they are at the octahedral sites. It has been found that the latter gives a better agreement with the observed intensities. No attempt has been made to work out the distribution amongst the Fe^{3+} and Mn^{3+} ions because their scattering powers are only slightly different. However, on the basis of the known octahedral site preference energies [Miller[46] (1959)] it appears reasonable to assume that Fe^{3+} ions occupy the tetrahedral sites. The situation does not change even if we have Mn^{4+} ions in the structure because they, like Mn^{3+} ions, have a very strong preference for the octahedral sites.

Table - 20

X-ray results for ($CuFeMnO_4$)

hkl	Intensity obs.	Intensity cal.	$1/d^2$obs.	$1/d^2$cal.	Lattice parameters
111	15	17.59	0.04226	0.04251	
220	35	35.00	0.1132	0.1133	
311	100	100.00	0.1571	0.1558	
222	5-10	7.3	0.1677	0.1700	
400	40	36.6	0.2268	0.2267	a = 8.398 Å
331	-	< 3	-	0.2692	
422	20	17	0.3389	0.3401	
511,333	50	49.3 11.6	0.3827	0.3825	
440	70	71.1	0.4535	0.4533	
531	-	2.75	-	0.4960	
620	5	5.20	0.5662	0.5668	
533,622	15	15.8	0.6083	0.6092	
444	5	<3	0.6793	0.6800	
711,551	-	<3	-	0.7226	
642	10	9.89	0.7861	0.7934	
731,553	20	19.58	0.8395	0.8360	

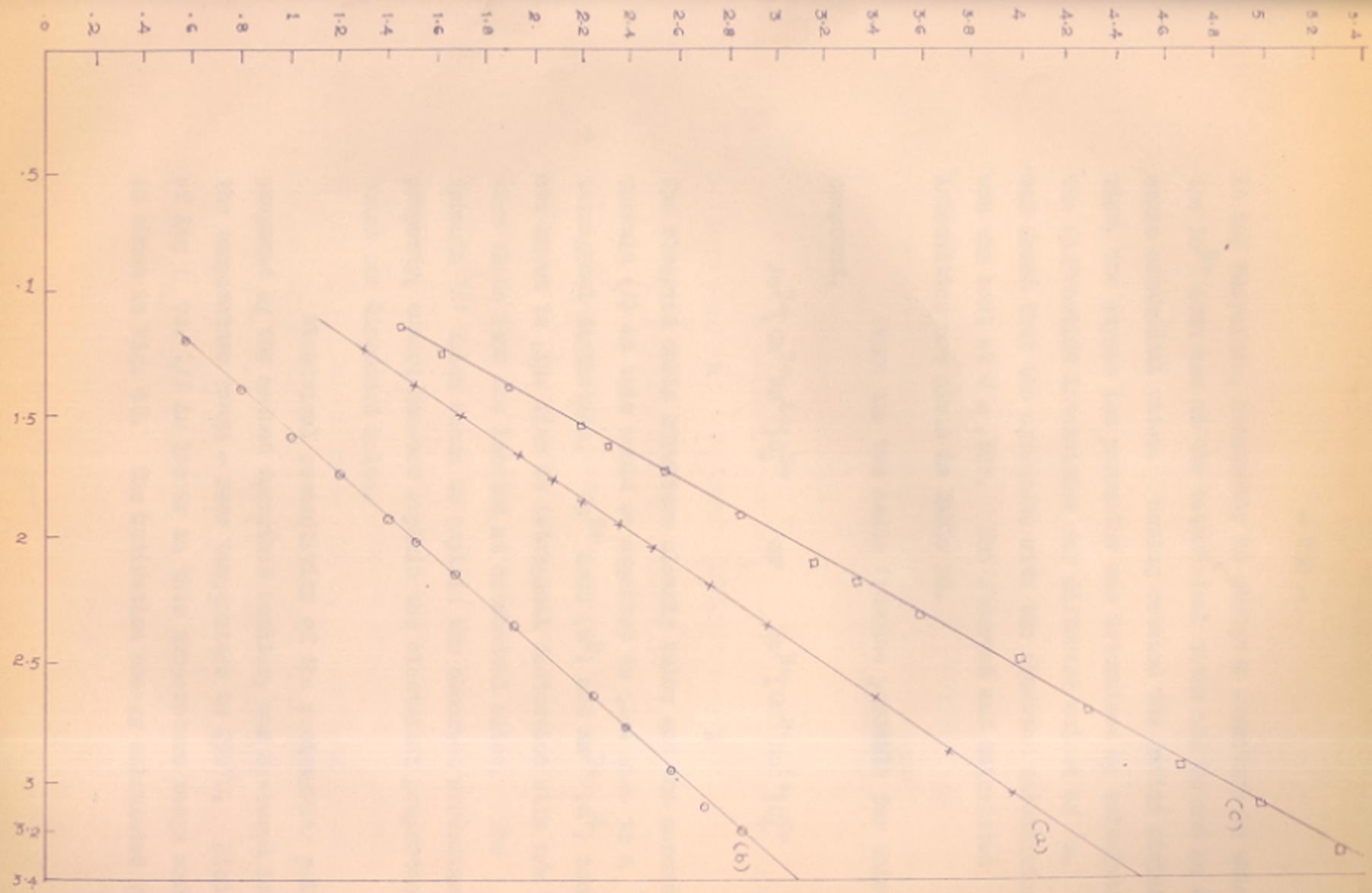

FIG - 42 VARIATION OF LOGP AS A FUNCTION OF THE RECIPROCAL OF TEMPERATURE FOR THE COMPOUNDS (Cu Fe Mn O4)(a); (Cu Mn O4)(b); (Ni Cr Mn O4)(c).

It is, therefore, reasonable to assign a structure in which the Fe^{3+} ions are at the tetrahedral sites and Cu and Mn ions share octahedral sites. Having settled the cation distribution, the oxygen ion parameter was determined by calculating the diffraction intensities for different values of u. It was found that the agreement with the observed intensities was the best at u = .381. The observed and calculated intensities are given in Table 50.

There are two ionic formulae possible for this compound.

$$Fe^{3+}[Cu^{1+}Mn^{4+}]O_4^{2-} \qquad \text{or} \qquad Fe^{3+}[Cu^{2+}Mn^{3+}]O_4^{2-}$$

A B

The observed cubic structure clearly rules out the second formula (B) as this would be expected to give rise to a tetragonal distortion. Cu^{2+} ions (d^9) and Mn^{3+} (d^4) ions are known to give rise to tetragonal distortion with c/a > 1, when these ions are located at octahedral sites. The formula 'A' which seems to explain the observed structural property, cannot however explain the electrical properties which are discussed below.

Electrical conductivity of the rectangular pellet, prepared by the method described earlier, was measured in the temperature range - room temperature to 250°C. Plot of log ρ vs. 1/T is linear in this temperature range and is shown in Fig. 42. The activation energy calculated from

the graph is 0.30 eV and the value of log ρ_0 is $\bar{7}.42$. The resistivity of the compound at room temperature is (log ρ = 4.564). The low activation energy for electrical conductivity indicates the existence of Mn^{3+}, Mn^{4+} pairs at the octahedral sites. Both the electrical and the structural properties can be explained if one assumes the ionic structure to be intermediate of (1) and (2) so that there are enough Mn^{3+} ions in the structure to give rise to a good conductivity, but not large enough to give a tetragonal distortion. Here we have a situation similar to that in copper manganite.

As mentioned earlier, two possible ionic formulae had been suggested for copper manganite namely :

(1) $Cu^{1+}[Mn^{3+}Mn^{4+}]O_4$ and (2) $Cu^{2+}[Mn_2^{3+}]O_4$

The first arrangement seemed to explain the electrical properties of the compound better as compared to the second whereas the reverse was true for the magnetic properties. Our results described in the last sections show that the results could be explained best if the formula is $Cu^{2+}_{.1}Cu^{1+}_{.9}[Mn^{3+}_{1.1}\ Mn^{4+}_{.9}]O_4$ which can be treated as a mixture of (1) and (2) in the ratio 90:10. This would explain the electrical magnetic and structural properties very well. In fact, the conclusion that in coppper manganite a large amount of Cu^{1+} and Mn^{4+} ions co-exist has been supported by the properties of the compound $CuFeMnO_4$.

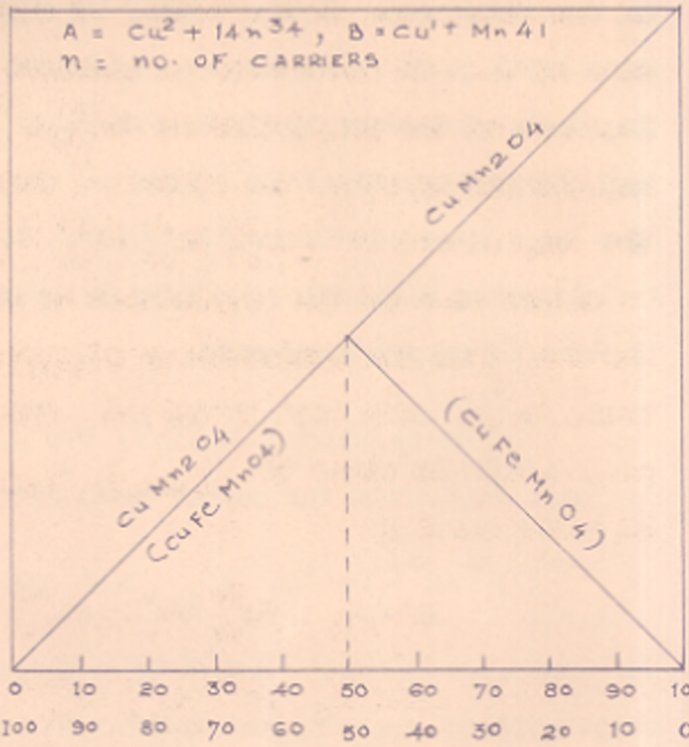

FIG - 43. VARIATION OF CARRIERS AS A FUNCTION OF COMPOSITION.

The observed activation energy of $CuFeMnO_4$ is comparable to that observed for copper manganite (0.25 eV). However the resistivity value is much higher as compared to copper manganite. This can be easily explained because of the difference in the number of charge carriers. In case of $CuMn_2O_4$ the number of carriers increases with the increase of the proportion of $Cu^{1+}[Mn^{3+}Mn^{4+}]O_4$ to $Cu^{2+}[Mn^{3+}]_2O_4$, whereas for $CuFeMnO_4$ the number of carriers is maximum for the composition $Fe^{3+}[Cu^{1+}_{.5}\ Cu^{2+}_{.5}\ Mn^{3+}_{.5}\ Mn^{4+}_{.5}]O_4$ and decreases on either side of the composition as can be seen from Fig. 43. The fact that the conductivity of copper manganite is many times larger than that of $CuFeMnO_4$ shows that actual composition is close to $A_{(.8-.9)}\ B_{(.2-.1)}$ for both manganites. In other words :

$$CuMn_2O_4 \quad Cu^{1+}_{.9}\ Cu^{2+}_{.1}\ [Mn^{3+}_{1.1}\ Mn^{4+}_{.9}]O_4$$

$$CuMnFeO_4 \quad Fe^{3+}[Mn^{3+}_{.1}\ Mn^{4+}_{.9}\ Cu^{2+}_{.1}\ Cu^{1+}_{.9}]O_4$$

The other reason for the relatively higher resistance for $CuMnFeO_4$ is the presence of both Mn and Cu ions at the octahedral sites. As explained earlier the mobility of a carrier depends on the number of available positions where a carrier can jump. Each octahedral site is surrounded by six other octahedral sites. However, for a random distribution of octahedral cations in $CuMnFeO_4$ three of these would be occupied by the Cu ions where the electrons from Mn^{3+} cannot jump. As explained earlier (page), the factor that enters the conductivity expression is the

product of $[Mn^{3+}]$ and $[Mn^{4+}]$. It can be seen that this factor is few times larger for $CuMn_2O_4$ as compared with $CuFeMnO_4$. This factor appears to be of the correct order of magnitude as can be seen by comparing the experimental values of log ρ_o for the two cases.

3.2.2. Copper chromite manganite [$CuCrMnO_4$]

Another interesting compound $CuMnCrO_4$ was synthesized by reacting a mixture of CuO, Mn_2O_3 and Cr_2O_3, in appropriate proportions, at 950°C for 55 hours in air. Completion of the reaction was checked by means of X-ray powder diffraction patterns taken on a 14 cms Debye-Scherrer camera with Mo-K_α radiations. The compound was found to be homogeneous and to have the cubic spinel structure. The lattice parameter, the cation distribution and the oxygen ion parameter were calculated as in the case of $CuFeMnO_4$. The unit cell edge 'a' is equal to 8.32 Å and the cation distribution is "normal" i.e. Cu ions occupy the tetrahedral sites and the Cr and Mn ions occupy the octahedral sites. The 'u' value has been found to be 0.392. The observed and calculated values of $1/d^2$ and the reflections intensities are given in Table 51. This compound has already been reported by Baltzer and Lopatin[31] (1964) but they have not determined the cation distribution nor have they studied the electrical properties. This study was necessary to see whether opposing distorting effects at the tetrahedral and

octahedral sites gave rise to the cubic symmetry. As mentioned earlier Miyahara[80] (1962) and Baltzer and Lopatin[81] have argued that Cu^{2+} ions at the tetrahedral sites tend to cause a tetragonal distortion with $c/a < 1$ and the Mn^{3+} ions at the octahedral sites tend to distort with $c/a > 1$. In case of $CuMn_2O_4$ the two effects just balance each other and hence the cubic symmetry is observed. At first sight, it is difficult to see how the two mutually opposing effects just balance and even if they do it is easy to see that the cubic symmetry will not be observed if we disturb the balance by replacing some of the distorting cations, from one of the sites. The compound $CuMnCrO_4$ was synthesized in an attempt to prepare such a compound. Cr^{3+} ions are known to have the strongest preference for the octahedral sites so that by replacing Mn^{3+} ions by Cr^{3+} ions one could maintain the normal structure. This has been proved to be true by the actual structure determination just discussed. If Cu^{2+} is able to balance the distorting effect of Mn^{3+} when in the ratio 1:2, there is no justifiable reason to believe that it will continue to do so even if the ratio has changed to 1:1. In fact at this concentration of Mn^{3+} ions at the octahedral sites there should be no distortion due to the Mn^{3+} ions alone as can be seen from the work of Finch, Sinha and Sinha[23] and Irani, Sinha and Biswas[22]. The minimum critical concentration of Mn^{3+} ions at the octahedral sites for producing tetragonal distortion is 10 per unit cell. Therefore, the copper ions at the

tetrahedral site should produce c/a < 1 unopposed by any effect due to Mn^{3+} ions at the octahedral sites. The fact that this does not happen clearly supports the formation of Mn^{4+} and Cu^{1+} in the structure $CuCrMnO_4$.

Table - 51

X-ray results for ($CuCrMnO_4$)

hkl	Intensity obs.	Intensity cal.	$1/d^2$ obs.	$1/d^2$ cal.	Lattice parameters
111	10	7.83	0.0438	0.0433	
220	40	42.35	0.1144	0.1156	
311	100	100	0.1586	0.1589	
222	5-10	< 3	0.1713	0.1734	
400	20	17.7	0.2303	0.2312	a = 8.32 Å
331	-	<1	-	0.2745	
422	20	17.43	0.3471	0.3468	
511,333	45	39.43 4.91	0.3960	0.3901	
440	60	59.77	0.4615	0.4624	
531	-	<1	-	0.5058	
620	-	<1	-	0.5781	
533,622	10	5.65 18.6	0.6221	0.6215	
444	-	<1	-	0.6936	
711,551	-	<1	-	0.7370	
642	10	8.74	0.8045	0.8093	
731,583	10	9.61	0.8429	0.8527	

The electrical conductivity for this compound was also measured at various temperatures. The variation of log ρ against 1/T is shown in the Fig. 42. An activation energy of conductivity obtained from the graph, is quite low (ΔE = 0.25 eV) and the conductivity is quite high (log $\rho_{R.T.}$ = 2.8451) as also log ρ_0 (= 1.2000). The fact that the conductivity of this compound is high and activation energy is low points out to the existence of Mn^{3+} and Mn^{4+} ions at the octahedral sites together with Cu^{1+} and Cu^{2+} at the tetrahedral sites. If the compound is treated as 1:1 solid solution between $CuMn_2O_4$ and $CuCr_2O_4$ a possible approximate formula would be :

$$Cu^{1+}_{.5}\ Cu^{2+}_{.5}\ [Mn^{3+}_{.5}Mn^{4+}_{.5}Cr^{3+}]O_4$$

The product of $[Mn^{3+}]$ and $[Mn^{4+}]$ which enters the pre-exponential factor of the conductivity expression would be intermediate between those for pure copper manganite ($\sim$10) and CuMnFeO ($\sim$ 0.1). The observed values for E and conductivity are also intermediate between those for the two compounds.

The stabilisation of Cu^{1+} in preference to Cu^{2+} as observed in the above series of compounds has also been observed by Lotgering[82] (1964) in $CuCr_2X_4$. As mentioned before this compound is ferromagnetic showing double exchange. The observed value of saturation magnetisation could be explained only by assuming the formation of Cu^{1+} and Cr^{4+}

due to the electron exchange $Cu^{2+} + Cr^{3+} \longrightarrow Cu^{1+} + Cr^{4+}$. If such an exchange can take place with Cr^{3+} ions it can surely do so with Mn^{3+} ions as Mn^{4+} is known to be more stable than Cr^{4+}.

3.3.3. Nickel chromite manganite [$NiCrMnO_4$]

The compound $NiCrMnO_4$ was synthesized to see the distortion produced due to Mn^{3+} ions at the tetrahedral sites. The free Mn^{3+} ions have the d^4 configuration in which all the electrons have the same energy but when they are put in the tetrahedral field of negative ions the degenerate d levels split into a lower doublet (e) and an upper triplet (t). In the case of a weak field the first two electrons will occupy the doublet and the other two electrons the triplet. This is a triply degenerate configuration and according to Jahn-Teller theorem the molecule must distort in such a way as to remove the degeneracy. The energy of the three levels d_{xy}, d_{ys}, d_{zx} plotted as a function of C/a, is shown in Fig. 44.

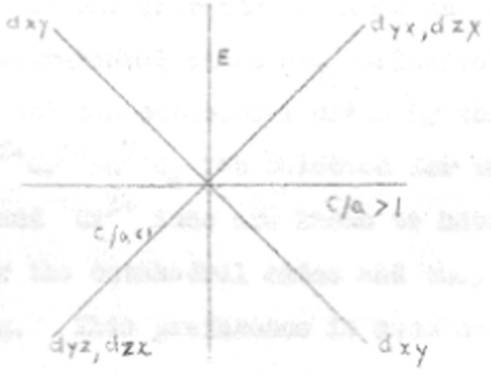

FIG - 44

In case of Mn^{3+} ions if $C/a > 1$ then one electron will occupy the level dxy and the other will be occupying the upper level which is doubly degenerate. This will give rise to a degenerate configuration which will be unstable according to Jahn-Teller theorem. On the other hand if $C/a < 1$, the two electrons will be occupying the levels dyz and dzx and the upper level will be empty. This configuration will be non-degenerate and should be stable according to the Jahn-Teller theorem. So far no compound of a spinel structure has been synthesized where Mn^{3+} ions at the tetrahedral sites are known to produce this type ($C/a < 1$) tetragonal distortion. / Mn_2O_3 and $Li^{1+}_{.5}Mn^{3+}_{2.5}O_4$ are known where both the tetrahedral and octahedral sites are occupied by Mn^{3+} ions. However, the structure is tetragonal with $C/a = 1.16$. This value of C/a is equal to that for Mn_3O_4 where the tetrahedral sites are occupied by non-distorting Mn^{2+} ions. This shows that Mn^{3+} ions at the tetrahedral sites do not affect the distortion. However, this is not a definite conclusion because there are two distorting ions ($Mn^{3+}_{oct.}$ and $Mn^{3+}_{tet.}$) of opposing requirement. It was therefore decided to prepare a compound in which the tetrahedral sites are exclusively occupied by the Mn^{3+} ions and the octahedral sites by the non-distorting cations. $Ni^{2+}Cr^{3+}Mn^{3+}O_4$ was selected for this purpose because Ni^{2+} and Cr^{3+} ions are known to have a strong preference for the octahedral sites and they are both non-distorting. This preference is much more than that of

the Mn^{3+} ions as can be seen from the calculated values of Miller and also from experimental results. $NiMn_2O_4$ is inverse whereas $NiCr_2O_4$ is normal showing the octahedral preference to be in the order $Cr^{3+} > Ni^{2+} > Mn^{3+}$.

The compound was synthesized by solid state reaction between nickel oxide, chromium oxide and manganese sesquioxide at 950°C for 55 hours. The reaction was complete as could be seen from the x-ray powder diffraction pattern. (Results in Table 52). The structure of the compound was found to be inverse cubic spinel which shows that Ni^{2+} and Cr^{3+} occupy octahedral site and Mn^{3+} occupy tetrahedral site.

From these results it is clear that although the Mn^{3+} ions are located at the tetrahedral sites as desired they have not produced the expected distortion with $c/a < 1$. To see if there was a change in the ionisation states of some of the cations, electrical conductivity of these samples was measured, as such a measurement is known to give some indication of such changes. The conductivity of this compound was found to be quite low ($\log \rho_{R.T.} = 5.337$) and the activation energy high, ($\Delta E = 0.416$ eV) and $\log \rho_0 = \bar{2}.72$.

From the results it appears unlikely that mixed valence states are present as the resistivity and activation energy are very high.

Table - 52

X-ray results for ($NiCrMnO_4$)

hkl	Intensity obs.	Intensity cal.	$1/d^2$ obs.	$1/d^2$ cal.	Lattice parameters
111	10	11.98	0.0430	0.0438	
220	23	21.74	0.1170	0.1169	
311	100	100	0.1609	0.1608	
222	5-10	5.3	0.1763	0.1754	
400	30	27.5	0.2356	0.2339	
331	-	<3	-	0.2778	a = 8.27 Å
422	10	9.3	0.3528	0.3510	
511,333	35	28.9 6.7	0.3934	0.3949	
440	50	55.75	0.4666	0.4678	
531	-	<2	-	0.5118	
620	-	4	-	0.5849	
533,622	10	10.85 5	0.6316	0.6434	
444	-	4.4	-	0.7018	
711,551	-	<3	-	0.7457	
642	-	4	-	0.8189	
731,553	10	11.23	0.8584	0.8628	

The observed cubic symmetry then remains anomalous. There is of course a possibility that the tetragonal-cubic

transition temperature may be below room temperature. In that case one would observe the expected distortion at low temperature. Further work is being done in this direction. There is another possibility that Mn^{3+} ions at the tetrahedral sites are in a spin paired state as shown in Fig. 45. This will explain the cubic symmetry of the present compound and the tetragonal structure with $c/a > 1$ for $Li_{\frac{1}{2}} Mn_{2\frac{1}{2}} O_4$ and γMn_2O_3.

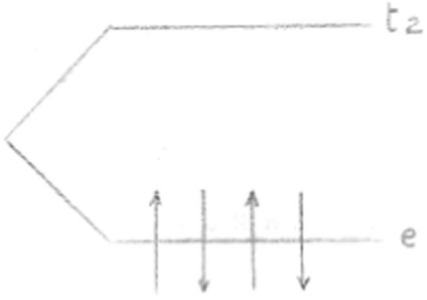

FIG - 45

+ + + +

SUMMARY

SUMMARY

Some new manganites crystallizing in spinel or hausmannite structure and containing both Mn^{3+} and Mn^{4+} ions at the octahedral sites have been synthesized. Their structural, electrical and magnetic properties have been studied.

Compounds with the general formula $ZnLi^{1+}_{2x}Mn^{3+}_{2-6x}Mn^{4+}_{4x}O_4$ were formed by reacting ZnO, Mn_2O_3 and Li_2O in appropriate proportions at elevated temperatures in air. X-ray diffraction patterns indicated the formation of a homogeneous phase on heating at 850°-900°C for about 100 hours. The electrical conductivity and thermoelectric coefficient of sintered samples have been measured as a function of temperature. The change of electrical conductivity with temperature follows the relationship $\sigma = \sigma_0 \exp -\frac{\Delta E}{kT}$. Thermoelectric properties indicate that compounds in which the number of Mn^{4+} ions is small ($0 \leq X \leq 0.1$) are p-type semiconductors, while those with $0.15 \leq X \leq 0.3$ are n-type semiconductors. Mobility shows an exponential dependence on temperature. This is similar to what has been observed for many oxides of 3d transition metals and indicates that the charge carriers are localised, and conduction takes place due to occassional exchange of holes or electrons between adjacent sites. Paramagnetic susceptibility of these compounds has been measured by the Gouy method in the temperature range 90°K to about 350°K. The magnetic

properties of these compounds are very interesting. Compounds in which the number of Mn^{4+} ions ($x \leq 0.1$) is small becomes paramagnetic and obey Curie-Weiss law. The compounds in which Mn^{3+} and Mn^{4+} ion concentrations are nearly equal ($0.15 \leq x \leq 0.25$) are ferrimagnetic.

An attempt was made to prepare another series of manganites containing Mn^{3+} and Mn^{4+} ions at octahedral sites. $ZnMn_2O_4$ and $CuMn_2O_4$ were therefore mixed in the mole ratio, x : 1-x and reacted at 1000°C for 72 hours. They were then quenched in air. In the composition range $x<0.05$, the substance had the cubic spinel structure and for $x > 0.25$ it had tetragonal hausmannite structure. In the range $0.05 \leq X \leq 0.25$ the product was a mixture of cubic and tetragonal phases. The electrical conductivity of these phases was measured as a function of temperature. Thermo-electric coefficient measurements indicated p-type conductivity for all these compounds. The variation of paramagnetic susceptibility with temperature indicates that all these compounds are ferrimagnetic. The compound $Zn_{0.5}Cu_{0.5}Mn_2O_4$ which is single-phased has a Curie temperature $\sim 95°K$, and $C = 5.4 \pm 0.1$.

The following compounds were prepared with a view to study the Jahn-Teller distortion :
$(Cu^{2+}Mn^{3+}Fe^{3+}O_4)$; $(Cu^{2+}Mn^{3+}Cr^{3+}O_4)$ and $(Ni^{2+}Cr^{3+}Mn^{3+}O_4)$
The crystal structure and the cation distribution have been determined and also the electrical properties of these have been studied.

+ + + +

References

1. Verwey, E.J.W. — Semiconducting materials, edited by H.K.Henish (1951).
2. Morin, F.J. — Phys. Rev. 93, 1195 (1954).
3. De Boer, J.H. and Verwey, E.J.W. — Proc. Phys. Soc., 49, suppl. 59 (1937).
4. Mott, N.F. — Proc. Phys. Soc., 62A, 416 (1949).
5. Jonker, G.H. and Van Santen, J.H. — Physica, 16, 337, 599 (1950).
6. C.Zener — Phys. Rev. 82, 403 (1951).
7. Heikes, R.R., McGuire, T.R. and Happel, R.J. — Phys. Rev. 121, 703 (1961).
8. Sabane, C.D. — Thesis, University of Poona, (1960).
9. Barth, T.F.W. and Posnjak, E. — Zeitschr. f. krist., 82, 325 (1932).
10. Sinha, A.P.B., Sanjana, N.R. and Biswas, A.B. — Acta cryst., 10, 439 (1957).
11. Sinha, A.P.B., Sanjana, N.R. Biswas, A.B. — Zeitschr. f. krist., 109, 420 (1957).
12. Sinha, A.P.B., Sanjana, N.R. Biswas, A.B. — J.Phys. Chem., 62, 291 (1958).
13. Sanjana, N.R. — Thesis, University of Bombay, (1958).
14. Bongers, P.F. — Thesis, University of Leiden, (1958).
15. Mason, B. — Amer.Min.,32, 426 (1947).
16. Mason, B. — Geol.Foren. Stockholm, Forch, 65, 97 (1943).
17. Wickham, D.G. and Croft, W.J. — Quarterly progress Reports of Solid State Research Group' Lincoln Laboratory, M.I.T. (1958).
18. Baltzer, P.K. and White, J.G. — J.Appl.Phys., 29, 445 (1958).

19. Kurlina, E.V., Prokhvatilov, V.G. and Sheftel, I.T. — Doklady Akad.Nauk U.S.S.R. 86, 305 (1952).

20. McMurdie, H. and Golovato, E.J. — J.Res. Nat. Bur. Stand. 41, 589 (1948).

21. Romeijn, F.C. — Philips Res. Rep. 8, 304-20 (1953).

22. Irani, K.S., Sinha, A.P.B. and Biswas, A.B. — J.Phys. Chem. of Solids 23, 711-727 (1962).

23. Finch, G.I., Sinha, A.P.B. and Sinha, K.P. — Proc. Roy. Soc. (London), A242, 28 (1957).

24. Wojtowicz, P.J. — J.Appl.Phys., 30S, 305 (1959).
Phys. Rev., 116, 32 (1959).

25. Konamori, J. — J.Appl.Phys., 31S, 148 (1959).

26. Wickham, D.G. and Croft, W.J. — J.Phys.Chem. of Solids, 7, 351-60 (1958).

27. Irani, K.S., Sinha, A.P.B. and Biswas, A.B. — J.Phys. Chem. of Solids, 17, 101 (1960).

28. Ikuo, AOKI — Chiba Univ., Oyô Butsuri, 21, 312 (1952).

29. Masahido Kamiyama and Ziro Maya — Oyô Butsuri, 21, 400 (1952).

30. Suchet, J. — J. Phys. Radium, 16, 417-22 (1955).

31. Heikes, R.R. and Johnston, W.D. — J. Chem. Phys., 26, 582 (1957).

32. Larson, E.G., Arnot, R.J., Wickham, D.G. — J.Phys.Chem. of Solids, 23, 1771 (1962).

33. Rosenberg, M., Nicolau, P., Manaida, R. and Pausescu, P. — J. Phys. Chem. of Solids, 24, 1419 (1963).

34. Bloch, F. — Z.Phys., 52, 555 (1928).

35. Bloch, F. — Z.Phys. 59, 208 (1930).

36. Wilson, A.H. — Proc. Roy. Soc., 133A, 458 (1931).

37. Morin, F.J. — Phys. Rev. 83, 1005-10 (1951).

38. J.Yamashita and T.Kurosawa. — J.Phys.Chem. of Solids, 5, 34-43 (1958).

39. J.Yamashita and T.Kurosawa.	J.Phys.Soc. of Japan, 15, 802 (1960).
40. J. Yamashita	J. Appl. Phys., Suppl. 32, 2215 (1961).
41. Holstein	Ann. Phys. 8, 325, 343 (1959).
42. Dogonadze, R.R., Chernenko, A.P. and Chizmadshev.	Sov. Phys. Solid State, 3, 2698 (1962).
43. Sinha, A.P.B. and Sinha, K.P.	Indian Journal of Pure and Applied Physics, 1, 286-290 (1963).
44. (a) Verwey, E.J.W. and Heilmann	J. Chem. Phys. 15, 174 (1947).
(b) Verwey, E.J.W., Broun, P.B. Garter, C.W., Romeijn, F.C. and Van Santen, J.H.	Z. Phys. Chem. 198, 6-22 (1951).
45. Garter, C.W.	Philips Res.Rep., 9, 295 (1954).
46. Miller, A.C.	J. Appl. Phys., Suppl. 30, 24S (1959).
47. Koops, C.G.	Phys. Rev., 83, 21 (1951).
48. Sewell, G.L.	Phil. Mag., 3, 1361 (1958).
49. Jonker, G.H.	J.Phys.Chem. of Solids, 9, 165-175 (1959).
50. S.Van Houten	J. Phys. Chem. of Solids, 17, 7-17 (1960).
51. Honda and Sonne	Sci. Repts. Tohoku Imp. Univ., 3, 139 (1944).
52. Moore, T.E., Merylinn, S. and Selwood	J.A.C.S., 72, 856 (1952).
53. Borovik, A.S., Romanov, V., and Orlova	Soviet Phy., U.S.S.R., 5, 1023 (1957).
54. Neel, L.	Ann.Phys., 3, 137 (1948).
55. Jacob, I.S.	J.Appl.Phys. Suppl.30, 301S (1959).
56. Yafet and Kittel	Phys. Rev. 87, 290 (1952).

57. Jacob, I.S. and Kouvel, J.S. — Phys. Rev., 122, 412 (1961).

58. Dwight, K. and Menyuk, N. — Phys. Rev., 119, 1470 (1960).

59. Kaplan, T.A. — Phys. Rev., 119, 1460 (1960).

60. Menyuk, N., Dwight, K., Lyons, D.H. and Kaplan, T.A. — J.Appl.Phys., 32, 138 (1961).

61. Lyons, D.H., Kaplan, T.A. Dwight, K. and Menyuk, N. — Phys. Rev., 126, 540 (1962).

62. Sinha, A.P.B. and Sinha, K.P. — J.Phys.Soc. of Japan, Suppl. 17, 218 (1962).

63. P.G.De Gennes — Phys. Rev., 118, 141 (1960).

64. Anderson, P.W. and Hasegawa, H. — Phys. Rev., 100, 675 (1955).

65. Guillaud, C. — J.Phys.Rad., 12, 239 (1951).

66. Miyahara, S. and Muramori, K. — J.Phys.Soc. of Japan, 15, 2354 (1960).

67. Pallot, M. and Maroni, R. — J. Phys. Rad., 12, 256 (1951).

68. Goodenough, J.B. and Loeb, A.L. — Phys. Rev., 98, 391 (1955).

69. Dunitz, J.D. and Orgel, L.E. — J.Phys.Chem. of Solids, 3, 20 (1957).

70. Jahn, H.A. and Teller, E. — Proc. Roy. Soc., A 161, 220 (1937).

71. Opik, U. and Pryce, M.H.L. — Proc.Roy.Soc., A=238, 425, (1957).

72. Liehr and Ballhausen — Ann.Phys., 3, 304 (1958).

73. Van Vleck, J.H. — J.Chem.Phys., 7, 472 (1939).

74. Bertaut, E.F., Bochirol, L. and Weil, L. — J. Phys. Radium, 11, 208 (1950).

75. Prince, E. and Treuting, R.G. — Acta Cryst., 9, 1025 (1956).

76. Miyahara, S. and Ohinishi, H. — J.Phys.Soc.Japan, 12, 1296 (1956).

77. McGuire, T.R., Howard, L.N. and Smart, J.S. — Ceramic Age, 60, 22 (1952).

78. Prince, E. — Acta Cryst. 10, 554 (1957).

79. Lotgering, F.K. — Philips Res. Rep., 11, 190 (1956).

80. Miyahara, S. — J. Phys. Soc. Japan, Suppl. 17, 181 (1962).

81. Baltzer, P.K. and Lopatin, E. — Paper read at 'International Conference on magnetism' (held at Nottingham, U.K.) Sep. 1964.

82. Lotgering, F.K. — Paper read at 'International Conference on magnetism', (held at Nottingham, U.K.) Sep. 1964.

+ + + +